Journal of Medicinal Chemistry

pubs.acs.org/jmc

Article

HER2 Kinase-Targeted Breast Cancer Therapy: Design, Synthesis, and *In Vitro* and *In Vivo* Evaluation of Novel Lapatinib Congeners as Selective and Potent HER2 Inhibitors with Favorable Metabolic Stability

Tamer A. Elwaie, Safinaz E. Abbas, Enayat I. Aly, Riham F. George, Hamdy Ali, Nikolai Kraiouchkine, Khaldoun S. Abdelwahed, Tamer E. Fandy, Khalid A. El Sayed, Zakaria Y. Abd Elmageed,* and Hamed I. Ali*

Cite This: https://dx.doi.org/10.1021/acs.jmedchem.0c01647

Read Online

ACCESS | Metrics & More | Article Recommendations | Supporting Information

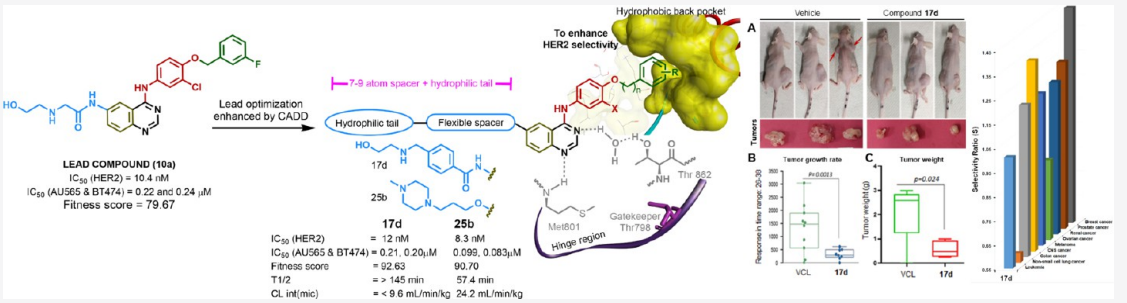

ABSTRACT: HER2 kinase as a well-established target for breast cancer (BC) therapy is associated with aggressive clinical outcomes; thus, herein we present structural optimization for HER2-selective targeting. HER2 profiling of the developed derivatives demonstrated potent and selective inhibitions (IC_{50}: 5.4−12 nM) compared to lapatinib (IC_{50}: 95.5 nM). Favorably, **17d** exhibited minimum off-target kinase activation. NCI-5-dose screening revealed broad-spectrum activities (GI_{50}: 1.43−2.09 μM) and **17d** had a remarkable selectivity toward BC. Our compounds revealed significant selective and potent antiproliferative activities (~20-fold) against HER2+ (AU565, BT474) compared to HER2(−) cells. At 0.1 IC_{50}, **15i**, **17d**, and **25b** inhibited pERK1/2 and pAkt by immunoblotting. Furthermore, **17d** demonstrated potent *in vivo* tumor regression against the BT474 xenograft model. Notably, a metastasis case was observed in the vehicle but not in the test mice groups. CD-1 mice metabolic stability assay revealed high stability and low intrinsic clearance of **17d** ($T_{1/2}$ > 145 min and $CL_{int(mic)}$ < 9.6 mL/min/kg).

INTRODUCTION

Cancer is the second main cause of death in the United States and worldwide.[1−6] The most common cancers among men and women are prostate and breast cancers (BCs), respectively.[1] BC is the most commonly diagnosed cancer and the main cause of cancer deaths among women globally. Approximately, two million patients are diagnosed with BC and more than 600,000 deaths occur each year.[7] In the United States, 276,480 new cases of female BC have been estimated and 42,170 deaths were reported in 2020.[8] The ErbB (HER) proteins are related to subclass I of the superfamily of receptor tyrosine kinases (RTKs) which plays a vital role in signal transduction pathways and the initiation of malignancy of several solid tumors. The ErbB family contains epidermal growth factor receptor (EGFR; also named ErbB1/HER1), ErbB2/HER2, ErbB3/HER3, and ErbB4/HER4.[9] All ErbBs are closely similar in their structures and consist of three domains, an extracellular ligand-binding domain, a transmembrane domain, and an intracellular kinase domain.[10] Unlike EGFR (ErbB1/HER1), ErbB2 (HER2) does not have a recognized activating ligand (ligandless receptor),[11] accordingly its overexpression can lead to cell transformation without the need of ligand interaction.[12,13] HER2 signalings are initiated by homo- or hetero-dimerization and these dimers have a lower dissociation rate with persistent signal transduction compared to other dimers. Subsequently, these intracellular cascades activate cell survival, proliferation, motility, and differentiation.[14,15] Dysregulation of the *HER2* gene disrupts cell proliferation and leads to the formation of aggressive tumor cells.[16] The HER2 RTK is amplified in

Received: September 21, 2020

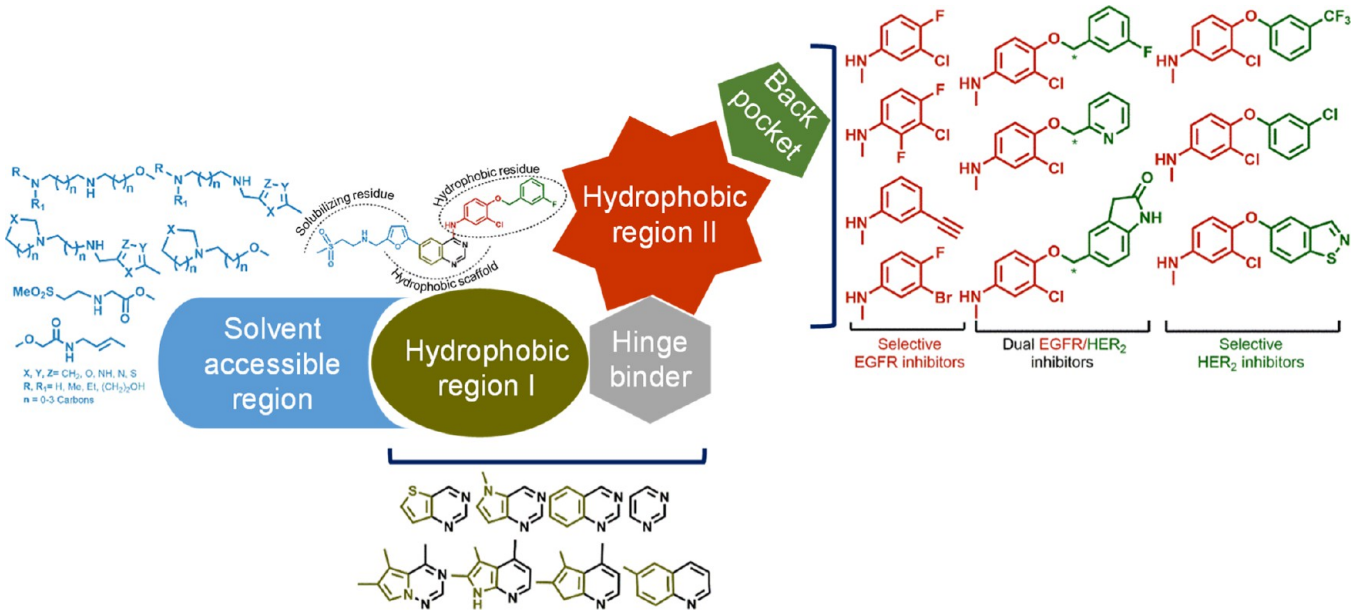

Figure 1. Binding mode of EGFR/HER2 inhibitors into their corresponding kinases and the fragments used for their design.

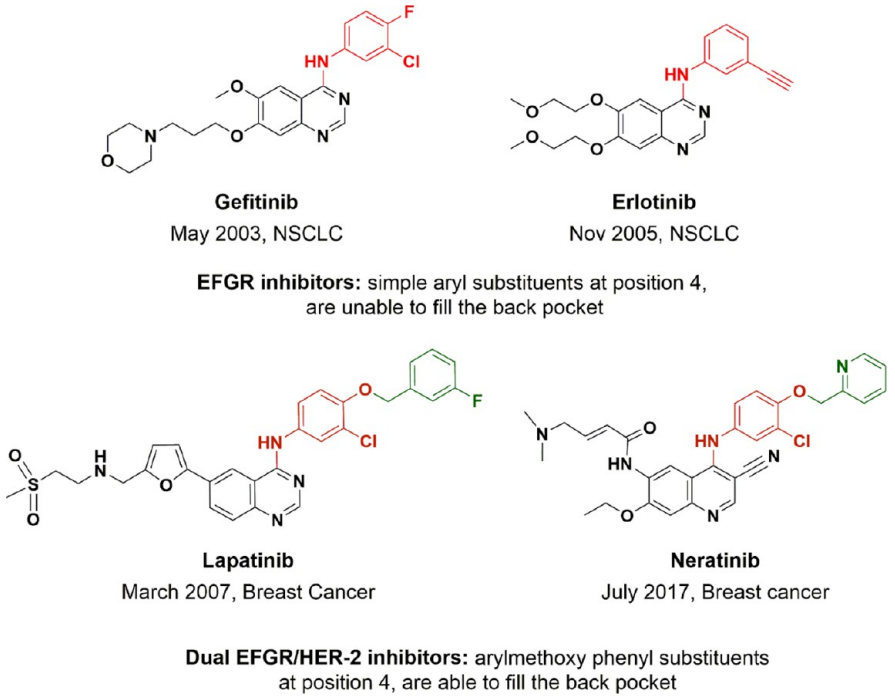

Figure 2. Chemical structure for the FDA-approved EGFR and dual EGFR/HER2 kinase inhibitors.

approximately 15−30% of BC and is associated with worse aggressive tumor forms.[17] HER2 overexpression has also been reported with high frequencies in the lung (NSCLC), gastroesophageal, ovarian, melanoma, and oral cancers.[18−20] HER2-positive (HER2+) BC often has a more aggressive phenotype than HER2-negative (HER2−) BC.[21] Worldwide, approximately 15−20% of BC cases are HER2+.[22] Because of the identification of the HER2 receptor amplification as an adverse prognostic factor in a special subtype of the metastatic BC, there has been a substantial improvement in the survival of these patients because of the development of anti-HER2-targeted therapies.[23] HER2 is a well-established therapeutic target for the treatment of BC.[24] Currently, there is a variety of FDA-approved HER2-targeted therapies for the treatment of HER2+ BCs including anti-HER2 monoclonal antibodies, such as trastuzumab and pertuzumab, antibody−drug conjugate such as trastuzumab-emtansine (T-DM1), and small-molecule pan-HER tyrosine kinase inhibitors (TKIs) such as lapatinib and neratinib.[23] The small-molecule TKIs have potential advantages over monoclonal antibody therapies, including their ability to inhibit multiple kinases and p95 HER2 (highly active truncated HER2 lacking most of the extracellular domain).[23,25] Likewise, TKIs have lower cardiopulmonary toxicities commonly associated with monoclonal antibody therapies[26−28] and have a higher ability to penetrate the blood−brain barrier with a greater therapeutic potential against brain metastases.[20]

https://dx.doi.org/10.1021/acs.jmedchem.0c01647
J. Med. Chem. XXXX, XXX, XXX−XXX

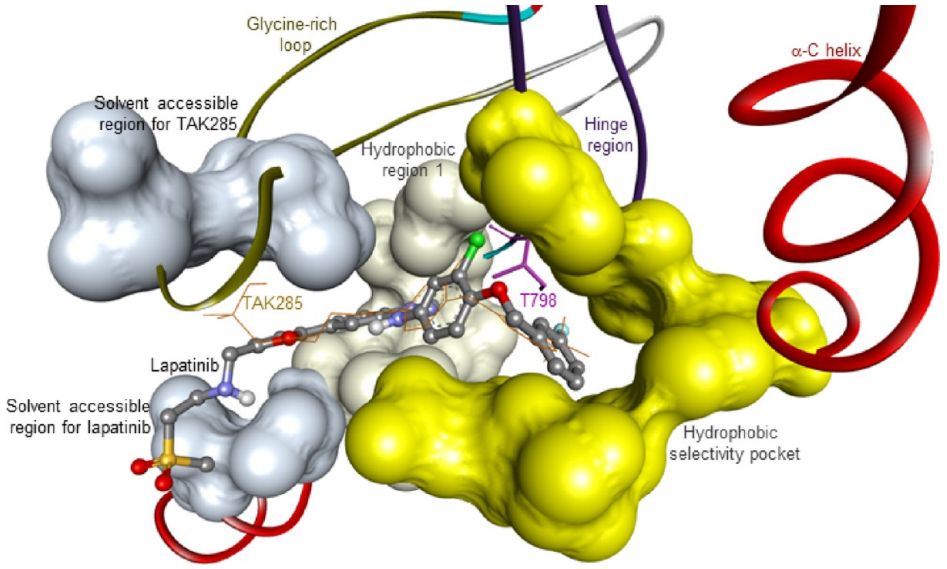

Figure 3. Docking mode of lapatinib (ball and sticks) and TAK285 (orange lines) into the HER2 kinase domain (PDB: 3PP0). Hydrophobic region 1 (L726, A751, L800, G804, L852, and M801); hydrophobic selectivity pocket (M774, L785, L796, T798, D863, and F864); solvent-accessible region for TAK285 (G727, S728, and V734); solvent-accessible region for lapatinib (C805 and D808); α-C helix (P761-V777), and the gatekeeper amino acid (T798).

In addition, the majority of BC patients who have an initial therapeutic response to the HER2-targeted antibody trastuzumab reveal poor prognosis within one year.[29] Unlike lapatinib, neratinib is a potent irreversible pan-HER kinase inhibitor but its clinical use may result in hepatotoxicity.[30] In favor of this strategy, four of the 25 FDA-approved medications in 2019 are kinase inhibitors.[31] The development of kinase inhibitors is based on the fundamental understanding of the general pharmacophoric features of these inhibitors (summarized in Figure 1) which are composed of (a) core scaffold serving as a hinge binder; (b) hydrophobic bulky moiety extended into the back pocket revealing HER2 kinase selectivity; and (c) hydrophilic solubilizing fragment harbored into the solvent-accessible region to conduct its pharmacokinetic role through balancing the logP of the inhibitors. The solvent-accessible region can tolerate a wide range of solubilizing groups modulating the cellular activity without affecting the enzymatic activity. Moreover, introducing particular functionalities into the solubilizing moiety would optimize the potency and selectivity profiles.[32] The 4-anilinoquinazoline is the most commonly used hinge binder scaffolds for EGFR kinase inhibitors, represented by the clinically approved drugs: gefitinib, erlotinib, and lapatinib (Figure 2).[33−35] Lapatinib was developed by GSK as the first dual EGFR/HER2 inhibitor and approved by the FDA in 2007 for treatment of BC. Its bulky 4-benzyloxyaniline substituent is essential for EGFR/HER2 dual inhibition. However, smaller anilines such as 3-ethynylaniline in erlotinib and 3-chloro-4-fluoro-aniline in gefitinib only inhibit EGFR.[36] Lapatinib binds to the inactive EGFR closed conformation displacing the αC-helix to "out" and gives the 3-fluorobenzyloxy group access to the hydrophobic back pocket.[32,37] This extra binding in the back pocket contributes to the dual EGFR/HER2 inhibition and has longer inhibition time when compared to gefitinib and erlotinib which do not have access into the back pocket.[38] In this regard, Abouzid et al. reported enhanced EGFR/HER2 activities of quinazoline derivatives through incorporating bulkier anilino moieties at position 4 in a manner similar to lapatinib. These moieties include 4-(4-aryl-2-imino pyridino) anilines, which could be oriented deep in the back of the ATP-binding site and mimicking the 3-chloro-4-[(3-fluorobenzyl)oxy]aniline group of lapatinib.[39] The HER2$^{T798I(M)}$ gatekeeper mutation and its analogous EGFR^{T790M} have been shown to confer the most common clinical resistance against lapatinib.[40] This resistance emerges from replacing a smaller polar Thr^{798} with bulkier Ile^{798} or Met^{798} residues, which causes unfavorable steric clashes between the gatekeeper mutant Ile^{798} amino acid and lapatinib.[40] Targeting other HER family members, such as EGFR (HER1), does not functionally suppress HER2 signaling and may introduce off-target toxicities such as diarrhea and rash.[41] Moreover, in BC cells that overexpress HER2, the inhibition of HER family members EGFR or HER4 does not functionally suppress HER2 signaling and consequently does not prevent tumor cell proliferation or survival.[42,43] Noteworthy, lapatinib, as an EGFR inhibitor, has another serious drawback by causing severe skin rash and diarrhea. Skin toxicity is typically manifested as mild to severe papulopustular rash in the majority of patients (45−100%) receiving EGFR inhibitors.[44−46] These adverse effects reveal serious physical and psycho-social complications, particularly for female patients with BC. For all the aforementioned limitations of current medications, there is an eventual need for developing novel selective HER2 inhibitors with enhanced efficacy against mutant isoforms to overcome the reported limitations of lapatinib. Based on the reported key binding features of lapatinib as a dual EGFR/HER2 inhibitor, guided by its binding mode through flexible docking into the HER2 kinase domain (Figure 3) and inspired by the importance of HER2 overexpression in BC progression, in this study, we present the design and development of new series of 6-substituted-4-anilinoquinazolines (**10a−c**, **15a−l**, **17a−d**, and, **25a−h**) as promising candidates for HER2 inhibition with improved potency and selectivity. The developed candidates can preferentially inhibit HER2 kinase and reduce the potential of EGFR-associated toxicities. In addition, our strategy is oriented to developing a variety of lapatinib analogues with

https://dx.doi.org/10.1021/acs.jmedchem.0c01647
J. Med. Chem. XXXX, XXX, XXX−XXX

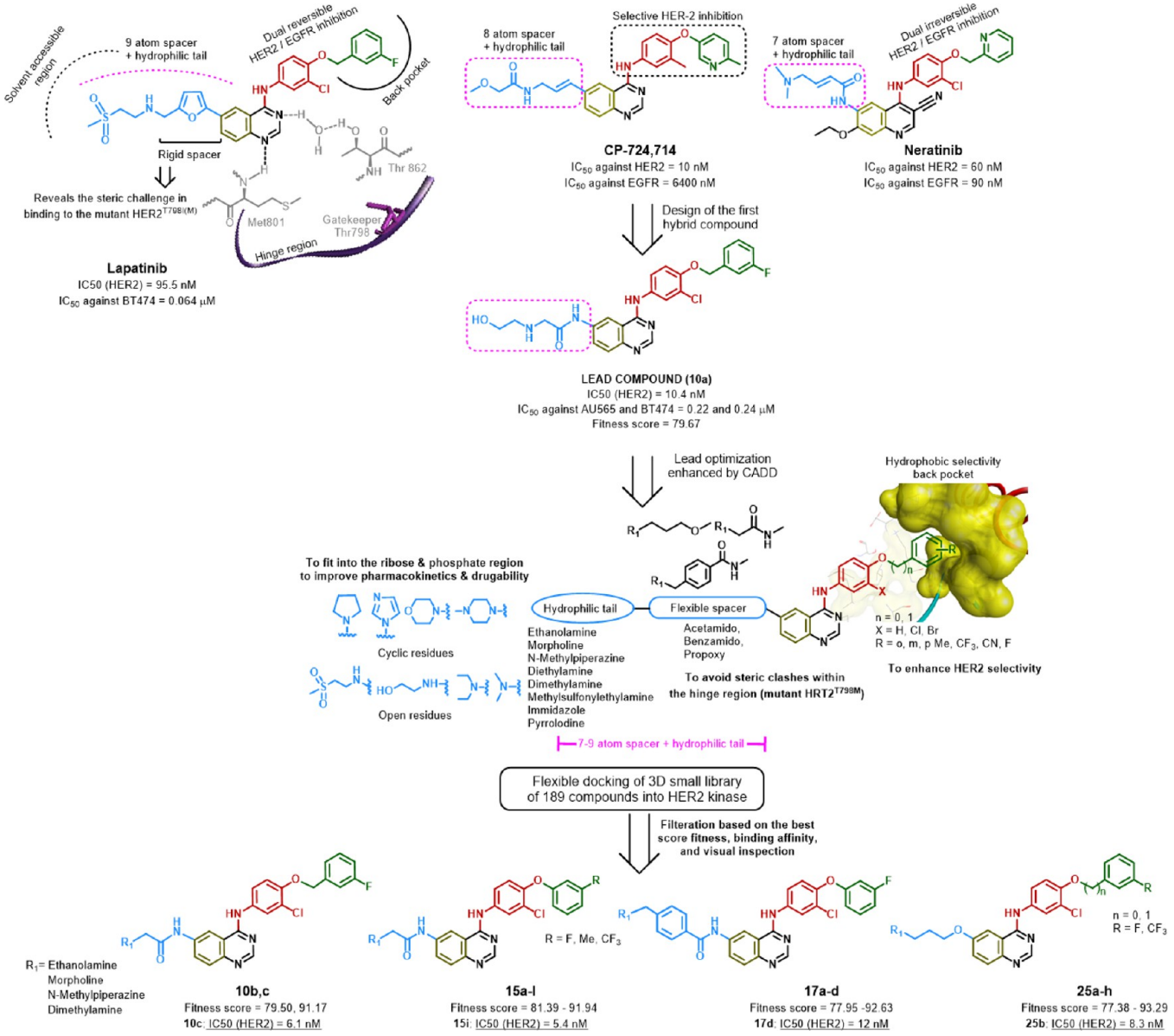

Figure 4. Rational design enhanced using CADD of the newly synthesized compounds.

some structural flexibility, this flexibility of the designed compounds may diminish the steric clashes within the gatekeeper amino acids of the HER2^{T798I} mutant BC and consequently provide better treatment options.

RESULTS AND DISCUSSION

Rational Design. The rational design of our compounds was based on the fundamental pharmacophoric features for the kinase inhibitors summarized in Figure 3 and according to the analysis of the binding pattern of the FDA-approved kinase inhibitors. Our template kinase inhibitors include the dual EGFR/HER2 inhibitors (lapatinib and neratinib) and the investigational selective HER2 inhibitor (CP-724,714).[47] Our efforts were focused on the design and synthesis of new hybrid molecules with the 6-substituted 4-anilinoquinazoline core to potentiate the selectivity against the target HER2 kinase by reversible inhibition and tackling the emergence of lapatinib acquired resistance. Guided by the reported EGFR/HER2 kinase inhibitors, we initially designed and synthesized the lead compound (**10a**; Figure 4) via incorporating a flexible spacer at position 6 of the quinazoline ring, namely, 6-acetamido, to mimic neratinib. This flexible design is aimed to avoid the steric clashes within the gatekeeper T798I(M) mutant kinase. A hydrophilic ethanolamine tail was introduced to the flexible spacer at position 6 through nucleophilic substitution. At position 4 "*N*-(4-(3-chloro-4-(3-fluorobenzyl)oxy)phenyl)-amino" moiety of lapatinib was retained. The lead compound (**10a**) revealed superior inhibition against HER2 kinase (IC_{50} = 10.4 nM) compared to lapatinib which exhibited inferior inhibition (IC_{50} = 95.5 nM). WST-8 assay for the lead compound was conducted using AU565 (only HER2+) and BT474 {triple positive, HER2+, estrogen (ER+), and progesterone (PR+)} BC cell lines. The lead compound (**10a**) exhibited promising antiproliferative activities (IC_{50} = 0.22 and 0.24 μM, respectively). These preliminary results have prompted us to enhance the efficiency of the lead compound through lead optimization, as depicted in Figure 4. To increase the selectivity of HER2 inhibition, the "*N*-(4-(3-

https://dx.doi.org/10.1021/acs.jmedchem.0c01647
J. Med. Chem. XXXX, XXX, XXX−XXX

Scheme 1. Synthesis of 2-Chloro-4-nitro-1-(3-(substituted)phenoxy/benzyloxy)benzene (3a−d) and 3-Chloro-4-(3-(substituted)phenoxy/benzyloxy)aniline (4a−d)[a]

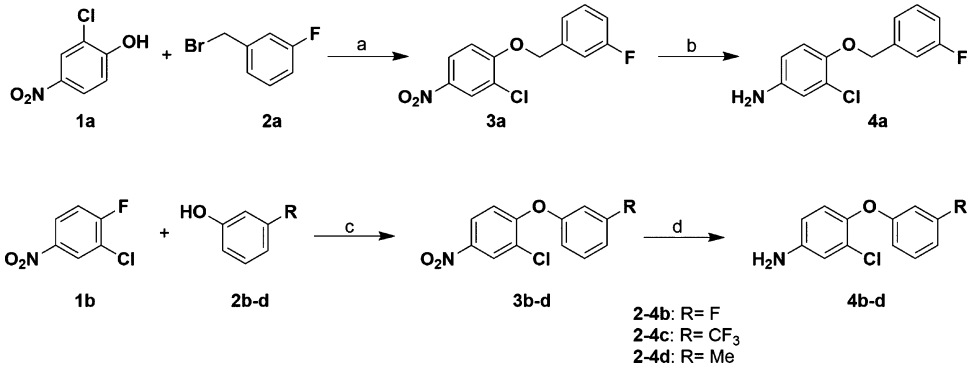

[a]Reagents and conditions: (a) DMF, K_2CO_3, 85 °C, 3 h; (b) Fe, $CaCl_2$, EtOH, H_2O, 80 °C, 8 h; (c) acetonitrile, K_2CO_3, 85 °C, 5 h; (d) $SnCl_2$, MeOH, reflux, under N_2, 2.5 h.

Scheme 2. Synthesis of *N*-(4-((3-Chloro-4-((3-fluorobenzyl)oxy)phenyl)amino)quinazolin-6-yl)-2-Substituted Acetamide (10a−c)[a]

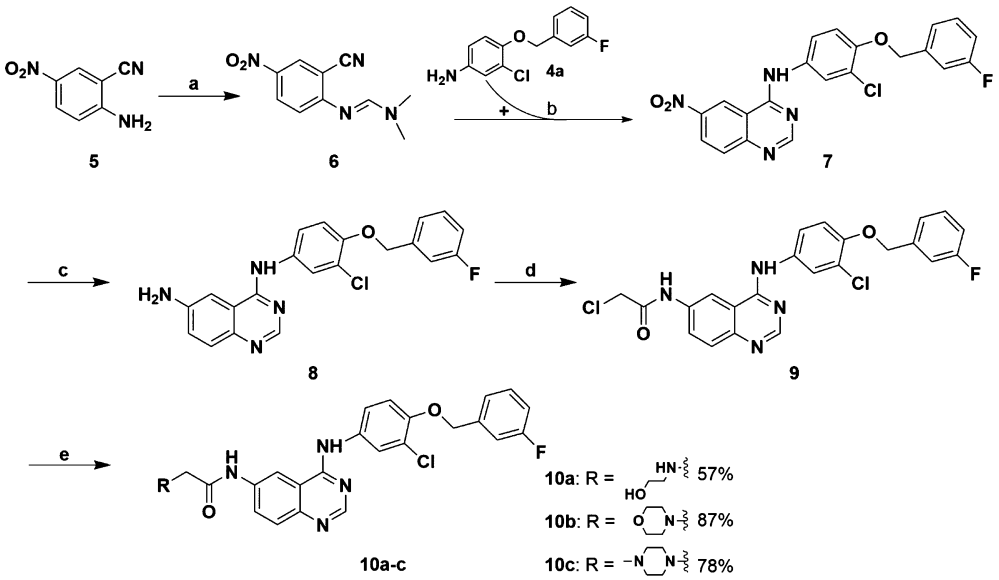

[a]Reagents and conditions: (a) DMF-DMA, reflux 2 h; (b) glacial HOAc, reflux, 3 h; (c) Fe, $CaCl_2$, EtOH, H_2O, 90 °C, 12 h; (d) $ClCH_2COCl$, $NaHCO_3$, acetone, 0 °C, under N_2, 1 h; (e) ethanolamine (5 equiv), MeOH, TEA, reflux, 4 h or appropriate secondary amine (50 equiv), reflux, 2 h.

chloro-4-(3-fluorobenzyl)oxy)phenyl)amino" moiety of lapatinib was replaced by phenoxy phenyl analogues that fit well into the back pocket of HER2. Optimization of HER2 inhibitory activity was conducted through replacing ethanolamine by morpholine, *N*-methyl piperazine, diethylamine, and dimethylamine at position 6 of the quinazoline scaffold to improve the pharmacokinetic properties. This hydrophilic tail was designed to fit into the ribose and phosphate region of the kinase ATP-binding site and improve the druggability. Different flexible spacers of acetamido, benzamido, and propoxy moieties were bridged between quinazoline and the hydrophilic tail. The flexibility of the used spacers is engendered by replacing the rigid 6-C−C bond in lapatinib by more flexible C−O or C−N bonds in the newly synthesized compounds, as shown in detail in Figure 4. The structural optimization was conducted using computer-aided drug design (CADD). A small library of 189 compounds (data are presented in the Supporting Information, Table S1) was designed by changing the substituents at position 4 and 6 of the quinazoline nucleus based on the literature database. At position 4, the lipophilic moiety was either substituted benzyloxy or phenoxy anilino moieties with the variables, including n = 0 or 1, X = H, Cl, or Br and R = o, m, or p CH_3, CF_3, CN, and F. At position 6, the flexible spacer was the acetamido, benzamido, or propoxy moiety and the hydrophilic terminal was the ethanolamino, morpholino, *N*-methyl piperazino, diethylamino, dimethylamino, methylsulfonylethylamino, immidazo, or pyrrolidino moiety. Then, the 3D structures of the developed compounds were energetically minimized to be explored as kinase inhibitors by docking into the crystal structure of HER2 kinase (PDB code: 3PP0),[48] in complex with its cocrystallized kinase inhibitor. The GOLD software package version 5.2.2 (Cambridge Crystallographic Data Centre, Cambridge, U.K.)[49] was used in this study, which is described in detail under the Molecular Docking part. The newly synthesized candidates were biologically evaluated in enzyme inhibitor-based assays and cell antiproliferative activity

https://dx.doi.org/10.1021/acs.jmedchem.0c01647
J. Med. Chem. XXXX, XXX, XXX−XXX

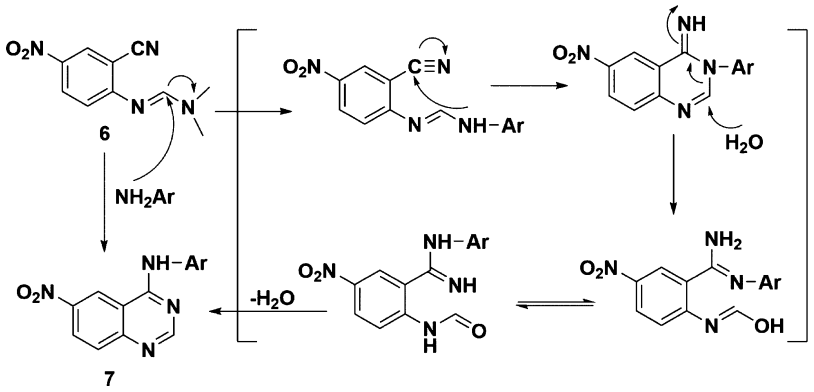

Figure 5. Proposed mechanism of Dimroth rearrangement for the preparation of 6-nitroquinazoline derivative (7).

Scheme 3. Synthesis of Target Compounds 15a–l and 17a–d[a]

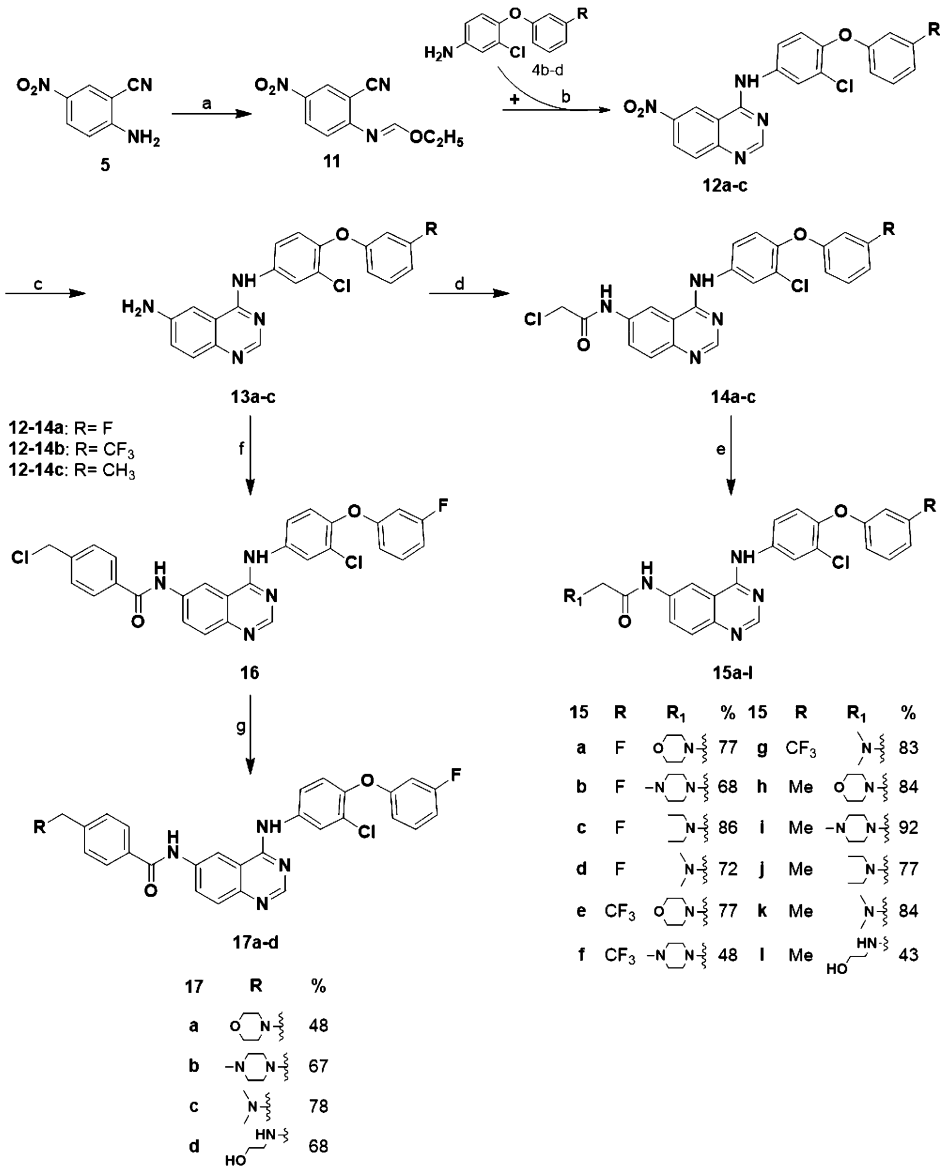

[a]Reagents and conditions: (a) triethylorthoformate, $(Ac)_2O$, reflux, 30 h; (b) glacial HOAc, reflux, 7 h; (c) $SnCl_2$, MeOH, reflux, under N_2, 1.5 h; (d) $ClCH_2COCl$, $NaHCO_3$, acetone, 0 °C, under N_2, 1 h; (e) appropriate secondary amine (50 equiv), reflux, 2 h or ethanolamine (5 equiv), MeOH, TEA, reflux, 4 h; (f) using **13a**, 4-(chloromethyl)benzoyl chloride, $NaHCO_3$, acetone, 0 °C, under N_2, 0.5 h; (g) excess appropriate secondary amine (50 equiv), reflux, 2 h or ethanolamine (5 equiv), MeOH, TEA, reflux, 4 h.

https://dx.doi.org/10.1021/acs.jmedchem.0c01647
J. Med. Chem. XXXX, XXX, XXX−XXX

ones. The following are the biological screening tests that had been carried out in the present work; *in vitro* protein kinase profiling was conducted to figure out the degree of selectivity obtained against the target HER2 using 20 different types of kinases, IC_{50} determination against wild and HER2 L755S mutant kinases, screening against National Cancer Institute-NCI 60 human cell panel, and the WST-8 antiproliferative assay using BT-474 and AU-565 BC cell lines (HER2+), as well as MCF7 and MDA-MB-231 BC cell lines (HER2−), were included. In addition, we also investigated the apoptotic inducing effect in BT-474 cells; western blot analysis was also established to study the effect of some selected candidates on inhibition of the HER2 downstream targets (ERK and AKT). *In vivo* antitumor efficacy and microsomal stability assay were also established for the most promising candidates.

Chemistry. In this part, we described the preparation of novel 6-substituted-4-anilinoquinazolines (**10a−c**, **15a−l**, **17a−d**, and **25a−h**) which were purified by flash column chromatography. The structures of the newly synthesized compounds were elucidated by different spectroscopic methods, including ^{1}H NMR, ^{13}C DEPT, ^{13}C NMR, and high-resolution mass spectrometry (HRMS).

The synthesis of the different substituted aniline derivatives (**4a−d**) is described in Scheme 1. Reaction of the commercially available 2-chloro-4-nitrophenol (**1a**) or 2-chloro-1-fluoro-4-nitrobenzene (**1b**) with 1-(bromomethyl)-3-fluorobenzene (**2a**) or the appropriate phenol derivative (**2b−d**) was carried out in dimethylformamide (DMF) or acetonitrile in the presence of potassium carbonate to afford the corresponding nitro derivatives (**3a−d**) in good yields of 73−89%.[50,51] Reduction of the nitro derivatives (**3a−d**) into their amino analogues (**4a−d**) were achieved by either heating with Fe/$CaCl_2$ in aqueous ethanolic solution to prepare (**4a**) intermediate or via reflux with $SnCl_2$ for 2.5 h in methanol under nitrogen to afford intermediates (**4b−d**). The reduction methods gave the desired intermediates in very good yields of 77−82%, in shorter reaction times, and with higher purity than the reported methods using H_2/Pt−C,[50,51] $SnCl_2$/EtOAc/reflux/24 h,[52,53] Na_2S/dioxane/70−80 °C/24 h (Zinin reaction),[54] or Fe/NH_4Cl/EtOH/reflux/2 h.[44] The ^{1}H NMR spectrum of **4c** revealed a broad signal at δ 5.42, exchanged with D_2O, representing the two protons of the NH_2 group. The impact of the acetamido linker at position 6 was investigated by applying Scheme 2, and the 3-chloro-4-((3-fluorobenzyl)oxy)aniline (**4a**) was incorporated into position 4 of the quinazoline nucleus through Dimroth rearrangement, as depicted in Scheme 2. The reaction of 2-amino-5-nitrobenzonitrile (**5**) with DMF-DMA (dimethylformamide-dimethylacetal) afforded the formimidamide intermediate (**6**) in a 90% yield, which was then cyclized upon reflux with compound **4a** in glacial acetic acid into 6-nitro-4-anilinoquinazoline derivative (**7**) through Dimroth rearrangement (Figure 5) as reported for similar derivatives.[55]

Reduction of (**7**) could be attained by a sodium dithionite/ammonia mixture or $SnCl_2$/methanol, but the yield was very low (30%) and the product requires purification by flash column chromatography. In the present study, reflux of iron in an alcoholic/aqueous solution of calcium chloride was implemented to efficiently afford a 6-amino-4-anilinoquinazoline derivative (**8**) in an excellent yield of 97% with high purity without further purification. Subsequently, compound **8** was acylated by 2-chloroacetyl chloride in acetone to afford the corresponding 2-chloroacetamido derivative (**9**) in 61% yield.

The target compounds **10a−c** were prepared through a nucleophilic substitution on the chloroacetamido moiety of compound **9** using ethanolamine or the appropriate cyclic secondary amines (morpholine and *N*-methyl piperazine) according to the procedure described in Scheme 2 to afford pure compounds in 57−87% yields. Compounds **10a−c** were confirmed by multiple spectroscopic data including their ^{1}H NMR spectra which exhibited two singlet signals at δ 5.25 and δ 3.19−3.35 for benzyloxy CH_2 protons and acetamido CH_2 protons, respectively. Besides, a quartet signal at δ 3.54−3.49 and a triplet signal at δ 2.69−2.66 were representing the four protons of the ethanolamine terminal in the target compound (**10a**), and two triplet signals at δ 2.55−3.69 were detected for the eight protons of the morpholino ring in compound (**10b**). Another two broad singlet signals at δ 2.41−2.57 were assigned for the eight protons of the piperazino ring in compound (**10c**). An additional panel of novel target compounds (**15a−l** and **17a−d**) was prepared to study the structure−activity relationship (SAR) and to enhance the selectivity, as shown in Scheme 3. The lapatinib anilino moiety at position 4, namely, 3-chloro-4-((3-fluorobenzyl)oxy) aniline in Scheme 2, was replaced by substituted phenoxyaniline fragments to enhance the selectivity against HER2 kinase, whereas the 6-acetamido linker was kept in compounds (**15a−l**) or replaced by a bulkier 6-methyl benzamido linker in compounds (**17a−d**). Reaction of 2-amino-5-nitrobenzonitrile (**5**) with triethylorthoformate in the presence of acetic anhydride produced the formimidate derivative (**11**), which was then cyclized upon reflux with the appropriately substituted phenoxyaniline (**4b−d**) to afford 6-nitro-4-anilinoquinazoline derivatives (**12a−c**) through Dimroth rearrangement. It was noteworthy that reduction of the 6-nitro-quinazolione derivatives (**12a−c**) to the corresponding 6-amino analogues (**13a−c**) was adequately accomplished using $SnCl_2$/MeOH, where they were obtained within short reaction time (1.5 h), in high purities and excellent yields (86−94%). In comparison, the other reported conditions using iron/$CaCl_2$/EtOH afforded these compounds within a longer reaction time (12 h) and in inferior purities and lower yields (52−65%). Also, a longer reaction time (24 h) is needed on using Na_2S/dioxane.

Compounds (**13a−c**) were subsequently acylated with 2-chloroacetyl chloride in acetone to yield the corresponding 2-chloroacetamido derivatives (**14a−c**), while compound (**16**) was prepared by acylation of intermediate (**13a**) with 4-(chloromethyl)benzoyl chloride to afford the corresponding 4-(chloromethyl)benzamido derivative (**16**). Two series of the target compounds (**15a−l**, 43−92% yields) and (**17a−d**, 48−78% yields) were synthesized through nucleophilic substitution of compounds (**14a−c**) and (**16**), respectively, with the appropriate secondary amines or ethanolamine, as described in Scheme 3. Partial hydrolysis was detected in compounds (**17a−d**) bearing a benzamido linker to their corresponding 6-amino quinazoline analogues as a result of the nucleophilic attack of the reacting amines on the reactive carbonyl group of the benzamido moiety. Therefore, the hydrolytic products were removed by flash column chromatography to get the target compounds in a pure form. Compounds (**15a−l**) were confirmed by ^{1}H NMR spectra exhibiting a singlet signal at δ 3.15−3.38 for the acetamido CH_2 protons, in addition to, ^{13}C DEPT revealed an inverted signal at δ 53.17−63.69, representing the acetamido CH_2 carbon. On the other hand, ^{1}H NMR spectra of (**17a−d**) revealed the characteristic AB doublet spin system signals of the phenylene residue at δ 7.46−

https://dx.doi.org/10.1021/acs.jmedchem.0c01647
J. Med. Chem. XXXX, XXX, XXX−XXX

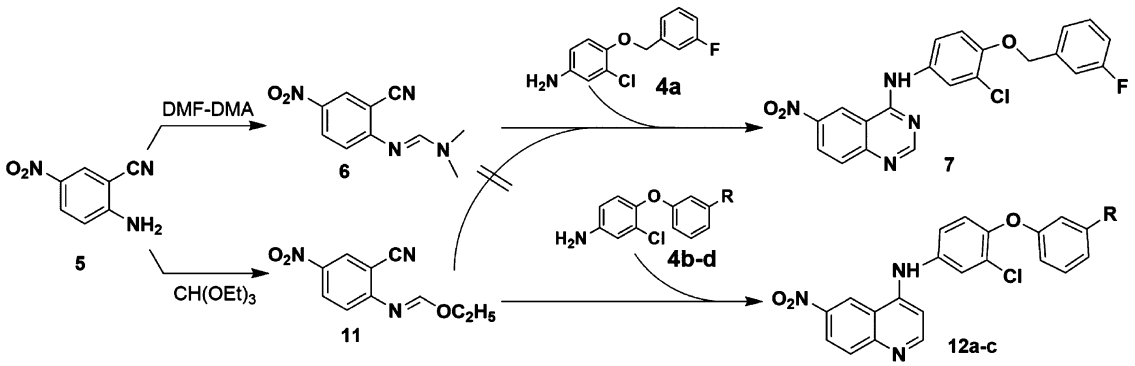

Figure 6. Two pathways conducted for the preparation of 6-nitroquinazoline derivatives.

Scheme 4. Synthesis of the Target Compounds 25a–h[a]

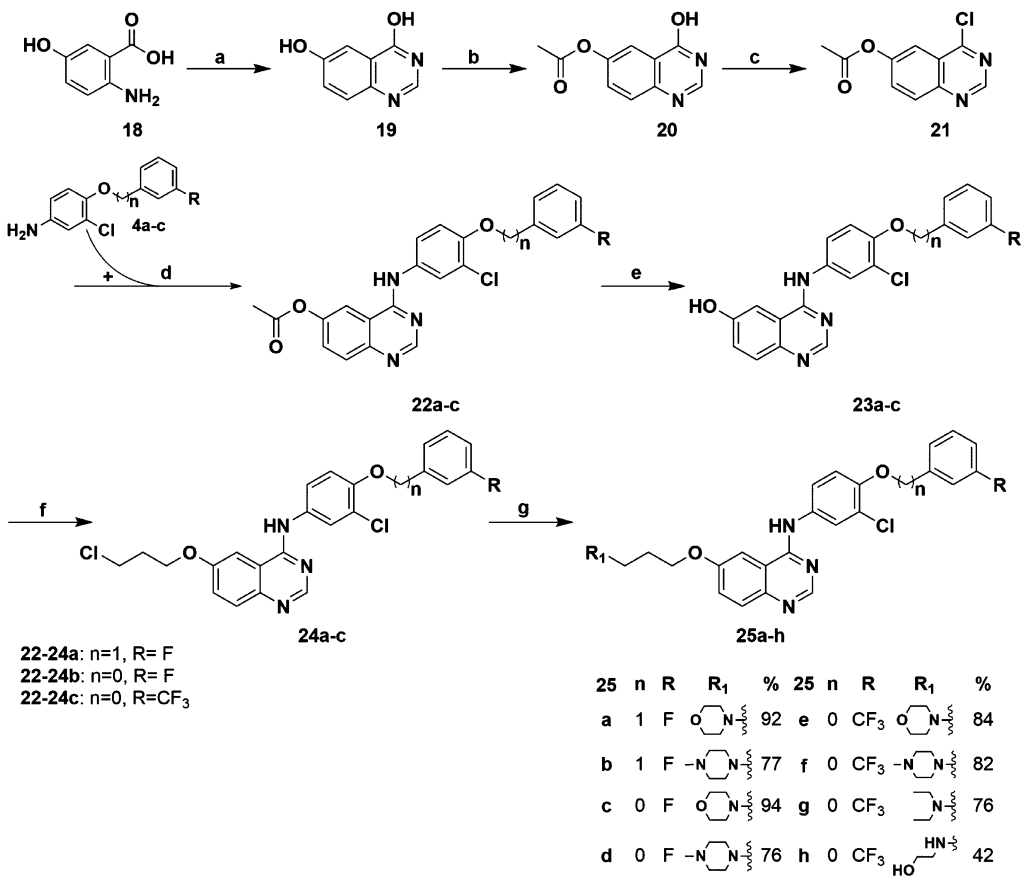

25	n	R	R1	%	25	n	R	R1	%
a	1	F		92	e	0	CF_3		84
b	1	F		77	f	0	CF_3		82
c	0	F		94	g	0	CF_3		76
d	0	F		76	h	0	CF_3		42

[a]Reagents and conditions: (a) NH_2CHO, 190 °C, 1 h; (b) AC_2O, pyridine, 100 °C, 2 h; (c) $SOCl_2$, DMF, 95 °C, 5 h; (d) acetonitrile, K_2CO_3, rt, 8 h (with **4a**); acetonitrile, K_2CO_3, reflux, 12 h (with **4b** or **4c**); (e) NH_4OH, MeOH, rt, 2 h, (f) $Cl(CH_2)_3Br$, K_2CO_3, TBAB, acetonitrile, reflux, 2 h; (g) appropriate amine (100 equiv), reflux, 2 h or ethanolamine (10 equiv), MeOH, TEA, reflux, 8 h.

8.03 and a characteristic ^{13}C DEPT inverted signal for benzyl CH_2 at δ 52.97–63.42.

It is noteworthy that the success of Dimroth rearrangement for the preparation of 6-nitroquinazoline derivatives (**7**) and (**12a–c**) depends on the used precursors of formimidamide (**6**) or the formimidate (**11**), as shown in Schemes 2 and 3, respectively. We have observed that intermediate (**6**) could be used properly to afford the desired 6-nitroquinazoline derivatives (**7**) and (**12a–c**). However, the intermediate (**11**) was not the appropriate precursor for the preparation of 6-nitroquinazoline derivative (**7**), as shown in Figure 6.

The synthesis of 4-substituted phenoxy/benzyloxy anilino quinazolin-6-ol and their 6-substituted propoxy analogues (**25a–h**) is depicted in detail in Scheme 4. The quinazoline-4,6-diol (**19**) was prepared using the Niementowski synthesis,[56] by heating the commercially available 5-hydroxy anthranilic acid (**18**) in formamide.

The ^1H NMR spectrum of (**19**) showed a characteristic singlet signal of the C-2 proton of the quinazoline nucleus at δ 7.90, whereas the two OH protons were detected at δ 10.05 and 12.02. In addition, the melting point was consistent with the reported one.[57,58] The phenolic OH at the C-6 position of (**19**) was selectively protected by acetylation via heating with

https://dx.doi.org/10.1021/acs.jmedchem.0c01647
J. Med. Chem. XXXX, XXX, XXX–XXX

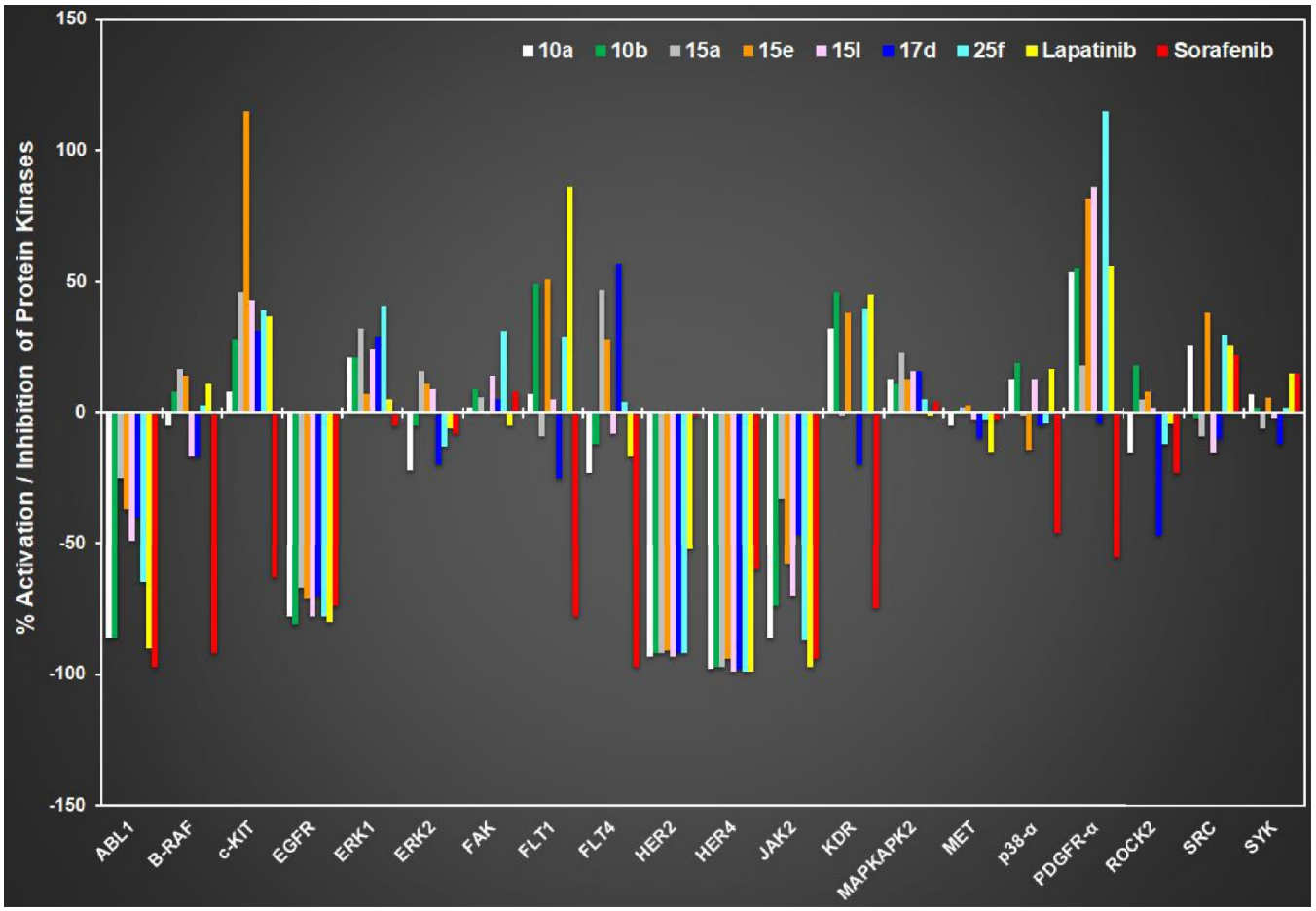

	ABL1	B-RAF	c-KIT	EGFR	ERK1	ERK2	FAK	FLT1	FLT4	HER2	HER4	JAK2	KDR	MAPKAPK2	c-MET	p38-α	PDGFR-α	ROCK2	SRC	SYK
10a	**-86**	-5	8	**-78**	21	-22	2	7	-23	**-93**	**-98**	**-86**	32	13	-5	13	54	-15	26	7
10b	**-86**	8	28	**-81**	21	-5	9	49	-12	**-92**	**-97**	**-74**	46	11	1	19	55	18	-2	2
15a	**-25**	17	46	**-67**	32	16	6	-9	47	**-92**	**-97**	**-33**	-1	23	2	-1	18	5	-9	-6
15e	**-37**	14	115	**-71**	7	11	0	51	28	**-91**	**-94**	**-58**	38	13	3	-14	82	8	38	6
15l	**-49**	-17	43	**-78**	24	9	14	5	-8	**-93**	**-99**	**-70**	0	16	-3	13	86	2	-15	-2
17d	**-40**	-17	31	**-70**	29	-20	5	-25	57	**-92**	**-98**	**-47**	-20	16	-10	-5	-4	**-47**	-10	-12
25f	**-65**	3	39	**-78**	41	-13	31	29	4	**-92**	**-99**	**-87**	40	5	-3	-4	115	-12	30	2
Lapatinib	**-90**	11	37	**-80**	5	-6	-5	86	-17	**-52**	**-99**	**-97**	45	-1	-15	17	56	-4	26	15
Sorafenib	**-97**	**-92**	**-63**	**-74**	-5	-8	8	**-78**	**-97**	-1	**-60**	**-94**	**-75**	4	-3	**-46**	**-55**	-23	22	15

Figure 7. Protein kinase profiling for compounds (**10a**, **10b**, **15a**, **15e**, **15l**, **17d**, and **25f**) at 10 μM single dose concentration, represented by % activity or % inhibition, against a panel of 20 kinases in comparison with two reference compounds lapatinib and sorafenib using the [γ-^{32}P]ATP radiometric assay method. (−) values: inhibition of target activity; (+) values: activation of target activity; >−25% changes in activity compared to the control were considered to be significant inhibition.

acetic anhydride at 100 °C for 2 h in the presence of pyridine as a basic catalyst to afford 4-hydroxy-6-quinazolinyl acetate (**20**).[57] The ^{1}H NMR spectrum of compound (**20**) exhibited a singlet signal at δ 2.31 attributed to the three protons of the CH_3 group accompanied by the disappearance of the C-6 phenolic OH signal at δ 10.05. Chlorination of (**20**) was carried out by heating with thionyl chloride.[57,59] The freshly prepared 4-chloro derivative (**21**) was unstable; therefore, it was immediately coupled with the appropriate aniline derivative (**4a**−**c**) by long-term reflux in isopropanol, in the presence of trimethylamine (TEA),[44,57] or in *N*-methyl pyrrolidinone.[42] However, using the reported methods, the desired compounds (**22a**−**c**) were obtained in very low yields (20−42%) with multispot side products. Thus, we significantly optimized the coupling reaction using acetonitrile/K_2CO_3, either at room temperature (for **22a**) or under reflux (for **22b**,**c**), to afford the desired intermediates in good purity and with higher yields (60−90%). The melting point of compound **22a** was consistent with the reported one (290−292 °C).[57] Compounds **22b** and **22c** were confirmed by their ^{1}H NMR spectral data with the appearance of the signals of eleven aromatic protons at δ 6.74−8.69. Hydrolysis of the acetylated intermediates (**22a**−**c**) to the corresponding quinazolin-6-ol derivatives (**23a**−**c**) was conducted using aqueous ammonia in methanol (1:3) at room temperature up to 12 h. The melting point of the compound (**23a**) was consistent with the reported one (>300 °C).[57] The new compounds (**23b** and **23c**) were confirmed by their ^{1}H NMR spectra showing a singlet exchangeable signal at δ 10.14 of the 6-OH proton with a concurrent disappearance of the singlet signal at δ 2.38 and the ^{13}C DEPT signal at δ 21.21−21.22 of the CH_3 group. Alkylation of compounds (**23a**−**c**) was carried out by reflux with 1-bromo-3-chloropropane in the presence of K_2CO_3 and a

https://dx.doi.org/10.1021/acs.jmedchem.0c01647
J. Med. Chem. XXXX, XXX, XXX−XXX

catalytic amount of tetrabutylammonium bromide (TBAB).[57,60]

The new compounds (**24b** and **24c**) were elucidated spectroscopically through the appearance of two triplets at δ 4.26−4.28 and δ 3.85 and one pentet at δ 2.25 corresponding to the six protons of the chloropropoxy moiety, along with the disappearance of a singlet signal at δ 10.14 of the 6-OH proton. In addition, their ^{13}C DEPT spectra revealed three inverted signals at δ 32.13−32.15, δ 42.43−42.46, and δ 65.59−65.61 which represent three CH_2 groups of the chloropropoxy moiety. The target compounds (**25a−g**) could be prepared through nucleophilic substitutions on (**24a−c**) with the appropriate secondary amines in dry acetonitrile, by heating under reflux in the presence of anhydrous K_2CO_3 a catalytic amount of potassium iodide.[61] In the current study, the target compounds (**25a−g**) were synthesized by refluxing the mixture of compounds (**24a−c**) with 100 equiv of appropriate secondary amine, including *N*-methyl piperazine, morpholine, and diethylamine. Compounds (**25a−g**) were afforded in excellent yields (76−94%) and high purity. On the other hand, because of the high nucleophilic reactivity of ethanolamine, compound **25h** could not be prepared under the same reaction condition adopted for (**25a−g**), where multispot degradation byproducts were obtained. Therefore, compound **25h** was prepared by heating under reflux a mixture of intermediate **24c** and excess ethanolamine (10 equiv) in MeOH, rather than the solvent-free reaction, in the presence of a catalytic amount of TEA to afford compound (**25h**) with 42% yield. ^{1}H NMR spectra of compounds **25a** and **25b** exhibited singlet signals at δ 5.14 and δ 5.25, respectively, for their characteristic benzylic protons ($OCH_2C_6H_4F$) with a concurrent appearance of two broad singlets at δ 2.48 and δ 3.74 for the eight protons of the morpholino moiety or at δ 2.30 and δ 2.38 for the eight protons of the piperazino moiety, respectively. In addition, the six protons of the propoxy linker were detected as two triplets and one pentet at δ 1.90−4.18. Moreover, ^{13}C DEPT spectra revealed six signals for the CH_2 groups, whereas compounds **25c−h** (missing benzylic protons) were confirmed by their aliphatic signals of the corresponding secondary or primary amines.

***In Vitro* Protein Kinase Inhibition Assay.** The protein kinase profiles of seven compounds (**10a**, **10b**, **15a**, **15e**, **15l**, **17d**, and **25f**) against a panel of 20 protein kinases using the [γ-^{32}P]ATP radiometric assay method were evaluated by Kinexus Bioinformatics Corporation, Vancouver, British Columbia, Canada. Two reference kinase inhibitors on the phosphotransferase activity were used including lapatinib (EGFR and HER2 dual selective TKI) and sorafenib (nonselective potent multikinase inhibitor). This assay was performed at 10 μM concentration in a single measurement by employing the standardized assay methodology outlined in the Experimental Section part.

Rationale for Selection of the 20 Kinase Panels. The EGFR (HER1), HER2, and HER4 kinases were selected as the most common targets in therapy of aggressive BC. ABL kinase was selected as an antitarget kinase in BC which was reported to negatively modulate HER2+ BC progression *in vivo*.[62,63] Meanwhile, BRAF, ERK1, and ERK2 kinases were picked out, being a downstream signal transducer in the EGFR family. The SRC activity was reported to be the main mode of resistance to Herceptin as the first-line therapy for HER2+ BC.[64] The FAK is overexpressed and activated in several advanced-stage solid cancers including multidrug-resistance BC.[65,66] JAK2 was selected because the JAK2-STAT3 signaling pathway is known as a crucial signaling pathway for regulating cancer progression and metastasis.[67] C-kit, c-Met, FLT1,4, KDR, and PDGFRα kinases are involved in angiogenesis and were reported as effective targets in the treatment of solid cancers. MAPKAPK2, ROCK2, and p38α kinases were used as examples of different target serine/threonine kinases to explore selectivity to our target tyrosine kinase.

Selection Criteria for the Test Compounds for Kinase Profiling. Seven compounds were screened for kinase profiling including the lead compound (**10a**) and its morpholino analogue (**10b**). Other different compounds bearing an acetamido spacer with a 4-phenoxyaniline moiety (**15a**, **15e**, and **15l**), compound **17d** bearing a benzamido spacer and a 4-phenoxyaniline moiety, and compound **25f** with a propoxy spacer and a 4-phenoxyaniline moiety. The selected candidates are representative of the optimized analogues of the lead compound (**10a**; generated by CADD).

Throughout this study, the inhibition of target activity by the compound was given negative (−) values while activation of target activity was given positive (+) values, and only >25% changes in activity compared to the control were considered to be significant. Six out of 20 kinases tested by compound **17d** exhibited moderate-to-high inhibition scores ranging from −40 to −98% including HER4 (−98%), HER2 (−92%), EGFR (HER1) (−70%), ROCK2 (−47%), JAK2 (−47%), and ABL1 (−40%), whereas two kinases showed an activation, including c-Kit (31%) and FLT4 (57%), as shown in Figure 7.

For compound **15a**, four kinases revealed moderate-to-high inhibition scores ranging from −33 to −97% including HER4 (−97%), HER2 (−92%), EGFR (−67%), and JAK2 (−33%). Similar to **17d**, c-Kit (46%) and FLT4 (47%) were moderately activated in the presence of the compound **15a** as well as ERK1 (32%). In the presence of **15e**, five kinases were inhibited ranging from −37 to −94% including HER4 (−94%), HER2 (−91%), EGFR (−71%), JAK2 (−58%), and ABL1 (−37%). The other five kinases were activated, including KDR (38%), SRC (38%), FLT1 (51%), PDGFR alpha (82%), and c-Kit (115%). Compound **15l** inhibited five kinases from moderate-to-high level ranging from −49 to −99% inhibition, including HER4 (−99%), HER2 (−93%), EGFR (−78%), JAK2 (−70%), and ABL1 (−49%), while two kinases were activated, including c-Kit (43%) and PDGFR-α (86%). Testing of compound **25f** revealed moderate-to-high inhibitions ranging from −65 to −98% against 5 kinases including HER4 (−99%), HER2 (−92%), JAK2 (−87%), EGFR (−65%), and ALB1 (−65%), with activations noted with c-Kit (39%), KDR (40%), ERK1 (41%), and PDGFR-α (115%). Compound **10a** exhibited high inhibition against HER4 (−98%), HER2 (−93%), ABL1 (−86%), JAK2 (−86%), and EGFR (−78%), whereas it activated KDR (32%) and PDGFR-α (54%). Similarly, compound **10b** showed high inhibition of HER4 (−97%), HER2 (−92%), ABL1 (−86%), EGFR (−81%), and JAK2 (−74%) and moderate activation toward KDR (46%), FLT1 (49%), and PDGFR-α (55%). Regarding the reference compounds used in this study, sorafenib as a potent nonselective multikinase inhibitor was tested at 10 μM against the same panel of 20 protein kinases. It showed strong inhibitions against ABL1 (−97%), FLT4 (−97%), JAK2 (−94%), and B-RAF (−92%), whereas it revealed moderate inhibitions against FLT1 (−78%), EGFR (−74%), c-Kit (−63%), HER4 (−60%), PDGFR-α (−55%), and P38-α (−46%). Lapatinib was used as a selective dual kinase

https://dx.doi.org/10.1021/acs.jmedchem.0c01647
J. Med. Chem. XXXX, XXX, XXX−XXX

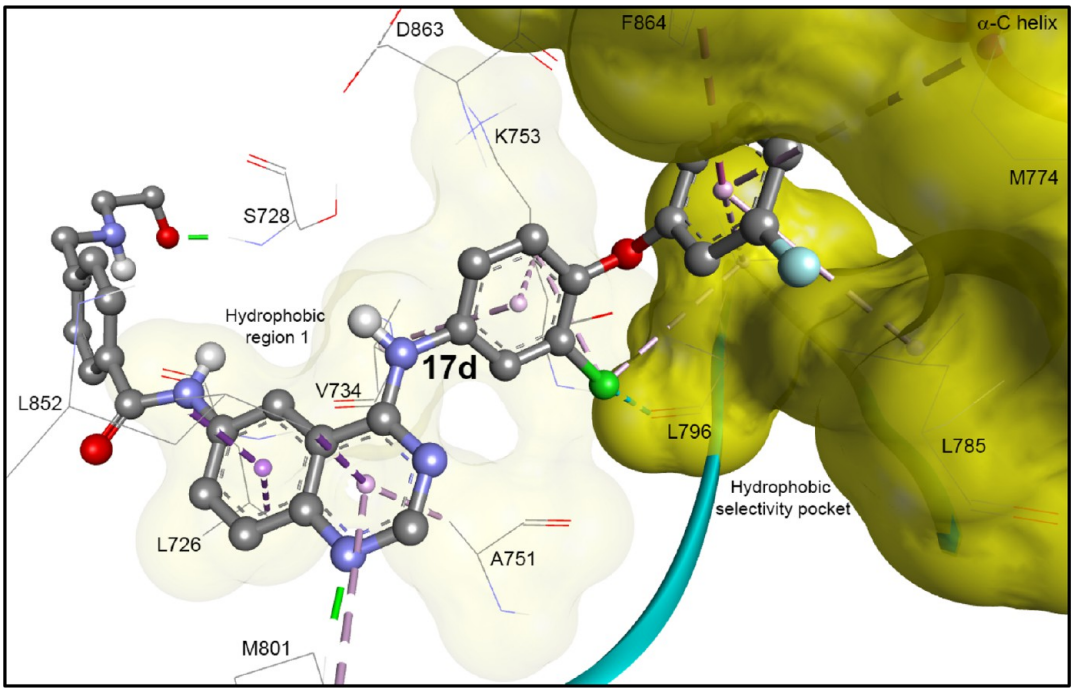

Figure 8. Docking of compound **17d** (ball and stick, colored by element) into human HER2 kinase (PDB code: 3PP0) within an rmsd of 3.1 Å from the native cocrystallized ligand (03Q). It exhibited two hydrogen bonds (green-dotted lines) with M801 and S728 in addition to multiple hydrophobic interactions. The color codes are hydrophobic (π−alkyl and alkyl−alkyl): ---; hydrophobic (π−π): ---; hydrophobic (π−σ): ---; halogen acceptor bonding: --- *m*-chloro atom interacts hydrophobically by a halogen acceptor with L796 and K753 residues.

inhibitor, which interrupts the HER2/neu and EGFR pathways. Five out of 20 tested kinases were moderately to strongly inhibited including HER4 (−99%), JAK2 (−97%), ABL1 (−90%), EGFR (−80%), and HER2 (−52%), while c-Kit, FLT1, KDR, and PDGFR-α kinases were moderately to highly activated within 37−86%, and these activations increase the possibility that in some cancer patients, lapatinib could in principle exacerbate their cancer.

The abovementioned results indicated that our newly synthesized compounds revealed a significant selective inhibition against HER2 and HER4 kinases within −92 to −99% and to a moderate extent against the subfamily closely related to RTK EGFR (HER1) within −67 to −81%. These results highly support our design for selective HER2 kinase inhibitors for the treatment of aggressive BC. Furthermore, the test compounds exhibited moderate-to-substantial kinase inhibitory effects against ABL1 and JAK2 kinases within −25 to −86% and −33 to −87%, respectively. In comparison with lapatinib as a dual EGFR/HER2 kinase inhibitor, compounds **10a**, **15a**, and **17d** and to a lower extent **10b** are considered as more safe compounds in activating c-KIT, FLT1, KDR, and PDGFR-α kinases. Various studies reported that PDGFR expression (including PDGFR-α and β and both show similar kind of functions) is associated with poor prognosis of BC patients via activating of Stat3 to support BC initiation and progression.[68−71] Accordingly and in comparison with lapatinib (activating PDGFR-α by 56%), compounds **15a** and **17d** (affecting PDGFR-α by 18% and −4, respectively) are considered as the safest and potent compounds for the treatment of aggressive HER2+ BC.

The potent inhibitory activity of compound **17d** against HER2 kinase (−92%) is highly correlated with its robust binding affinity into human HER2 kinase (PDB code: 3PP0) with a GoldScore fitness of 92.63 compared to 84.59 for the native bound ligand. Compound **17d** was docked into HER2 kinase by two hydrogen bonds between its quinazoline-N^{1}H and terminal ethanolamine-OH and NH moiety of M801 and NH of S728 amino acids, respectively. Besides, hydrophobic interaction plays a crucial role in the binding of compound **17d** into the intensively hydrophobic HER2 kinase domain, where its planar quinazoline ring interacts hydrophobically with L726, L852, Ala751, and M801 by π−σ and π−alkyl interactions, as clearly depicted in Figure 8. Moreover, its *m*-chloro-6-aniline moiety interacts comprehensively by π−alkyl interactions with the V734 and K753 bond, whereas the *m*-chloro atom interacts hydrophobically by the halogen acceptor with L796 and K753 residues. Noticeably, the terminal phenoxy moiety was deeply harbored into the hydrophobic HER2 selectivity pocket through four π−π and π−alkyl interactions with F864, M774, L785, and L796. Accordingly, compound **17d** demonstrated a GoldScore (external vdw) of 62.94.

***In Vitro* HER2 Kinase Inhibitory Activity (IC_{50}) against Wild and L755S Mutant Kinases.** The ADP-Glo Assay method was performed for kinase profiling of five compounds (**10a**, **10c**, **15i**, **17d**, and **25b**) to evaluate their IC_{50} using concentrations 0.5 nM to 25.0 μM. Two protein kinases (HER2 wild-type and HER2 L755S mutant) were used in a single measurement. Lapatinib was used as a positive control at the same used concentrations.

In Vitro HER2 Kinase Inhibitory Activity against Wild Type. Compounds **10c**, **15i**, **17d**, and **25b** revealed the most potent activities against HER2+ BC cell lines (BT474 and AU565; IC_{50}: 0.08−0.20 μM), in comparison with the lead compound **10a** (IC_{50}: 0.22−0.24 μM), respectively.

Out of these compounds, **15i**, **17d**, and **25b** were further selected by NCI for 5-dose assay against NCI60 cancer cell lines. Therefore, these compounds were selected for further evaluation of their IC_{50} against wild-type HER2 kinase. At the

https://dx.doi.org/10.1021/acs.jmedchem.0c01647
J. Med. Chem. XXXX, XXX, XXX−XXX

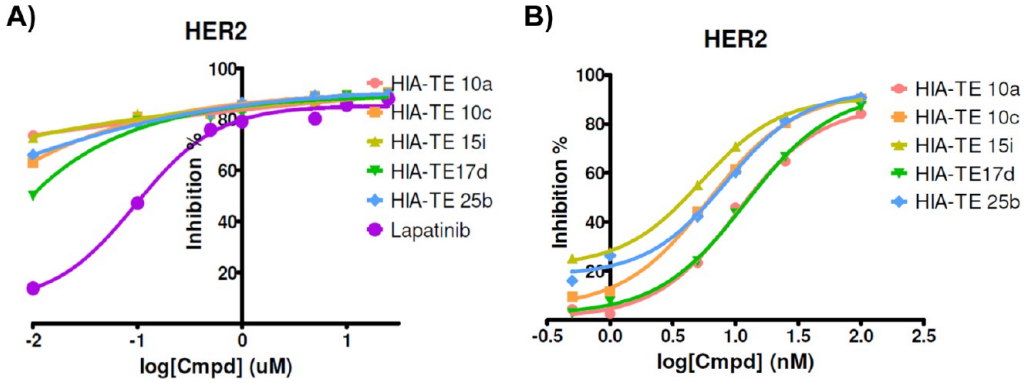

Figure 9. % IC_{50} graph and calculations for the five compounds (**10a**, **10c**, **15i**, **17d**, and **25b**) and lapatinib tested against HER2 wild-type kinase using the ADP-Glo assay method at (A) concentrations 0.01−25.0 μM and (B) concentrations 0.5−100 nM.

initially used concentrations (0.01−25 μM), all the test compounds exhibited high inhibitions (50−91%) greater than lapatinib (14−88%; IC_{50} = 95.5 nM) against HER2 wild-type kinase, as shown in Figure 9A. Therefore, concentrations of 0.5−100 nM were further used to calculate the IC_{50} of the test compounds. At 100 nM, compound **25b** revealed the highest inhibition (91%) and at 0.5 nM, all the compounds exhibited inhibition of HER2 wild-type kinase at 3−25%, as shown in Figure 9B. All five test compounds (**10a**, **10c**, **15i**, **17d**, and **25b**) have IC_{50} scores ranging from 5.4 to 12.0 nM. In all cases, IC_{50} values for the test compounds were far lower than the IC_{50} value for lapatinib 95.5 nM, as listed in Table 1.

Table 1. IC_{50} of Compounds 10a, 10c, 15i, 17d, and 25b in Comparison with Lapatinib Tested against HER2 Wild-Type Kinase at Concentrations Ranging from 0.5 nM to 25 μM Using the ADP-Glo Assay Method

	IC_{50} (nM)	95% confidence intervals	SEM (nM)	R^2	DOF
10a	10.4	5.512−19.430	±1.159	0.9958	5
10c	6.1	4.679−7.969	±1.064	0.9993	5
15i	5.4	4.291−6.666	±1.052	0.9995	5
17d	12.0	8.412−17.114	±1.085	0.9989	5
25b	8.3	3.757−18.404	±1.202	0.9922	5
lapatinib	95.5	43.97−207.40	±1.276	0.9939	5

In Vitro HER2 Kinase Inhibitory Activity against L755S Mutant Type. HER2 pathway reactivation by the HER2/L755S mutation was found to be the common somatic mutation which constitutes a mechanism of acquired resistance to lapatinib-containing HER2-targeted therapies in preclinical HER2+ BC models.[72] The most frequently altered codon in HER2 exon 19 that encodes the tyrosine kinase intracellular domain was L755 (10 mutations, L755S);[73] therefore, the kinase domain mutant HER2 L755S was used in this study in which HER2 is mutated in 14.05% of breast carcinoma patients with ERBB2 L755S present in 0.74% of all breast carcinoma patients,[74,75] as depicted in Figure 10. However, none of the compounds showed a strong inhibition with the HER2-L755S mutant kinase, and the inhibitions ranged from 12% at the lowest concentration of 0.1 μM of the test compounds up to the highest inhibition of 39% at a concentration of 25 μM (Table 2). The lapatinib followed the same pattern of inhibition as the test compounds. According to these results, there were no IC_{50} values determined for the compounds tested with HER2 L755S mutant kinase as the highest inhibition score was only 39%.

It is known that the L755S mutation correlates with activated HER2 signaling and transformation, but this may require complementary mutations.[76] It has also been previously reported that HER2 T733I and L755S mutations are associated with resistance to inhibition by lapatinib *in vitro*.[77−79]

Antiproliferative Activity Assay. The antiproliferative activity of the newly synthesized compounds was conducted by WST-8 assay against a panel of four different HER2-expressing BC cell lines. The selected panel has different genetic backgrounds including wild-type luminal AU565 cell line with abnormally high expressing HER2,[80] TPBC (HER2+/ER+/PR+) BT474 cells, estrogen and progesterone receptor-positive (ER+/PR+) MCF7 cells, and triple-negative (MDA-MB-231) cells. These four BC cell lines represent two different genetic backgrounds of tumor suppressor p53, including AU565/p53 wild type (wt), BT474/p53 mutant (mt), MCF-7/p53 (wt), and MDA-MB-231/p53 (mt). Phenotyping and molecular features of the cell lines used in our study are listed in Table 3.

Lapatinib is an FDA-approved dual EGFR/HER2 TKI for the treatment of HER2+ metastatic BC was used as a positive control.

Our compounds revealed statistically significant selective and potent antiproliferative activities against HER2+ BC cells (AU565 and BT474) of mean ± SEM (0.295 ± 0.03207 μM) compared to HER2− BC cells (MCF7 and MDA-MB-231) of mean ± SEM (5.817 ± 0.9121 μM). Notably, all the synthesized compounds were tested against human metastatic high expressing HER2 BC cells (AU565) and revealed potent antiproliferative activities with an IC_{50} of 0.099−0.923 μM range. Compounds **10b**, **15h**, **15i**, **15k**, **25a**, and **25b** are highly potent with IC_{50} less than 0.2 μM, as shown in Table 4. Remarkably, compound **25b** (IC_{50} = 0.099) showed the most potent activity and most comparable one to lapatinib (IC_{50} = 0.064 μM). To a lower extent, 75% of other compounds exhibited antiproliferative activity less than 0.5 μM in the range of 0.205−0.456 μM against the same cell line.

These results indicate that our designed compounds significantly target HER2 kinase, which is highly expressed in AU565 BC cells. Interestingly, 23 out of 27 (85%) of the designed compounds showed an improved IC_{50} of 0.081−0.540 μM against triple-positive BT474 BC cells with more potency than HER2 BC cells (AU565). These results also

https://dx.doi.org/10.1021/acs.jmedchem.0c01647
J. Med. Chem. XXXX, XXX, XXX−XXX

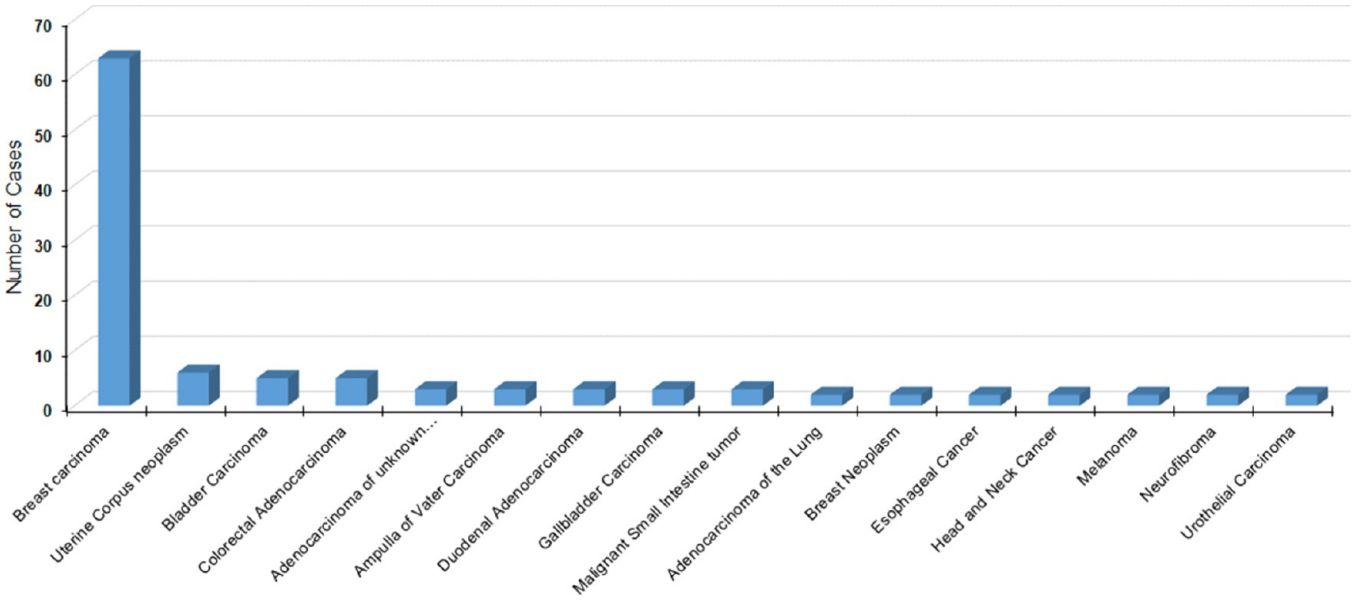

Figure 10. Top disease cases with HER2 L755S (data retrieved from refs 66 and 67).

Table 2. % Activity Change in Compounds 10c, 15i, 17d, and 25b in Comparison with Lapatinib Tested against HER2 L755S Mutant Kinase at Concentrations Ranging from 0.1 to 25 μM Using the ADP-Glo Assay Method

	0.1 μM	0.5 μM	1.0 μM	5.0 μM	10 μM	25 μM
10c	−16	−21	−26	−29	−32	−33
15i	−12	−20	−20	−24	−33	−28
17d	−15	−19	−20	−22	−27	−29
25b	−12	−19	−22	−25	−31	−39
lapatinib	−14	−18	−23	−31	−35	−37

indicate that the quinazoline derivatives selectively target HER2 kinase in addition to other oncologic pathways, which have been investigated and discussed under apoptosis assay and western blotting. Noticeably, multitargeting of the triple-positive BT474 BC cell was detected by 85% of the tested compounds. This augmented effect was noticed to a higher extent for compounds **15d**, **15l**, **17a**, **25d**, **25f**, and **25h** up to 6 times antiproliferative activity compared to their IC_{50} toward AU565 BC cells (HER2+), whereas compounds **10b,c**, **15a−c**, **15e,f,h,i,k**, **17b−d**, **25a−c**, **25e**, and **25g** exhibited a lower boost (up to 2.0 times) of antiproliferative activity by targeting other receptors/pathways. Likewise to their effects against AU565 cells, compounds **10b−c**, **15d,h,i,k,l**, and **25a,b,f** exhibited high antiproliferative activity toward BT474 cells with $IC_{50} \leq 0.2$ μM, as depicted in Figure 11. Strikingly, compounds **15h**, **15i**, **25a**, and **25b** revealed the most potent and comparable activities to lapatinib with an IC_{50} of 0.091, 0.081, 0.081, and 0.083 μM, respectively. The potent antiproliferative activity of compound **25b** against HER2+ BC cells is a reflection of its high binding affinity (GoldScore fitness 90.70) into human HER2 kinase compared to 84.59 for the native bound ligand. Compound **25b** was docked proximately superimposed on the native cocrystallized 03Q ligand within a root-mean-square deviation (rmsd) of 1.1 Å. It bound to the binding site of the titled kinase by one hydrogen bond between its quinazoline-N^1H and HN moiety of M801 as a key amino acid, as shown in Figure 12. Despite compounds **15h**, **15i**, **25a**, and **25b** that showed the lowest IC_{50}, compound **15d** displayed the highest augmentation of antiproliferative activity by targeting triple-positive BT474 BC cells (IC_{50} = 0.107 μM) of ∼6.0 times more potency than AU565 (0.663 μM). The antiproliferative activities of the tested compounds were noticeably diminished using other BC cells lacking HER2 kinase such as estrogen and progesterone receptor-positive (ER+/PR+) MCF7 cells and triple-negative (MDA-MB-231) cells (IC_{50} ranges from 0.321 to 18.119 and 0.737 to 30.162 μM, respectively). In contrast, the IC_{50} ranges of the HER2+ BC cells (AU565 and BT474) are from 0.099 to 0.923 and 0.081 to 0.540 μM, respectively. This means that MCF7 and MDA-MB-231 cells are less sensitive to the inhibitory effects of the tested compounds than the BC cells harboring HER2 kinase. Nevertheless, the majority (74−89%) of our designed quinazoline derivatives exhibited superior

Table 3. Characterization, Molecular Information, Culture Conditions, and Clinical Features for the Four BC Cell Lines Used in Our Study; the Information was Retrieved from Ref 73[a80]

cell line	HER2	ER	PR	P53	origin	subtype	tumor	culture medium	references
AU565	+	−	−	NA	metastasis	H	AC	DMEM/F12	81,83
BT474	+	+	+	mt	primary	LB	IDC	DMEM/F12	81,82,84−87
MCF7	−	+	+	wt	metastasis	LA	IDC	RPMI, DMEM	7,9,81,83
MDA-MB-231	−	−	−	mt	metastasis	TNB	AC	RPMI, DMEM	3,4,7,9,86

[a]HER2: human epidermal growth factor receptor 2; ER: estrogen receptor; PR: progesterone receptor; NA: not available; wt: wild type; mt: mutant type; H: HER2 positive; LA: luminal A; LB: luminal B; TNB: triple-negative B; RPMI: Roswell Park Memorial Institute (RPMI) 1640 medium; DMEM: Dulbecco's modified Eagle medium; AC: adenocarcinoma; and IDC: invasive ductal carcinoma.

https://dx.doi.org/10.1021/acs.jmedchem.0c01647
J. Med. Chem. XXXX, XXX, XXX−XXX

Table 4. Antiproliferative Activity (IC_{50}; μM) of Compounds 10a−25h against Four BC AU565, BT474, MCF7, and MDA-MB-231 Cell Lines

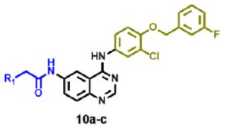

10a-c

Compound	R_1	AU565	BT474	MCF7	MDA-MB-231
10a (Lead compound)		0.220	0.240	8.620	8.776
10b		**0.130**	**0.117**	7.969	11.600
10c		**0.134**	**0.133**	**1.781**	**1.360**

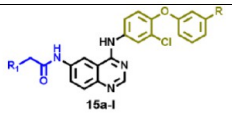

15a-l

Compound	R	R_1	AU565	BT474	MCF7	MDA-MB-231
15a	F		0.545	0.373	18.119	30.162
15b	F		0.491	0.221	5.991	5.447
15c	F		0.684	0.532	5.684	3.924
15d	F		0.663	**0.107**	**0.321**	6.555
15e	CF_3		0.364	0.298	11.168	8.846
15f	CF_3		0.441	0.369	2.074	2.559
15g	CF_3		0.408	0.478	5.097	2.659
15h	CH_3		**0.152**	**0.091**	9.644	13.783
15i	CH_3		**0.135**	**0.081**	2.647	4.503
15j	CH_3		0.219	0.265	2.678	2.828
15k	CH_3		**0.154**	**0.134**	2.703	4.513
15l	CH_3		0.304	**0.132**	10.778	7.833

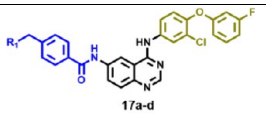

17a-d

Compound	R_1	AU565	BT474	MCF7	MDA-MB-231
17a		0.923	0.540	6.219	11.509
17b		0.767	0.506	**1.621**	1.902
17c		0.225	0.339	2.642	5.000
17d		0.205	0.204	5.636	5.233

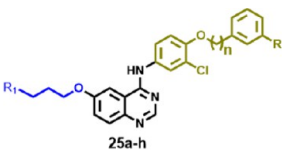

25a-h

Compound	n	R	R_1	AU565	BT474	MCF7	MDA-MB-231
25a	1	F		**0.149**	**0.081**	6.191	7.316
25b	1	F		**0.099**	**0.083**	**1.933**	**0.737**
25c	0	F		0.311	0.283	8.326	10.160
25d	0	F		0.419	0.221	**0.913**	1.699
25e	0	CF_3		0.348	0.246	5.528	6.732
25f	0	CF_3		0.447	0.200	**1.685**	1.063
25g	0	CF_3		0.289	0.213	**1.600**	**1.371**
25h	0	CF_3		0.456	0.262	**1.507**	**1.948**
Lapatinib				**0.064**	**0.064**	6.301	10.373

inhibition of MCF7 and MDA-MB231 cells than lapatinib. Compounds **10c**, **15d**, **25b**, **17b**, **25d**, and **25f−h** inhibited cell proliferation of MCF7 cells with IC_{50}: 0.321−1.933 μM, implying their greater potency (up to 20 times) more than lapatinib (IC_{50}: 6.301 μM), and specifically, compounds **15d** (IC_{50}: 0.321 μM) and **25d** (IC_{50}: 0.913 μM) exhibited the lowest IC_{50} values. Remarkably, the antiproliferative activities of compounds **15d**, **15f**, **15i**, **15k**, **17b**, **25b**, **25d**, and **25f−h** against MCF7 cells (IC_{50}: 0.321−2.647 μM) are highly consistent with their augmented antiproliferative effects

https://dx.doi.org/10.1021/acs.jmedchem.0c01647
J. Med. Chem. XXXX, XXX, XXX−XXX

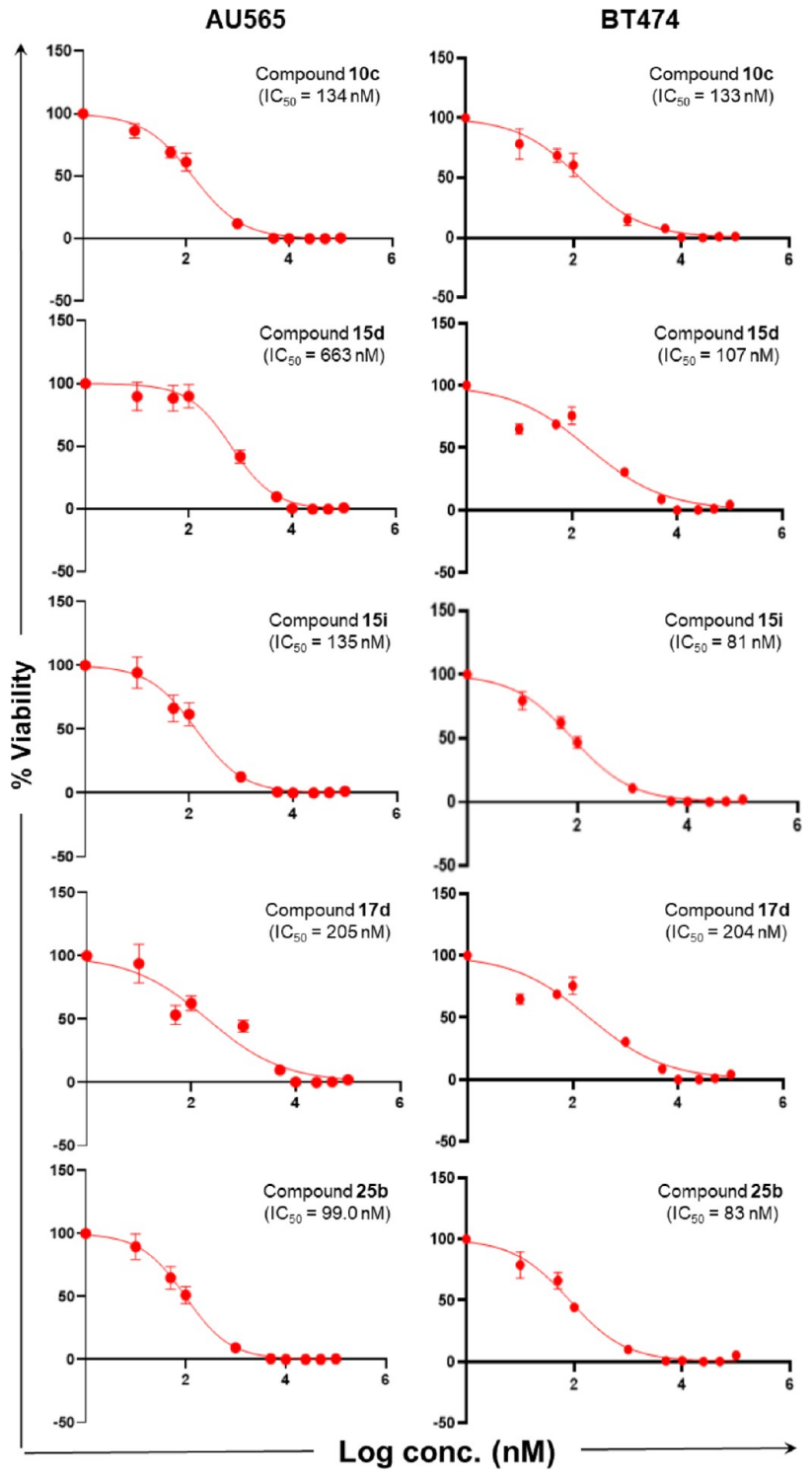

Figure 11. Dose−response curves for cell viability by WST-8 assay of AU565 and BT474 cells and their corresponding IC_{50} values (standard error are given). Cells were treated with compounds **10c**, **15d**, **15i**, **17d**, and **25b** at concentrations 0.01−100 μM for 72 h. Compounds were tested in three independent experiments.

shown toward AU565 and BT474 breast cell lines. These results support the suggestion that our compounds are selectively targeting HER2+ (in AU565 cells) and get boosted by targeting other receptors as shown in triple-positive (HER2+/ER+/PR+) BT474 cells, and to a lower extent, they can influence the estrogen and progesterone receptors (ER+/PR+) as depicted in MCF7 cells in the absence of HER2 as a main target. On the other hand, the majority of the tested compounds (~67%) displayed poor antiproliferative activities against triple-negative (MDA-MB-231) BC cell lines with IC_{50}: 4.503−30.162 μM, which represents 15−100% times higher IC_{50} than that against HER2-expressing cells (AU565 and BT474). This is clearly explained by the absence of HER2 and other boosting targets such as ER/PR expressed in these cells. To a lower extent, compounds **10c**, **15c**, **15f**, **15g**, **15j**, **17b**, **25b**, **25d**, and **25f−h** exhibited an acceptable

https://dx.doi.org/10.1021/acs.jmedchem.0c01647
J. Med. Chem. XXXX, XXX, XXX−XXX

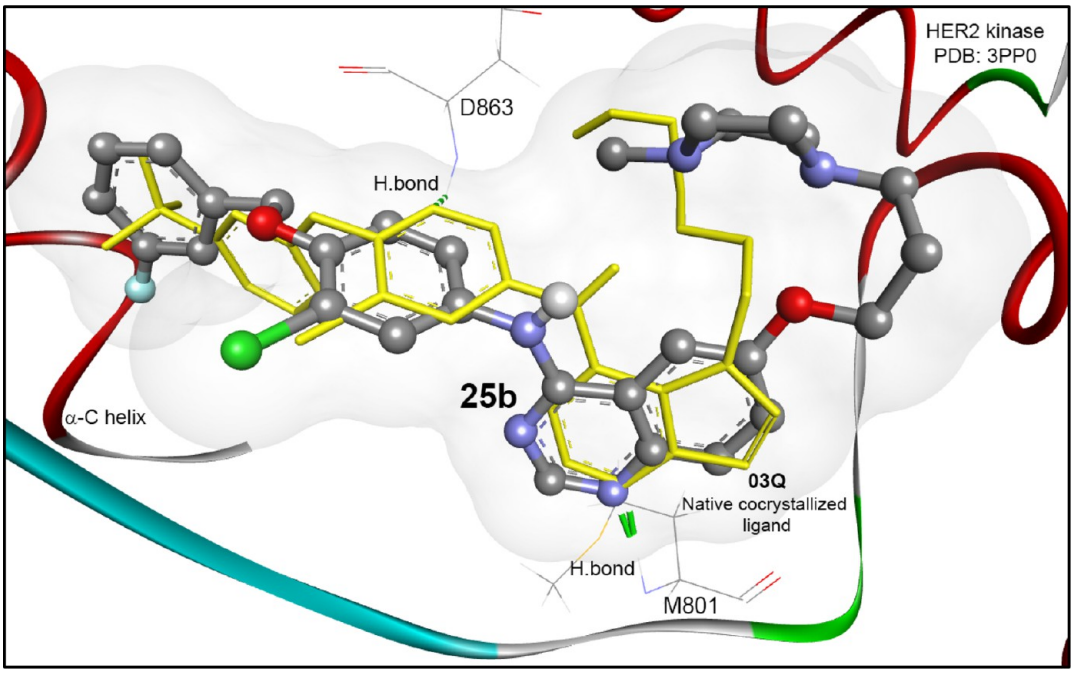

Figure 12. Docking of compound **25b** (ball and stick, colored by element) into human HER2 kinase (PDB code: 3PP0). It exhibited one hydrogen bond (green dotted lines) with M801. It was docked within an rmsd of 1.10 Å from the native cocrystallized 03Q ligand (shown as yellow sticks).

IC_{50} in the range of 0.737−3.924 μM, that is, up to 13 times less active than their corresponding activities against AU565 and BT474 breast cell lines. The reasonable explanation of this slight activity against triple-negative (MDA-MB-231) BC cell lines is the expression of 3% of HER2 kinase in comparison with 100% in triple-positive (HER2+/ER+/PR+) BT474 cells, whereas MDA-MB-231 cells expressed about 9 times EGFR (also known as HER1) more than BT474 cells.[88] Furthermore, HER1 which is overexpressed in 15−30% of breast carcinoma[89,90] is frequently associated with poor prognosis in triple-negative BC.[91−93] The aforementioned facts might explain the slight activities of some compounds toward triple-negative (MDA-MB-231) BC cell lines.

***In Vitro* Primary Single-Dose (10 μM Concentration) Screening against the NCI 60 Human Cell Panel.** The detailed discussion of single-dose and 5-dose screening toward NCI 60 human cancer cell lines and the cytotoxicity mean graphs from NCI is presented in the Supporting Information. Single-dose testing was performed at 10 μM concentration against 60 cell lines, representing nine tumor subpanels. As depicted in Figure S1, many of the test-substituted quinazoline compounds exhibited distinctive patterns of selectivity and sensitivity against different NCI cell panels. Remarkably, compounds **15f**, **15i**, **17c**, **17d**, **25b**, **25d**, and **25f−h** exhibited mean cell growth and lethality in the range of 11.85−19.30% and −1.30 to −31.03%, respectively. Therefore, these potent compounds in addition to **15g**, **15k**, **17a**, and **25e** were selected by the DTP program in NCI for further 5-dose screening using the mean growth percent of 47.7% as a minimum criterion for inhibition. Compounds **15f**, **15i**, **17c**, **17d**, **25b**, **25d**, and **25f−h** exhibited broad spectrum cell growth inhibition and lethality against BC up to −78.7%. All test compounds exhibited significant inhibition and lethality in the range of 18.8 to −66.0% against MDA-MB-468 cells. Compounds **15f**, **17c**, **25b**, and **25g** exhibited significant lethality in the range of −11.7 to −78.7% against MCF7, MDA-MB-231, HS578T, and MDA-MB-468 cells, whereas compounds **15i**, **17d**, **25f**, and **25h** showed lethality in the range of −18 to −74.6% against MCF7, MDA-MB-231, and MDA-MB-468 cells. Unfortunately, none of the six human BC cells used by the DTP in NCI was the HER2+ cell. Among these six cancer cells, four cells, namely, MDA-MB-231, HS578T, BT549, and MDA-MB-468, are characterized by the lack of expression of the three main molecular markers (ER, PR, and HER2) and referred as triple-negative,[84,94] whereas MCF-7 and T-47D breast cell lines are ER+/PR+, making them an ideal model to study hormone response.[84]

In Vitro Five-Dose Full NCI 60 Cell Panel Screening. Surprisingly, out of 20 compounds tested initially at a single high dose (10^{-5} M), 13 compounds were selected to be screened by five-dose concentration against the full NCI 60 cell panel. These compounds, namely, **15f**, **15g**, **15i**, **15k**, **17a**, **17c**, **17d**, **25b**, **25d**, **25e**, **25f**, **25g**, and **25h**, exhibited significant growth inhibitions in the single-dose screen. The criteria for efficiently capturing these thirteen compounds and progressing them to the 5-dose antiproliferative activity were based on careful analysis of historical DTP screening data. In this assay, the test compounds were incubated at five different concentrations (0.01, 0.1, 1.0, 10, and 100 μM). Three dose−response parameters (GI_{50}, TGI, and LC_{50}) were calculated for each compound against each cell line (Table S2). Compounds **15i**, **25b**, and **25g** demonstrated the most potent antiproliferative activities against the tested NCI 60 cell panel. Compounds **15i** and **25b** exhibited the same pattern of potency against MDA-MB-468, the triple-negative BC cells with GI_{50} = 0.4 μM (Figure S2).

*Sensitivity of the Test Compounds toward **9** Subpanels of NCI 60 Cell Lines.* To a higher extent, the test compounds **15i** and **25b** exhibited impressive anticancer activity against most of the NCI 60 cell lines representing nine different subpanels with GI_{50} values between 0.4 and 2.1 μM. The best inhibitions were revealed against BC cell lines with average GI_{50} values of

https://dx.doi.org/10.1021/acs.jmedchem.0c01647
J. Med. Chem. XXXX, XXX, XXX−XXX

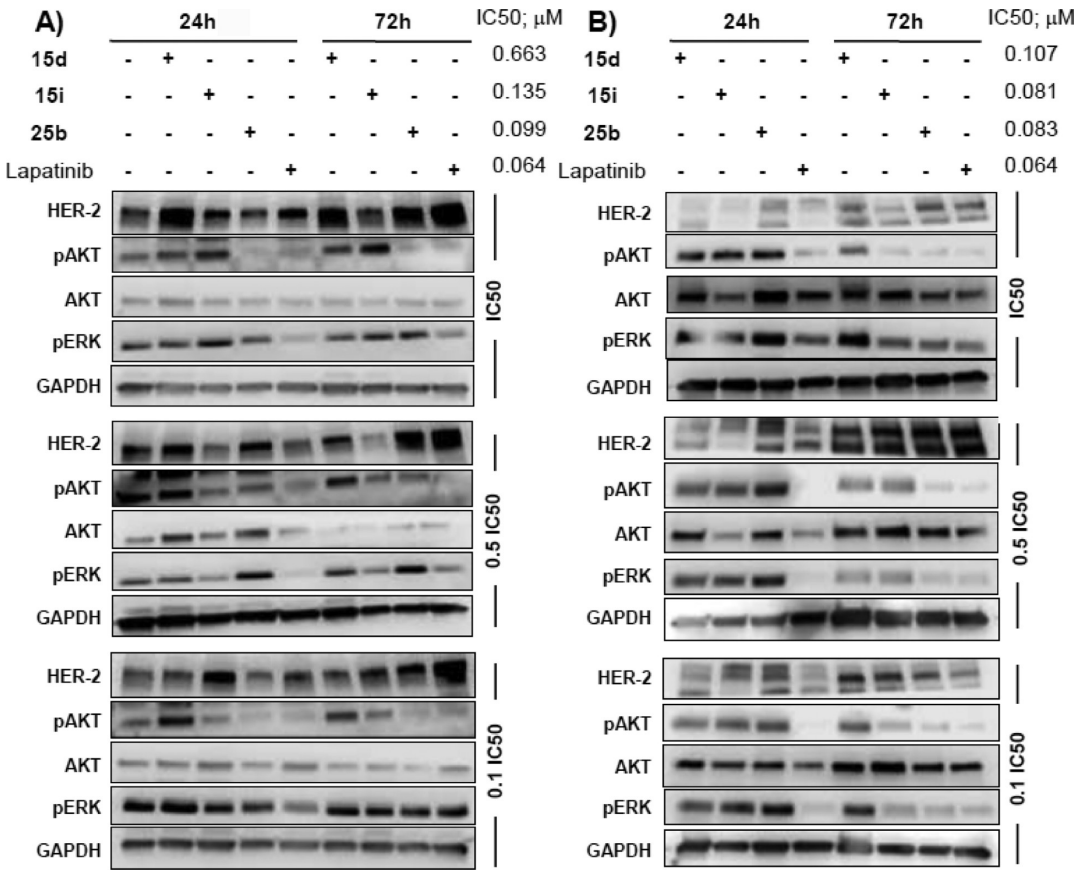

Figure 13. Effect of optimized compounds on the HER2 signaling pathway in BC cells. AU565 (A) and BT474 (B) cells were treated with compounds **15d**, **15i**, and **25b** at concentrations of their IC_{50}, 0.5 IC_{50}, and 0.1 IC_{50} for each compound at 24 and 72 h. Lapatinib was used as an authenticated control for the test compounds. Western blot analysis was performed and GAPDH was used as a reference loading control. Data represented results collected from at least two independent experiments.

1.21 and 1.37 μM, respectively. Noticeably, BC MDA-MB-468 cells were inhibited selectively by many compounds including **15i**, **15k**, **17d**, **25b**, **25e**, **25g** and **25h** with GI_{50} equal to 0.4, 0.2, 0.6, 0.4, 0.5, 0.9, and 0.6 μM, respectively. The selectivity ratio (S) of the screening results of the selected test 13 compounds against NCI-60 human tumor cell lines at the five-dose level was calculated as reported[95] by dividing its average GI_{50} toward a full panel of NCI 60 cell lines (MID-all) by its average GI_{50} toward cell lines of a particular subpanel (MID), that is, higher value indicates better selectivity. As per this criterion, the majority (77−85%) of the test compounds exhibited a remarkable selectivity profile toward BC (S: 1.05−1.44), as shown in Table S3 and depicted in Figure S3. Regarding the selectivity against a particular subpanel of NCI-60 cell lines, compounds **15k**, **17a**, **17d**, **25e**, and **25f** were found to be the most significantly selective toward BC cells with a selectivity ratio (S) of 1.24, 1.27, 1.44, 1.24, and 1.26, respectively, as obviously shown in Figure S3.

Annexin V PI/FITC Apoptosis Assay. Based on the previous reports[29,96,97] that show that lapatinib induces cell cycle arrest and apoptosis in HER2-positive BC cells, Annexin V fluorescein isothiocyanate/propidium iodide (FITC/PI) apoptosis assay was conducted for the most potent compounds revealing augmented effects in BT474 cells (**10c**, **15d**, **15i**, **17d**, and **25b**). These compounds were chosen for the apoptosis assay based on their powerful antiproliferative activities and/or augmented effect on targeting triple+ BT474 cells in comparison with their effects on HER2+ AU565 cells. The BT474 cells were treated with the selected compounds and labeled by Annexin V PI/FITC, followed by flow cytometric analysis. Compounds **10c**, **15d**, **15i**, **17d**, and **25b** induced early-phase apoptosis of BT474 in a dose-dependent manner by 3−10-fold compared to the control cells, as shown in Figure S4. Remarkably, compound **10c** at the lowest concentration (0.2 μM) showed significant early-phase apoptosis of about sevenfold induction compared to the control cells. This activity was increased to 10-fold compared to the control at 0.5, 1.0, and 5 μM. To a lower extent, compounds **25b**, **15i**, **15d**, and **17d** exhibited early-phase apoptosis up to sixfold at 0.5−5.0 μM concentration compared to the control. Regarding the late apoptotic changes as identified by PI staining, compound **10c** showed a notable increase (2−5-folds) in late apoptosis at 0.5−5.0 μM concentrations compared to their counterparts. At the same concentration, compounds **25b** and **15i** induced late-phase apoptosis to a lower level (≤3-fold) compared to the control cells, whereas compounds **15d** and **17d** have insignificant changes in late-phase apoptosis of the BT474 cell lines. To some extent, these results can partially explain the preferential effects, particularly for compounds **15d** and **15i** on HER2+ AU565 cells (IC_{50}: 0.663 and 0.135 μM) in comparison with their effects on the triple-positive BT474 cells (IC_{50}: 0.107 and 0.081 μM, respectively). Despite some of these apoptotic results are partially consistent with the WST-8 and NCI 60 cell line antiproliferative assays, we cannot speculate to correlate these assays to each other. Additionally, these compounds may

https://dx.doi.org/10.1021/acs.jmedchem.0c01647
J. Med. Chem. XXXX, XXX, XXX−XXX

exhibit their antitumor effects by downregulating other different hallmarks of cancer[98,99] without affecting apoptosis. Hence, further assays were conducted to investigate the mechanism by which our compounds reveal their antitumor effects through other pathways than the apoptosis. Further Annexin V apoptosis assays using MCF7 and MDA-MB-231 cells were conducted with the potent compounds **10c**, **15i**, and **25b** which revealed antiproliferative activities of IC_{50} ranges of 1.78−2.65 and 0.74−4.50 μM, respectively, as shown in Figure S5. In contrast to their apoptotic results using BT474 cells, the tested compounds (**10c**, **15i**, and **25b** at 5.0 μM) exhibited insignificant effects on the early- and late-phase apoptosis of MCF7 and MDA-MB-231 cell lines. These results anticipate the specificity of our optimized compounds toward HER+ harboring cells.

Cell Growth Inhibition by Modulation of HER2 Downstream Signaling Pathways. Compounds **15d**, **15i**, and **25b** were selected to investigate their effects on the expression of HER2 kinase and its downstream signaling proteins. These three compounds were selected for further assessment at the molecular level because they exhibited the most potent antiproliferative activities against the HER2+ BC cells, in addition to the significant augmented activity of compound **15d** in the triple (+) BT-474 cells. Moreover, the apoptosis induction effect of these compounds was proved to be enhanced. Furthermore, these compounds were the best representatives for the derivatives bearing a 4-substituted phenoxy anilino moiety (**15d** and **15i**) and those bearing a 4-substituted benzyloxy anilino moiety (**25b**). It is well-known that the activation of HER signaling triggers several downstream signaling pathways, mainly mitogen-activated protein kinase/extracellular-related kinase (MAPK/ERK) and phosphatidylinositol-4,5-bisphosphate 3-kinase (PI3K)/Akt pathways.[100] The effects of the three test compounds as well as lapatinib, as a positive control, on HER2 and its main downstream signaling pathways were assessed by immunoblotting. The expression level of HER2 and the activities of ERK1/2 and Akt were compared in cellular lysates prepared from HER2+ BC cell lines (AU565 and BT474) at different time points and concentrations. The AU565 and BT474 cells were treated with IC_{50}, 0.5 IC_{50}, and 0.1 IC_{50} concentrations for each compound including lapatinib. The treated cells were harvested from each concentration after 24 and 72 h, and HER expression and activities of ERK1/2 and Akt were determined by western blot analysis as described.[101] Using AU565 BC cells, our results indicated that IC_{50} concentrations of compound **25b** and lapatinib dramatically reduced the Akt activity after 24 and 72 h of treatment. This inhibitory effect of ERK kinase was significantly exhibited by lapatinib after 24 h and to a lower extent after 72 h. Compound **25b** and lapatinib demonstrated mild inhibition of HER2 expression after 24 h, whereas compounds **15d** and **15i** did not show any detectable inhibitions on these kinases (Figure 13A). At a lower concentration of 0.5 IC_{50}, compound **15i** showed a significant reduction in HER2 expression compared to lapatinib at 24 h but not at 72 h. Peculiarly, the tested compounds, as well as lapatinib, inhibited Akt expression (total Akt) after 72 h. However, only compound **25b** and lapatinib were able to demonstrate the inhibitory effect on Akt activity. At a concentration of 0.5 IC_{50}, compound **15i** showed inhibition of pERK expression almost similar to that of lapatinib after 24 and 72 h. Remarkably, compounds **15i** and **25b** reduced pAKT competitively to lapatinib at 0.1 IC_{50} concentration after 24 h. At the same concentration and time point, compound **25b** inhibited HER2 expression comparable to lapatinib, as depicted in Figure 13A.

The effect of the three test compounds and lapatinib on HER2 expression as well as its downstream targets was further investigated using the BT474 triple-positive BC cell line. Our results showed that at IC_{50} concentrations, all compounds, specifically compound **15i**, and lapatinib revealed a substantial reduction in HER2 expression after 24 h of treatment. In the same way, compounds **15i**, **25b**, and lapatinib significantly inhibited the activity of Akt as indicated by the notable reduction of phosphorylated AKT after 72 h (Figure 13B). At 0.5 IC_{50} and 0.1 IC_{50} concentrations, most of the compounds particularly compound **25b** and lapatinib revealed a dramatic inhibition in the activity of both Akt and ERK1/2 after 72 h (Figure 13B). A close look at the overall immunoblotting analysis using AU565 and BT474 cells indicates that all the three tested compounds were able to inhibit the expression/activity of HER2 and/or at least one of its downstream targets in at least at a one-time point or three used concentrations.

Furthermore, the HER2 signaling pathway in BC BT-474 cells was evaluated using western blot analysis for compound **17d**. The cells were treated at IC_{50} (0.204 μM), 0.5 IC_{50}, and 0.1 IC_{50} concentrations within two-time points (24 and 48 h). GAPDH was used as a loading control. Using BT474 BC cells, our results indicated that at 0.1 and 0.5 IC_{50} concentrations, compound **17d** has particularly reduced HER2 and pAKT expressions compared to the control 24 h, whereas this effect was exhibited at IC_{50} at 48 h. To a lower extent, compound **17d** exhibited a mild inhibitory effect against Akt and pERK1/2 after 24 and 48 h, as shown in Figure 14.

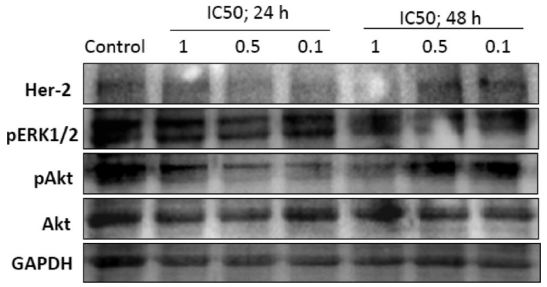

Figure 14. Western blot analysis for compound **17d** to evaluate the HER2 signaling pathway in BC cells (BT-474). The cells were treated with different concentrations at IC_{50} (0.204 μM), 0.5 IC_{50}, and 0.1 IC_{50} at 24 and 48 h. GAPDH was used as a loading control.

***In Vivo* Antitumor Efficacy for the Most Potent Optimized Scaffolds Using the BT474 Athymic Nude Mice ($Foxn^{1nu}/Foxn^{1+}$) Xenograft Mouse Model.** Encouraged by the potent inhibitory activity of compounds **17d** and **25b** regarding their low IC_{50} against BT474 cell lines as demonstrated by the WST-8 assay data, we were excited to know whether this inhibition can be reproduced in the preclinical BC model.

*Rationale for the Selection of Compounds **17d** and **25b** for the In Vivo Study.* The selection criteria of compounds **17d** and **25b** for evaluation of their *in vivo* anticancer activity depended on the overall activity of these compounds and NOT limited to the antiproliferative activities. Regarding the selection of compound **25b** for *in vivo* testing, compounds **15i**, **25a**, and **25b** revealed COMPARABLE or almost SAME potency against BT474 cells, IC_{50} values (0.08 μM; Table 4).

https://dx.doi.org/10.1021/acs.jmedchem.0c01647
J. Med. Chem. XXXX, XXX, XXX−XXX

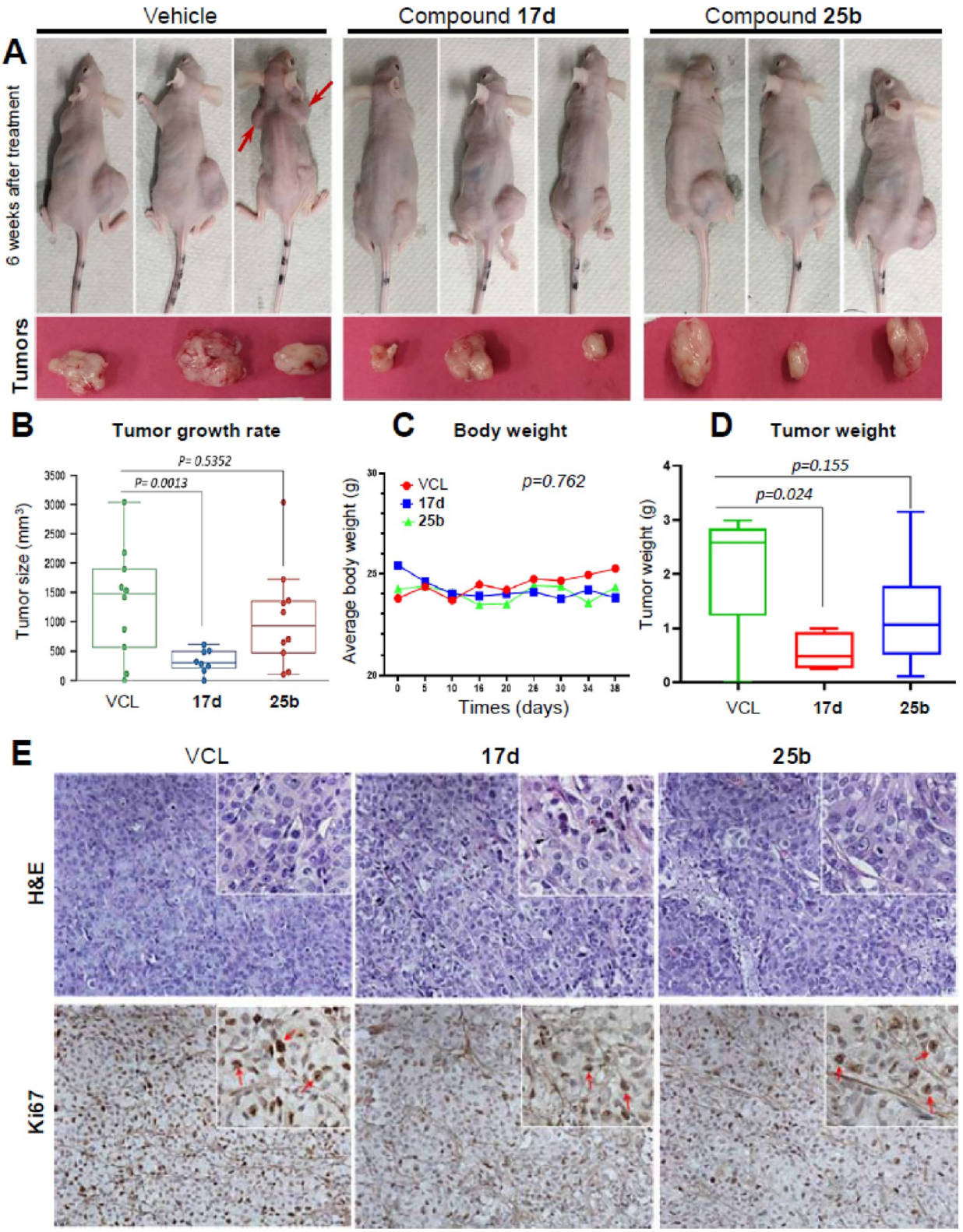

Figure 15. Effect of compounds **17d** and **25b** on tumor growth of BT474 cells in the preclinical mouse model. (A) Represented images of mice implanted with 2×10^6 BT474 cells on the dorsal flank. After growing of the nodules, mice were randomized 5 mice per group and received the vehicle and compound **17d** and **25b**, respectively; then, all mice were sacrificed 6 weeks after the initial treatment. The remarkable metastases in the vehicle group are pointed out by red arrows. At the end of the experiment, tumor tissues were resected and preserved. (B) Tumor growth was measured twice a week for 6 weeks after treatments. (C,D) Whole-body weight per each mouse was recorded twice a week and the resected tumors were weighed per each animal. (E) Formalin-fixed paraffin-embedded xenograft tissues were stained with hematoxylin (H) and eosin (E), and proliferative index Ki67 for the three groups as indicated. Significance considered at $p < 0.05$ regarding mice that received vehicle. The magnification for H&E and Ki67 staining was 200× and for inserts was 400×.

https://dx.doi.org/10.1021/acs.jmedchem.0c01647
J. Med. Chem. XXXX, XXX, XXX−XXX

Table 5. Mouse Microsomal Stability Assay Result of the Test Compounds[a]

test compound	R^2	$T_{1/2}$ (min)	$CL_{int(mic)}$ (μL/min/mg)	$CL_{int(liver)}$ (mL/min/kg)	remaining (T = 60 min) (%)	remaining (NCF = 60 min) (%)
17d	0.9822	**>145**	**<9.6**	<38.0	102.7	100.2
25b	0.9749	**57.4**	**24.2**	95.7	46.4	93.5
testosterone	0.9991	5.0	279.1	1105.4	0.0	103.7
diclofenac	0.9978	60.0	23.1	91.5	50.2	101.8
propafenone	0.9968	2.1	668.1	2645.6	0.0	105.5

[a]NCF: no cofactor. No NADPH regenerating system is added to NCF samples (replaced by buffer) during the 60 min incubation. If the NCF remaining is less than 60%, then non-NADPH-dependent metabolism occurs; R^2: correlation coefficient; $T_{1/2}$: half-life; $CL_{int(mic)}$: intrinsic clearance; $CL_{int(mic)} = 0.693/T_{1/2}$/mg microsome protein per mL; $CL_{int(liver)} = CL_{int(mic)} \times$ mg microsomal protein/g liver weight × g liver weight/kg body weight mg microsomal protein/g liver weight: 45 mg/g for all species; and liver weights: 88 g/kg for a mouse.

Compound **25b** is considered as the best candidate in this series (1) with similar activities, (2) being previously selected by NCI as a promising candidate for 5-dose assay, (3) with its potent inhibitory activity against HER2 kinase (IC_{50} of 8.3 nM), and (4) it shares the 4-benzyloxyaniline moiety of lapatinib and could be considered as a well-optimized analogue by a comparative *in vivo* study.

On the other hand, compound **17d** was selected for *in vivo* testing being; (1) revealing superior kinase profiling selectivity over the targeted HER2 kinase, with a particular insignificant effect on the off-targeted PDGFRα kinase (−4.0%), which was overactivated by lapatinib (56%) and other test compounds (18−115%), (2) **17d** was selected by NCI for 5-dose assay and revealed the highest sensitivity toward BC cell lines within NCI60 cell lines, and (3) it has the 4-phenoxyaniline moiety and could be considered as the best example for studying the beneficial effect of this moiety on the *in vivo* efficacy, compared to the 4-benzyloxyaniline moiety of lapatinib.

In this study, female athymic nude mice ($Foxn^{1nu}/Foxn^{1+}$) were used to examine these two compounds **17d** and **25b**. When the volume of the engrafted tumors reached around 100−150 mm^3, the tested compounds were administered at 50 mg/kg, by oral gavage 5×/week, and continued over 55 days.[80,81] To evaluate the treatment response of the BT474 xenograft growth in mice, the tumor growth curves of the three tested groups were analyzed and compared among each other using the R package TumGrowth according to Enot et al. (2018).[102] The tumor growth curves of the three groups were subjected to type II ANOVA and pairwise comparisons across groups using this statistical package. According to the statistical data and as depicted in Figure 15A, oral treatment of the nude female mice with 50 mg/kg of compound **17d** substantially inhibited the BT474 tumor growth compared to either the vehicle control (p = 0.0013) or compound **25b** treated group (p = 0.01). Mice treated with compound **25b** demonstrated mild growth inhibition at the same dose; however, this reduction did not reach a significant value when compared to the vehicle control group (p = 0.5352), as shown in Figure 15B. More details were illustrated in Figure S6 illustrating the average tumor growth rate (tumor size with error bars vs time) for the three mice groups that received the vehicle, compound **17d** and **25b**, respectively. These data were further confirmed when using the average tumor weight of the three treatment groups after animals were sacrificed. The average tumor weights for the **17d** group (0.572 g) were significantly less than that of the vehicle control group (2.046 g) and the p-value of the comparison was 0.024 (ANOVA/Tukey test). The average tumor weight of the vehicle control group (2.046 g) is still higher than that of the **25b** compound group (1.223 g). However, there was no significant difference recorded when both groups were compared (p = 0.155, ANOVA/Tukey), as depicted in Figure 15D. Histologically, the H&E stain of the xenograft tumor tissues indicated that the cells are originated from the xenograft and had the typical morphology of cancer cells. This was unequivocally observed in the vehicle-treated tissues with round cells and enlarged nuclei. Interestingly, large areas of necrosis were observed in compounds **17d**- and **25b**-sensitive tumors, as depicted by red arrows in Figure 15E (upper panel), the higher magnification showing fibrosis and inflammation in compounds **17d**- and **25b**-treated tumors. On the other hand, the xenograft tissues stained by the ki67 antibody indicated that the proliferative cells are most abundant in the vehicle control group, whereas they are dramatically reduced on treatment by compound **17d** and to a less extent by compound **25b**, as clearly depicted in Figure 15E (lower panel). Interestingly, a metastasis case was observed in the vehicle group but not detected in the mice treated by the test compounds, as obviously pointed out with red arrows in Figure 15A, whereas no metastasis was detected in the other groups treated by the compounds **17d** and **25b**. This study anticipates that compound **17d** is a potential replacement therapy for lapatinib to sensitize HER2-overexpressing BCs and significantly reduce the tumorigenesis and metastasis of the HER2+ BC. Nevertheless, the *in vivo* efficacy of compound **25b** is less active as compared to compound **17d**.

Fortunately, our findings are fit in-line with the reported postulations[103,104] that the superior *in vitro* activity of the lipophilic 3-fluoro benzyl derivatives (as **25b**) would not translate into a better *in vivo* efficacy because of their higher protein binding.

On the other hand, Mohamed et al. reported the O-dealkylation on the 3-fluorobenzyl moiety of lapatinib as an abundant metabolic pathway.[105] Similarly, the metabolic study of pyrotinib indicated that the O-dealkylated metabolite exhibited weak activity against HER2 kinase because of the loss of interaction with the HER2 back pocket.[106] Accordingly, to investigate the metabolic stability of compounds **17d** (bearing 3-fluorophenyl moiety) and **25b** (bearing 3-fluorobenzyl moiety), a microsomal stability assay was conducted.

CD-1 Mouse Microsomal Stability Assay. Compounds **17d** and **25b**, 5 μL at a final concentration of 100 μM, were incubated with pooled mouse liver microsomes (final concentration 0.56 mg/mL) in phosphate buffer 0.1 M (pH 7.4) in a 37 °C water bath, and the reaction was initiated by the addition of an NADPH cofactor. The reaction was allowed for different time points, 5, 15, 30, 45, and 60 min and after quenching of the reactions, each bioanalysis plate was sealed and shaken for 10 min prior to LC−MS/MS analysis. The equation of first-order kinetics was used to calculate $T_{1/2}$ and

https://dx.doi.org/10.1021/acs.jmedchem.0c01647
J. Med. Chem. XXXX, XXX, XXX−XXX

Table 6. Optimization of the Docking into HER2 Kinase (PDB: 3PP0)

					hydrogen bonds between compounds and HER2 kinase		
compd	GoldScore	S(hb-ext)[a]	S(vdw-ext)[b]	flexible residues	atom of compd	amino acid	rmsd[c] (Å)
trial 1	87.29	3.8604	63.3455	M801	quinazoline-N^1H	HN of M801	3.11
				D863	terminal CH_2O	HN of C805	
				T798			
trial 2	94.26	3.9375	68.4816	M801	quinazoline-N^1H	HN of M801	3.17
				D863	pyridine-N	HN of D863	
					terminal CH_2O	HN of C805	
trial 3	89.75	2.0682	66.9045	M801	quinazoline-N^1H	HN of M801	2.44
					pyridine-N	HO of T862	
					pyridine-N	HN of D863	
trial 4	91.40	6.4519	64.8467	M801	quinazoline-N^1H	HN of M801	1.54
					pyridine-N	HN of D863	
					pyridine-N	HO of T862	
					terminal CH_2OH	O=C of D863	
trial 5	85.52	6.8702	61.0202	rigid	quinazoline-N^1H	HN of M801	0.99
					terminal CH_2OH	O=C of D863	
native ligand[d]					quinazoline-N^1H	HN of M801	
					pyridine-N	HN of D863	

[a] S(hb_ext)[a] GoldScore protein−ligand hydrogen bonding. [b] S(vdw_ext): GoldScore external Vdw (van der Waals interactions between the protein and ligand). [c] rmsd: Root-mean-square deviation. [d] 03Q: 2-(2-[4-((5-chloro-6-[3-(trifluoromethyl)phenoxy]pyridin-3-ylamino)-5*H*-pyrrolo[3,2-*d*]pyrimidin-5-yl]ethoxy)ethanol).

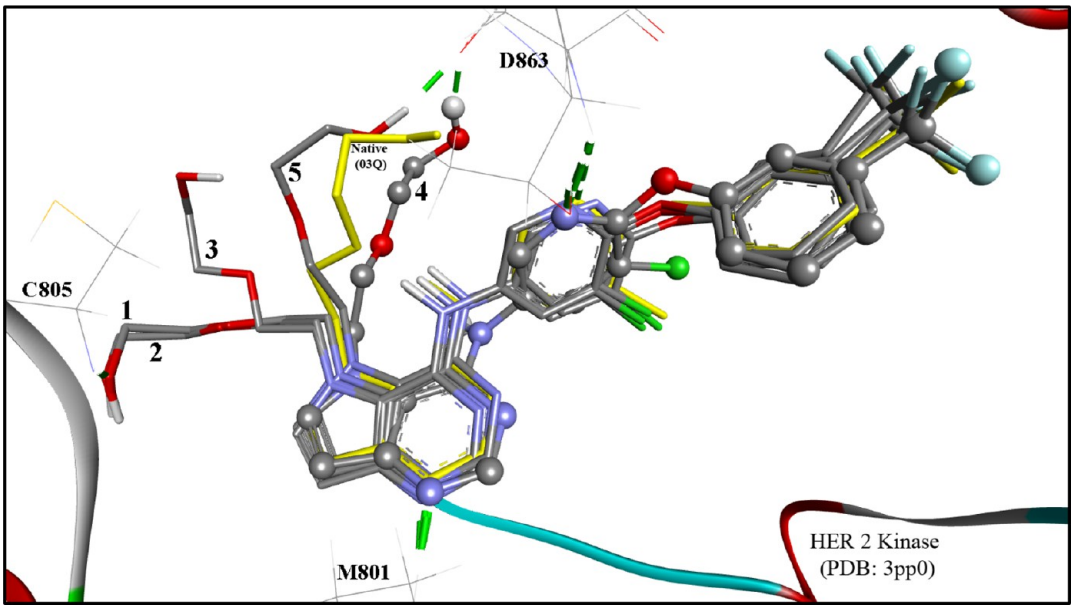

Figure 16. Optimization of the docking protocol of the cocrystallized ligand (03Q) into HER2 kinase (PDB: 3PP0). The five docked trials are labeled (1−5) in comparison with the native bound ligand (03Q, shown as yellow sticks) in which trial 4 (shown as ball and sticks) utilizing M801 as a flexible residue with 50,000 operations exhibited the best-optimized protocol with an rmsd of 1.54 Å and four hydrogen bonds.

$CL_{int(mic)}$ (μL/min/mg). Testosterone, propafenone, and diclofenac were used as positive controls as reference compounds with high and medium clearance, respectively.

As shown in Table 5, compound **17d** that revealed higher $T_{1/2}$ = >145 min compared to compound **25b** $T_{1/2}$ = 57.4 min along with lower intrinsic clearance was observed with compound **17d**, $CL_{int(mic)}$ = <9.6 mL/min/kg compared to **25b**, $CL_{int(mic)}$ = 24.2 mL/min/kg. Accordingly, compound **25b** is likely to be rapidly cleared *in vivo* resulting in a short duration of action. This underpins the less sufficient antitumor activity of **25b** compared to **17d** in the *in vivo* animal model.

Molecular Docking. *Docking Validation and Protocol Optimization.* The scoring function of the GOLD program was validated by checking the extent of the resemblance of the best-docked conformation of the cocrystallized ligand with the reported biological method.[107] Therefore, we initiated this study by redocking of the cocrystallized ligand (03Q: 2-(2-[4-((5-chloro-6-[3-(trifluoromethyl)phenoxy]pyridin-3-ylamino)-5*H*-pyrrolo[3,2-*d*]pyrimidin-5-yl]ethoxy)ethanol)) into chain B (75% overall quality) of the HER2 kinase domain (PDB: 3PP0). The docking protocol was optimized by running five trials of docking including rigid and flexible docking, as listed in Table 6. Trial 4, involving a flexible docking with M801

https://dx.doi.org/10.1021/acs.jmedchem.0c01647
J. Med. Chem. XXXX, XXX, XXX−XXX

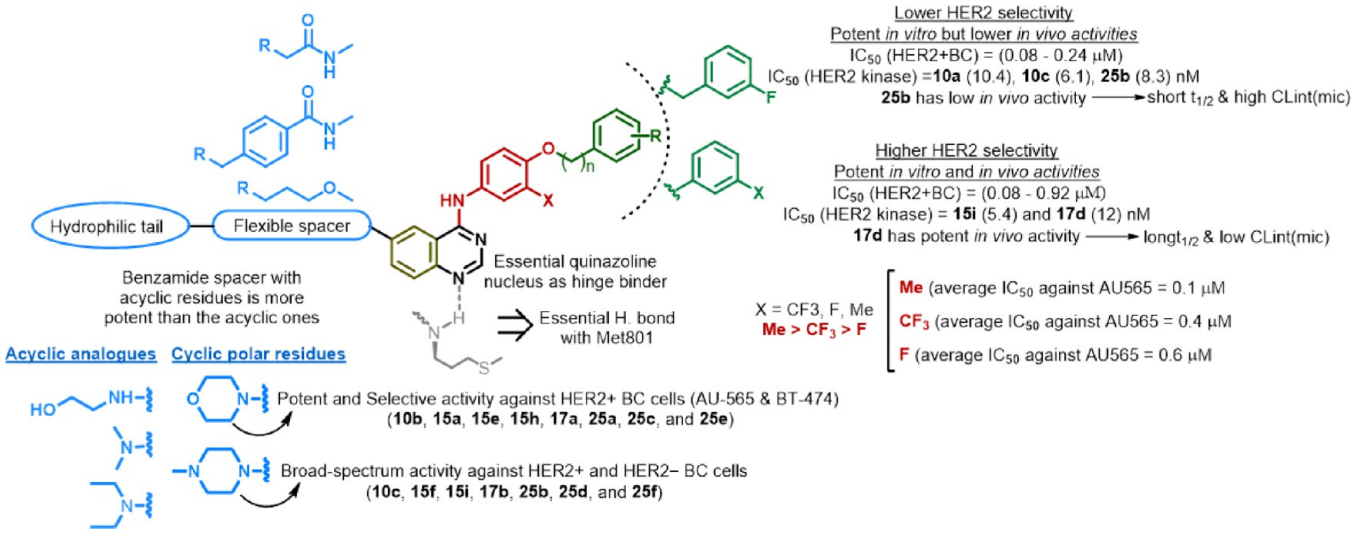

Figure 17. SAR studies of the newly synthesized 4,6 disubstituted quinazolines.

residue and 50,000 operations, exhibited the best-optimized protocol with an rmsd of 1.54 Å and four hydrogen bonds, as shown in Figure 16. The binding modes for the 03Q native ligand obtained in trial 4 were greatly consistent with its reported cocrystal structure bound to HER2 kinase.

GoldScore Fitness of the Designed Quinazoline Derivatives into HER2 Kinase. The GoldScore algorithmic function was applied in this molecular docking because it affords superior docking results than the ChemScore function in GOLD as a powerful molecular docking program.[49] All the docking results, including GoldScore fitness, *S*(hb-ext), *S*(vdw-ext), hydrogen bonds between the ligand and HER2 kinase, and rmsd between the docked pose and the native cocrystallized ligand, are listed in the Supporting Information, Table S4. Our compounds were docked into the human HER2 kinase domain revealing Gold fitness scores ranging from 77.38 to 93.29. Compounds **10c**, **15f**, **15i**, **15j**, **17d**, **25b**, and **25h** exhibited the most noteworthy GoldScore fitness of 90.14−93.29 in comparison with the cocrystallized compound 03Q of 91.40. The majority of the test compounds (17 out of 27) were docked proximately superimposed on the native ligand within ≤2.50 Å. They docked into the ATP-binding site through up to three hydrogen bonds to a higher extent with M801 (NH) and C805 (NH) amino acids.

Structure−Activity Relationship. In this study, three key structural features of the designed compounds were discussed. These include the polar terminal residues at position 6, the anilino substitution at position 4, and the flexible spacer between the quinazoline ring and the terminal hydrophilic moieties, as depicted in Figure 17. Regarding the antiproliferative assay, compounds **10b**, **15a**, **15e**, **15h**, **17a**, **25a**, **25c**, and **25e** bearing a morpholine terminal residue revealed potent and selective activity against HER2+ BC cells (BT-474 and AU-565). These compounds exhibited IC_{50} in sub-micromolar concentrations (IC_{50} = 0.08−0.9 μM) with a noticeably diminished activity against HER2− BC cells MCF7 and MDA-MB-231 (IC_{50} = 5.5−30 μM). Meanwhile, compounds having an *N*-methylpiperazine residue (**10c**, **15f**, **15i**, **17b**, **25b**, **25d**, and **25f**) exhibited a broad spectrum of activity against BC cell lines. Their antiproliferative strengths vary ranging from strong (IC_{50} = 0.08−0.7 μM) against HER2+ BC cells to moderate activity (IC_{50} = 0.7−2.5 μM) against HER2− BC cells. Compounds having acyclic polar residues (ethanolamine, dimethylamine, and diethylamine) along with an acetamido or propoxy spacer exhibited inferior activity of 2−3 times less than compounds bearing a terminal morpholine or *N*-methyl piperazine moiety. However, the reverse was observed in the presence of a bulkier benzamide linker, where compounds with acyclic polar residues exhibited 2−5 times more potential than compounds bearing cyclic terminal residues.

Thus, the steric effect of the substituents at position 6 of the quinazoline scaffold has a significant impact on the antiproliferative activity, where these substituents will accommodate into the solvent-accessible region of HER2 kinase. It is noteworthy that the methyl substitution on the phenoxyaniline moiety at position 4 dramatically enhanced the cytotoxic activity of compounds within 4 to 6 times higher than substitution by a trifluoromethyl or fluoro moiety. Considering that compounds have the same spacer and terminal residues, compounds **15h**, **15i**, and **15k** with a methyl substituent on the phenoxyaniline ring at position 4 exhibited IC_{50} with an average of 0.1 μM against AU565 BC cells. Meanwhile, compounds **15e−15g** and compounds **15a**, **15b**, and **15d** bearing a trifluoromethyl and fluoro group, respectively, revealed an average of IC_{50} = 0.4 and 0.6 μM, respectively.

Regarding the protein kinase profiling assay, compounds **10a**, **10b**, **15a**, **15e**, **15l**, **17d**, and **25f** demonstrated the same pattern of inhibitory activity and selectivity against the HER kinase family (EGFR, HER2, and HER4) with higher particular potency against the target HER2 kinase (−91 to 93%) and with moderate-to-weak inhibition on other non-target 17 kinases. Regardless of the type of the spacer or the polar terminal residue, the test quinazoline derivatives bearing 4-substituted phenoxyaniline moieties (**15a**, **15e**, **15l**, **17d**, and **25f**) showed remarkable selectivity against the target HER2 kinase (−91 to −92%) and moderate inhibition against EGFR (−65 to −78%). Compound **17d** having a benzamide spacer and ethanolamine terminal residue demonstrated the best selectivity among the test compounds with −92% inhibition of HER2, −70% for EGFR, −47% for ROCK2, −47% for JAK-2, and −40% for ABL1 kinase. Nevertheless, the test quinazoline derivatives (**10a** and **10b**) substituted with a benzyloxyaniline moiety at position 4 exhibited inferior selectivity against HER2 of −92 to −93%, EGFR of −78 to −81%, JAK-2 of −74 to

https://dx.doi.org/10.1021/acs.jmedchem.0c01647
J. Med. Chem. XXXX, XXX, XXX−XXX

−86%, and ABL of −86%. However, the tested compounds **10a**, **10c**, and **25b** or **15i** and **17d** bearing benzyloxyaniline or phenoxyaniline moieties at position 4 revealed superior HER2 inhibition with an IC_{50} of 10.4, 6.1, and 8.3 nM or 5.4 and 12 nM, respectively, compared to lapatinib IC_{50} of 95.5 nM. It is noteworthy that the benzyloxyaniline moiety is metabolically labile to O-dealkylation which may result in high clearance and low *in vivo* activity, as observed in the *in vivo* efficacy of **25b**. Accordingly, we can conclude that the substitution at position 4 with a phenoxyaniline or benzyloxyaniline moiety mainly affects the selectivity against HER2 kinase and the metabolic stability *in vivo*. Additionally, the polar substitution at position 6 can also modulate the cellular activity of the tested compounds.

CONCLUSIONS

In summary, novel 27 4,6-disubstituted quinazoline derivatives were designed and synthesized guided by the binding mode of the current dual EGFR/HER2 inhibitor, lapatinib. This design was conducted through multistep reactions to incorporate different flexible spacers at position 6 of the quinazoline ring, namely, acetamido, methylbenzamido, or propoxy. This was followed by a nucleophilic substitution with several polar fragments. At position 4, the *N*-(4-(3-chloro-4-(3-fluorobenzyl)oxy)phenyl) amino moiety of lapatinib was replaced by the *N*-(4-(3-chloro-4-(3-substituted-phenoxy)-phenyl)amino) moiety to properly fit into the lipophilic back pocket with an enhanced selectivity against the target HER2 kinase. Increasing the selectivity against HER2 kinase was assumed to minimize the EGFR inhibition-associated side effects such as severe rash and diarrhea. The synthetic methodologies involved in this project have been optimized to report the most appropriate reaction conditions affording the targeted and intermediate compounds at a higher yield and purity. The *in vitro* protein kinase profiling for the lead compound (**10a**) and the other representative analogues (**10b**, **15a**, **15e**, **15l**, **17d**, and **25f**) at 10 μM single-dose concentration against 20 kinases demonstrated a superior significant selectivity than lapatinib. Our compounds revealed inhibitions within a range of −92 to −99% against HER2 and HER4 kinases and within −67 to −81% against EGFR (HER1). Remarkably, the screened compounds specifically **17d** exhibited negligible activation or even mild inhibition of other nontarget kinases which were activated by lapatinib. These results anticipate lower side effects and toxicity of compound **17d**. This preferential selectivity of the test compounds was an encouraging result to evaluate the cytotoxic activity of the newly synthesized quinazolines against HER2 BC cell lines and HER2-negative cells for comparison. The majority of synthesized compounds demonstrated potent and selective antiproliferative activities toward HER2+ BC cell line AU-565. Furthermore, many compounds revealed augmented activity against triple-positive cells (BT-474) with noticeably diminished activity against HER2-negative BC cells (MCF7 and MDA-MB-231). Against wild-type HER2 kinase, the privileged compounds (**10a**, **10c**, **15i**, **17d**, and **25b**) demonstrated higher inhibitory activity against HER2 kinase with IC_{50} values in the range of 5.4−12 nM compared to lapatinib (95.5 nM). On the other hand, the western blot analysis indicated that the phosphorylation of HER2 downstream signaling through AKT and ERK pathways was impaired in BT-474 and AU-565 cells treated with compounds **15d**, **15i**, and **25b** at different concentration points of IC_{50}, 0.5 IC_{50}, and 0.1 IC_{50} for each compound. The apoptosis assay for compounds **10c**, **15i**, **17d**, and **25b** revealed induction of the early-phase apoptosis in BT-474 cells 3−10-fold compared to the negative control. Furthermore, out of 20 compounds tested at 10 μM single dose in the full NCI 60 cell panel, 13 compounds (**15f**, **15g**, **15i**, **15k**, **17a**, **17c**, **17d**, **25b**, **25d**, **25e**, **25f**, **25g**, and **25h**) were selected to be evaluated at five concentration levels, where compound **17d** demonstrated the highest selectivity against BC. The SAR study expounded that the terminal polar moieties not only affect the drug-likeness and pharmacokinetic properties of the compound but also modulate the cellular activity. We have noticed that compounds bearing a morpholino moiety or its acyclic analogue ethanolamine revealed potent and selective antiproliferative activities against HER2(+) BC cell lines (BT-474 and AU-565). Meanwhile, the *N*-methylpiperazino-bearing compounds exhibited extended moderate activity against the other HER2(−ve) BC cell lines. Inspired by the potent antiproliferative and enzymatic activities of compounds **17d** and **25b** bearing the 4-substituted phenoxyanilino and 4-substituted benzyloxyanilino moiety, respectively, were selected to be tested for their *in vivo* antitumor efficacy using the BT-474 athymic nude mice ($Foxn^{1nu}/Foxn^{1+}$) xenograft model. Even though compound **25b** exhibited higher antiproliferative activity in WST-8 assay (IC_{50} = 0.083 μM) than compound **17d** (IC_{50} = 0.204 μM), both compounds behaved differently in *in vivo* evaluation. Compound **17d** substantially inhibited the BT-474 tumor growth compared to either the vehicle control or compound **25b**-treated groups. This was attributed to the higher $T_{1/2}$ and lower intrinsic clearance of compound **17d** ($T_{1/2}$ = >145, $CL_{int(mic)}$ = <9.6 mL/min/kg), compared to compound **25b** ($T_{1/2}$ = 57.4 min, $CL_{int(mic)}$ = 24.2 mL/min/kg). Interestingly, metastasis was observed in the nude mice treated by the vehicle which was not detected in the other groups treated by compounds **17d** and **25b**. Altogether, we eventually identified compound **17d** as a promising candidate for HER2+ BC therapy deserving further investigations.

EXPERIMENTAL SECTION

Chemistry. This part is concerned with the synthetic schemes adopted for the synthesis of the designed compounds and the description of the synthetic chemical steps used, aided by a literature survey for each route. All the synthesized compounds were purified using flash column chromatography and then subjected to a comprehensive spectrometric analysis including ^{1}H NMR, ^{13}C DEPT, and ^{13}C NMR. In addition, all 27 key target compounds have been further analyzed by HRMS. Using integrated analytical methods, the purity of the synthesized compounds was confirmed at ≥95% by ultrahigh-performance liquid chromatography/MS (UHPLC/MS) and NMR methods. All different spectra of our compounds have been uploaded in the Supporting Information for publication. Thin-layer chromatography (TLC) analysis of reaction mixtures was performed using Sigma-Aldrich silica gel 60 Å, F254 TLC plates, and visualized under UV. Flash column chromatography was carried out on RediSep R_f-Teledyne ISCO cartilages, 230−450 mesh using CombiFlash R_f 200-Teledyne ISCO. The reaction progress was monitored using an Advion Expression-L Mass spectrophotometer using TLC plate extraction or ASAP techniques. ^{1}H, ^{13}C DEPT, and ^{13}C NMR spectra were recorded in $CDCl_3$ or dimethyl sulfoxide (DMSO) at ambient temperature using a Bruker 300 MHz spectrometer. Coupling constants were expressed in Hz and the abbreviations used for multiplicity are as follows: s = singlet, d = doublet, t = triplet, q = quartet, p = pentet, m = multiplet, and br = broad. ^{1}H and ^{13}C NMR chemical shifts are reported in ppm downfield of tetramethylsilane and are, respectively, referenced to the

https://dx.doi.org/10.1021/acs.jmedchem.0c01647
J. Med. Chem. XXXX, XXX, XXX−XXX

residual solvent (δ = 7.26 and 77.36 ppm for $CDCl_3$, δ = 2.54 and 40.45 ppm for DMSO-d_6). High-resolution mass spectra (HRMS) were obtained on LC/MS-TOFAgilent 6210 using electrospray ionization (ESI). Melting points were recorded on a Stuart melting point smp20 apparatus using Kimax Glass Capillary Tubes, 100 mm.

2-Chloro-1-((3-fluorobenzyl)oxy)-4-nitrobenzene (3a). To a mixture of 2-chloro-4-nitrophenol (**1a**) (3.47 g, 20.0 mmol) and potassium carbonate (2.76 g, 20.0 mmol) in DMF (20 mL), 3-fluorobenzyl bromide (**2a**) (3.81 g, 2.47 mL, 20.2 mmol) was added. After being stirred at 85 °C for 3 h, water (40 mL) was added and the mixture was extracted with ethyl acetate (EtOAc). The organic layer was washed with saturated brine (30 mL), dried over anhydrous sodium sulfate (Na_2SO_4), and concentrated in vacuum to yield **3a** (4.10 g, 73% yield) as a light-yellow solid.[108,109]

2-Chloro-4-nitro-1-(3-(substituted)phenoxy)benzene (3b–d). To a mixture of 2-chloro-1-fluoro-4-nitrobenzene (**1b**) (3.50 g, 20.0 mmol) and potassium carbonate (2.76 g, 20.0 mmol) in acetonitrile (20 mL) was added appropriate phenol **2b–d** (20.0 mmol). After being stirred at 85 °C for 5 h, the reaction mixture was filtered while hot and the filtrate was concentrated under reduced pressure to afford **3b–d**.[110,111]

*2-Chloro-1-(3-fluorophenoxy)-4-nitrobenzene (**3b**).* (4.7 g, yield 89%), yellow solid.

*2-Chloro-4-nitro-1-(3-(trifluoromethyl)phenoxy)benzene (**3c**).* (5.2 g, yield 83%), yellow solid.

*2-Chloro-1-(3-methylphenoxy)-4-nitrobenzene (**3d**).* (4.1 g, yield 78%), faint yellow oil.

3-Chloro-4-((3-fluorobenzyl)oxy)aniline (4a). To a suspension of (**3a**) (3.6 g, 12.8 mmol) and reduced iron [2.3 g, 38.4 mmol (3 mol equiv)] in ethanol (50 mL), a solution of calcium chloride (1.5 g, 12.8 mmol, 5 mL water) was added. The mixture was stirred at 85 °C for 8 h. The formed black solid was removed by filtration.

Then, the filtrate was centrifuged for 30 min and then filtered again. The clear filtrate was concentrated under vacuum. The residue was washed with water, filtered, dried, and purified by silica gel column chromatography (eluent, EtOAc/hexane = 1:3) to yield **4a** (2.5 g, 77% yield) as yellowish white crystals.[44]

General Procedure for the Synthesis of 3-Chloro-4-(3-(substituted)phenoxy)aniline (4b–d). A mixture of the appropriate nitro derivative (**3b–d**) (5 mmol) and stannous chloride (4.7 g, 25 mmol) in methanol (20 mL) was stirred at reflux for 2.5 h under a nitrogen atmosphere. Excess methanol was removed under reduced pressure, the remaining residue was dissolved in ethyl acetate (200 mL), and the obtained solution was neutralized with an aqueous saturated solution of sodium bicarbonate and stirred for 1 h. The resulting gelatinous precipitate was centrifuged for 15 min and then discarded by filtration. The clear filtrate was transferred into a separating funnel and the organic phase was separated. The aqueous phase was extracted with ethyl acetate (2 × 20 mL), and the organic fractions were combined, dried over anhydrous sodium sulfate, and concentrated under vacuum to afford the corresponding aniline derivatives **4b–d**.

*3-Chloro-4-(3-fluorophenoxy)aniline (**4b**).* (0.97 g, yield 82%), yellow oil solidifies on cooling.[44]

*3-Chloro-4-(3-(trifluoromethyl)phenoxy)aniline (**4c**).* (1.13 g, yield 79%) brown oil solidifies on cooling.[108,109] ^{1}H NMR (300 MHz, DMSO-d_6): δ 7.57–7.52 (t, J = 7.9 Hz, 1H, Ar-5′-H), 7.38–7.36 (d, J = 7.8 Hz, 1H, Ar-4′-H), 7.10–7.06 (m, 2H, Ar-2′,6′-H), 7.00–6.97 (d, J = 8.6 Hz, 1H, Ar-5-H), 6.75–6.76 (d (m-coupling), J = 1.6 Hz, 1H, Ar-2-H), 6.61–6.57 (dd, J = 8.6, 1.7 Hz, 1H, Ar-6-H), 5.42 (s, 2H, NH_2, exchanged with D_2O).

*3-Chloro-4-(3-methylphenoxy)aniline (**4d**).* (0.87 g, 75%), colorless oil.[44]

Synthesis of *N*′-(2-Cyano-4-nitrophenyl)-*N*,*N*-dimethylformimidamide (6). A stirred mixture of 2-amino-5-nitrobenzonitrile (**5**) (2.5 g, 15.3 mmol) and *N*,*N*-dimethylformamide dimethylacetal (5 mL, 37.6 mmol, 2.4 equiv) was heated under reflux for 2 h and then cooled to room temperature. The resulting precipitate was filtered, washed with ether (3 × 25 mL), and then dried to afford *N*′-(2-cyano-4-nitro-phenyl)-*N*,*N*-dimethyl-formamidine (**6**) as a yellow solid (3 g, 90% yield, mp 153–155 °C, as reported).[112]

Synthesis of 4-(3-Chloro-4-(3-fluorobenzyloxyl)-phenylamino)-6-nitroquinazoline (7). Compound (**6**; 2 g, 9.17 mmol) was held at reflux for 3 h with 3-chloro-4-((3-fluorobenzyl)-oxy)aniline (**4a**) (2.3 g, 9.17 mmol) in glacial acetic acid (10 mL). The formed precipitate was filtered while hot and washed with diethylether (3 × 10 mL) to afford the corresponding nitroquinazoline derivative (**7**) as a yellow to orange solid (3.6 g, 92.5% yield, mp; 280 °C, as reported).[110,113]

Synthesis of 4-(3-Chloro-4-(3-fluorobenzyloxyl)-phenylamino)-6-aminoquinazoline (8). To a suspension of the 6-nitro derivative (**15**; 2.12 g, 5 mmol) and reduced iron (0.85 g, 15 mmol) in ethanol (50 mL), a solution of calcium chloride (0.6 g, 5 mmol, 5 mL water) was added. The mixture was stirred at 90 °C for 12 h. The formed black solid was removed by filtration, and the filtrate was centrifuged for 30 min and then was filtered. The clear filtrate was concentrated under vacuum to afford **8** as a pure yellow solid (97% yield, mp; 190 °C, as reported).[100,110]

2-Chloro-*N*-(4-((3-chloro-4-((3-fluorobenzyl)oxy)phenyl)-amino)quinazolin-6-yl) Acetamide (9). To a solution of 6-aminoquinazoline (**8**) (1.3 g, 3.2 mmol) in acetone (20 mL), $NaHCO_3$ (0.3 g, 3.5 mmol) was added. The reaction mixture was stirred under nitrogen at 0 °C. This was followed by the dropwise addition of solution of 2-chloroacetylchloride (0.4 g, 3.4 mmol) in acetone (2 mL). The reaction mixture was stirred for 1 h at 0 °C.

The excess solvent was removed under reduced pressure. Cold water (20 mL) was added to the remaining residue and the resulting suspension was neutralized with a saturated solution of $NaHCO_3$, if necessary. The formed solid was then filtered, dried, and washed with diethylether (3 × 15 mL) to afford compound **9** as a pure yellow solid. (0.9 g, yield 61%, mp >300 °C); ^{1}H NMR (300 MHz, DMSO): δ 11.31 (s, 1H, NH, exchanged with D_2O), 11.21 (s, 1H, NH, exchanged with D_2O), 8.97 (s, 1H, Ar-2-H), 8.82 (s, 1H, Ar-5-H), 8.06–8.03 (d, J = 8.6 Hz, 1H, Ar-8-H), 7.96–7.93 (d, J = 8.8 Hz, 1H, Ar-7-H), 7.86 (s, 1H, Ar-2′-H), 7.61–7.59 (d, J = 7.9 Hz, 1H, Ar-6″-H), 7.49–7.47 (d, J = 7.2 Hz, 1H, Ar-6′-H), 7.34–7.31 (m 3H, Ar-5′,2″, 4″-H), 7.22–7.16 (t, J = 7.8 Hz, 1H, Ar-5″-H), 5.30 (s, 2H, CH_2, O***C*H*$_2$**C_6H_4F), 4.44 (s, 2H, CH_2, acetamido). ^{13}C DEPT (75 MHz, DMSO): δ 150.81 (1C, Ar-2-CH), 131.04 (1C, Ar-5″-CH), 129.50 (1C, Ar-8-CH), 126.69 (1C, Ar-7-CH), 124.95 (1C, Ar-6″-CH), 123.82 (1C, Ar-6′-CH), 122.53 (1C, Ar-2′-CH), 115.40 (1C, Ar-5′-CH), 114.59 (1C, Ar-4″-CH), 114.39 (1C, Ar-2″-CH), 113.45 (1C, Ar-5-CH), 69.83 (1C, CH_2, O***C*H*$_2$**C_6H_4F), 43.89 (1C, CH_2, acetamido); MS (APCI$^+$): m/z 471.1 $[M + H]^+$.

Synthesis of *N*-(4-((3-Chloro-4-((3-fluorobenzyl)oxy)-phenyl)amino)quinazolin-6-yl)-2-((2-hydroxyethyl)amino)-acetamide (10a). A mixture of the chloroacetamido intermediate (**9**) (0.47 g, 1 mmol) and 2-aminoethanol (0.25 g, 0.3 mL, 5 mmol) in methanol (20 mL) was held at reflux for 4 h in the presence of triethylamine (15 drops). Methanol was then removed under reduced pressure, and the remaining residue was dissolved in dichloromethane (DCM) and purified by flash column chromatography with ethylacetate/MeOH (90:10%) as an eluent to yield compound **10a**.

White solid, mp 140–145 °C, (0.28 g, yield; 57%); ^{1}H NMR (300 MHz, DMSO-d_6): δ 10.15 (s, 1H, NH, exchanged with D_2O), 9.76 (s, 1H, NH, exchanged with D_2O), 8.60 (s, 1H, Ar-2-H), 8.51 (s, 1H, Ar-5-H), 8.07–8.04 (d, J = 9 Hz, 1H, Ar-8-H), 7.99 (d, J = 2.5 Hz (m-coupling), 1H, Ar-2′-H), 7.78–7.75 (d, J = 9 Hz, 1H, Ar-7-H), 7.73–7.69 (dd, J = 9.0, 2.5 Hz, 1H, Ar-6′-H), 7.51–7.44 (m, 1H, Ar-4″-H), 7.34–7.29 (m, 2H, Ar-5′,2″-H), 7.27–7.24 (d, J = 9, Ar-6″-H), 7.21–7.16 (t, J = 9 Hz, 1H, Ar-5″-H), 5.25 (s, 2H, CH_2, O***C*H*$_2$**C_6H_4F), 4.68–4.65 (t, J = 4.9 Hz, 1H, OH, exchanged with D_2O), 3.54–4.49 (q, J = 5 Hz, 1H, CH_2, OH***C*H*$_2$**CH_2NH), 3.37 (s, 2H, CH_2, acetamido), 2.69–2.66 (t, J = 5.3 Hz, 2H, CH_2, $OHCH_2$***C*H*$_2$**NH); ^{13}C DEPT (75 MHz, DMSO-d_6): δ 153.67 (1C, Ar-2-CH), 131.07 (1C, Ar-5″-CH), 130.96 (1C, Ar-8-CH), 128.84 (1C, Ar-7-CH), 127.24 (1C, Ar-6″-CH), 124.54 (1C, Ar-6′-CH), 123.77 (1C, Ar-2′-CH), 115.00 (1C, Ar-5′-CH), 114.69 (1C, Ar-4″-CH), 114.34 (1C, Ar-2″-CH), 112.13 (1C, Ar-5-CH), 69.83 (1C, CH_2, O***C*H*$_2$**C_6H_4F),

https://dx.doi.org/10.1021/acs.jmedchem.0c01647
J. Med. Chem. XXXX, XXX, XXX–XXX

60.83 (1C, CH_2, OH**CH_2**CH_2NH), 53.16 (1C, CH_2, acetamido), 52.18 (1C, CH_2, OHCH$_2$**CH_2**NH); ^{13}C NMR (75 MHz, DMSO): δ 171.18 (1C, C═O), 167.28 (1C, Ar-4-C), 161.05 (1C, Ar-3″-C) 157.77 (1C, Ar-4′-C), 153.67 (1C, Ar-2-CH), 150.01 (1C, Ar-6-C), 146.91 (1C, Ar-8a-C), 140.11 (1C, Ar-1″-C), 136.81 (1C, Ar-1′-C), 133.86 (1C, Ar-3′-C), 131.06 (1C, Ar-5″-CH), 130.96 (1C, Ar-8-CH), 128.84 (1C, Ar-7-CH), 127.24 (1C, Ar-6″-CH), 124.54 (1C, Ar-6′-CH), 123.76 (1C, Ar-2′-CH), 115.72 (1C, Ar-4a-C), 115.28 (1C, Ar-5′-CH), 114.72 (1C, Ar-4″-CH), 114.33 (1C, Ar-2″-CH), 112.13 (1C, Ar-5-CH), 69.85 (1C, CH_2, O**CH_2**C_6H_4F), 60.84 (1C, CH_2, OH**CH_2**CH_2NH), 53.16 (1C, CH_2, acetamido), 52.17 (1C, CH_2, OHCH$_2$**CH_2**NH); HRMS (ES$^+$): m/z calcd for $C_{25}H_{24}ClFN_5O_3$ [M + 1]$^+$, 496.1552; found, 496.1547.

General Procedure for the Synthesis of Compounds 10b and 10c. A mixture of compound **9** (0.47 g, 1 mmol) and the appropriate secondary amine, 1-methyl piperazine or morpholine (50 mmol), was heated under reflux temperature for 2 h. The reaction mixture was then cooled to room temperature, poured onto iced-water (30 mL) portion wise while stirring, and 0.2 g of NaCl was added, where a precipitate was formed. The resultant precipitate was filtered, washed with water, and dried. Trituration of the dried precipitate with diethylether (3 × 15 mL) afforded the desired products (**10b** and **10c**) as pure compounds with no need for further purification.

*N-(4-((3-Chloro-4-((3-fluorobenzyl)oxy)phenyl)amino)-quinazolin-6-yl)-2 Morpholino Acetamide (**10b**).* Yellowish white solid, mp 175−180 °C, (0.4 g, yield; 87%); ^{1}H NMR (300 MHz, DMSO-d_6): δ 10.01 (s, 1H, NH, exchanged with D_2O), 9.77 (s, 1H, NH, exchanged with D_2O), 8.62 (s, 1H, Ar-2-H), 8.51 (s, 1H, Ar-5-H), 8.01−7.97 (dd, J = 8.7, 1.9 Hz, 2H, Ar-8, 2′-H) 7.77−7.74 (d, J = 8.8 Hz, 1H, Ar-7-H), 7.72−7.68 (dd, J = 8.9, 2.3 Hz, 1H, Ar-6′-H), 7.50−7.43 (m, 1H, Ar-4″-H), 7.34−7.30 (m, 2H, Ar-5′, 2″-H), 7.27−7.24 (d, J = 9, Ar-6″-H), 7.21−7.15 (t, J = 9 Hz, 1H, Ar-5″-H), 5.25 (s, 2H, CH_2, O**CH_2**C_6H_4F), 3.69−3.66 (t, J = 6, 4H, 2CH_2, morpholino), 3.21 (s, 2H, CH_2, acetamido), 2.58−2.55 (t, J = 6, 4H, 2CH_2, morpholino); ^{13}C DEPT (75 MHz, DMSO): δ 153.77 (1C, Ar-2-CH), 131.05 (1C, Ar-5″-CH), 130.95 (1C, Ar-8-CH), 128.73 (1C, Ar-7-CH), 127.81 (1C, Ar-6″-CH), 124.67 (1C, Ar-6′-CH), 123.76 (1C, Ar-2′-CH), 115.27 (1C, Ar-5′-CH), 114.74 (1C, Ar-4″-CH), 114.33 (1C, Ar-2″-CH), 112.85 (1C, Ar-5-CH), 69.89 (1C, CH_2, O**CH_2**C_6H_4F), 66.57 (2C, 2CH_2, morpholino), 62.38 (1C, CH_2, acetamido), 53.72 (2C, 2CH_2, morpholino); ^{13}C NMR (75 MHz, DMSO): δ 168.80 (1C, C═O), 164.29 (1C, Ar-4-C), 161.06 (1C, Ar-3″-C), 157.83 (1C, Ar-4′-C), 153.76 (1C, Ar-2-CH), 150.09 (1C, Ar-6-C), 147.06 (1C, Ar-8a-C), 140.21 (1C, Ar-1″-C), 136.63 (1C, Ar-1′-C), 133.84 (1C, Ar-3′-C), 131.05 (1C, Ar-5″-CH), 130.94 (1C, Ar-8-CH), 128.73 (1C, Ar-7-CH), 127.80 (1C, Ar-6″-CH), 124.67 (1C, Ar-6′-CH), 123.74 (1C, Ar-2′-CH), 115.65 (1C, Ar-4a-C), 115.27 (1C, Ar-5′-CH), 114.78 (1C, Ar-4″-CH), 114.33 (1C, Ar-2″-CH), 112.85 (1C, Ar-5-CH), 69.92 (1C, CH_2, O**CH_2**C_6H_4F), 66.57 (2C, 2CH_2, morpholino), 62.38 (1C, CH_2, acetamido), 53.73 (2C, 2CH_2, morpholino); HRMS (ES$^+$): m/z calcd for $C_{27}H_{26}ClFN_5O_3$ [M + 1]$^+$, 522.1708; found, 522.1705.

*N-(4-((3-Chloro-4-((3-fluorobenzyl)oxy)phenyl)amino)-quinazolin-6-yl)-2-(4-methylpiperazin-1-yl)acetamide (**10c**).* Grayish brown solid, mp 155−158 °C, (0.4 g, yield; 78%); ^{1}H NMR (300 MHz, DMSO-d_6): δ 9.93 (s, 1H, NH, exchanged with D_2O), 9.77 (s, 1H, NH, exchanged with D_2O), 8.59 (s, 1H, Ar-2-H), 8.51 (s, 1H, Ar-5-H), 8.02−7.99 (d, J = 9 Hz, 1H, Ar-8-H), 7.98−7.97 (d, J = 3 Hz (m-coupling) 1H, Ar-2′-H), 7.77−7.74 (d, J = 9 Hz, 1H, Ar-7-H), 7.72−7.68 (dd, J = 9, 3 Hz, 1H, Ar-6′-H), 7.50−7.43 (m, 1H, Ar-4″-H), 7.34−7.29 (m, 2H, Ar-5′, 2″-H), 7.27−7.24 (d, J = 9, Ar-6″-H), 7.21−7.15 (t, J = 9 Hz, 1H, Ar-5″-H), 5.25 (s, 2H, CH_2, O**CH_2**C_6H_4F), 3.19 (s, 2H, CH_2, acetamido), 2.57 (br s, 4H, 2CH_2, piperazino), 2.41 (br s, 4H, 2CH_2 piperazino), 2.18 (s, 3H, CH_3); ^{13}C DEPT (75 MHz, DMSO): δ 153.76 (1C, Ar-2-CH), 131.07 (1C, Ar-5″-CH), 130.96 (1C, Ar-8-CH), 128.77 (1C, Ar-7-CH), 127.65 (1C, Ar-6″-CH), 124.67 (1C, Ar-6′-CH), 123.79 (1C, Ar-2′-CH), 115.29 (1C, Ar-5′-CH), 114.69 (1C, Ar-4″-CH), 114.34 (1C, Ar-2″-CH), 112.63 (1C, Ar-5-CH), 69.83 (1C, CH_2, O**CH_2**C_6H_4F), 62.14 (1C, CH_2, acetamido), 54.98 (2C, 2CH_2, piperazino), 53.28 (2C, 2CH_2, piperazino), 46.20 (1C, CH_3); ^{13}C NMR (75 MHz, DMSO): δ 169.01 (1C, C═O), 164.28 (1C, Ar-4-C), 161.05 (1C, Ar-3″-C), 157.81 (1C, Ar-4′-C), 153.76 (1C, Ar-2-CH), 150.06 (1C, Ar-6-C), 147.02 (1C, Ar-8a-C), 140.19 (1C, Ar-1″-C), 136.64 (1C, Ar-1′-C), 133.78 (1C, Ar-3′-C), 131.07 (1C, Ar-5″-CH), 130.96 (1C, Ar-8-CH), 128.77 (1C, Ar-7-CH), 127.65 (1C, Ar-6″-CH), 124.83 (1C, Ar-6′-CH), 123.79 (1C, Ar-2′-CH), 115.65 (1C, Ar-4a-C), 115.28 (1C, Ar-5′-CH), 114.70 (1C, Ar-4″-CH), 114.33 (1C, Ar-2″-CH), 112.63 (1C, Ar-5-CH), 69.83 (1C, CH_2, O**CH_2**C_6H_4F), 62.14 (1C, CH_2, acetamido), 54.99 (2C, 2CH_2, piperazino), 53.28 (2C, 2CH_2, piperazino), 46.20 (1C, CH_3); HRMS (ES$^+$): m/z calcd for $C_{28}H_{29}ClFN_6O_2$ [M + 1]$^+$, 535.2025; found, 535.2024.

Ethyl-*N*-(2-cyano-4-nitrophenyl)formimidate (11). 2-Amino-5-nitrobenzonitrile (**5**; 5 g, 30.6 mmol) was held at reflux in triethyl orthoformate (50 mL) for 30 h in the presence of acetic anhydride (10 drops). The reaction mixture was cooled to room temperature, poured onto ice water, and stirred for half an hour. The formed precipitate was filtered under vacuum and left to dry to yield compound **11**. Yellow solid, 5.6 g, yield 88%.[114]

General Procedure for the Synthesis of Compounds (12a−c). Compound (**11**; 2.19 g, 10 mmol) was held at reflux for 7 h with the appropriate aniline derivative (**4b−d**) (10.2 mmol) in glacial acetic acid (20 mL). The reaction mixture was then poured onto the ice/water mixture and stirred for 30 min with the addition of 0.2 g of NaCl, and the precipitate formed was filtered, washed with diethylether, and dried. The obtained solid was recrystallized from methanol to afford the corresponding nitroquinazoline derivative (**12a−c**) as a fluffy yellow solid.

*N-(3-Chloro-4-(3-fluorophenoxy)phenyl)-6-nitroquinazolin-4-amine (**12a**).* (3.1 g, yield 76%); ^{1}H NMR (300 MHz, DMSO-d_6): δ 10.47 (s, 1H, NH, exchanged with D_2O), 9.61 (s, 1H, Ar-5-H), 8.75 (s, 1H, Ar-2-H), 8.55−8.52 (d, J = 9 Hz, 1H, Ar-7-H), 8.23 (s, 1H, Ar-2′-H), 7.94−7.88 (m, 2H, Ar-2″, 8-H), 7.46−7.38 (m, 1H, Ar-6′-H), 7.31−7.28 (d, J = 8.5 Hz, 1H, Ar-4″-H), 6.99−6.93 (t, J = 8.4 Hz, 1H, Ar-5″-H), 6.87−6.83 (d, J = 10.5 Hz, 1H, Ar-5′-H), 6.79−6.76 (d, J = 8.5 Hz, 1H, Ar-6″-H); ^{13}C DEPT (75 MHz, DMSO-d_6): δ 157.90 (1C, Ar-2-CH), 131.89 (1C, Ar-8-CH), 130.06 (1C, Ar-5″-CH), 127.15 (1C, Ar-7-CH), 124.5 6 (1C, Ar-5′-CH), 123.15 (1C, Ar-6′-CH), 122.60 (1C, Ar-5-CH), 121.15 (1C, Ar-2′-CH), 113.02 (1C, Ar-6″-CH), 110.19 (1C, Ar-4″-CH), 104.72 (1C, Ar-2″-CH); MS (APCI$^-$): m/z 411.5[M + 1]$^+$.

*N-(3-Chloro-4-(3-(trifluoromethyl)phenoxy)phenyl)-6-nitroquinazolin-4-amine (**12b**).* (3.5 g, yield; 78%), mp 185−187 °C, as reported.[50]

*N-(3-Chloro-4-(m-tolyloxy)phenyl)-6-nitroquinazolin-4-amine (**12c**).* (3.3 g, yield: 82%), ^{1}H NMR (300 MHz, DMSO-d_6): δ 10.48 (s, 1H, NH, exchanged with D_2O), 9.63 (s, 1H, Ar-5-H), 8.75 (s, 1H, Ar-2-H), 8.57−8.54 (dd, J = 9.1, 1.9 Hz, 1H, Ar-7-H), 8.19 (s, 1H, Ar-2′-H), 7.95−7.92 (d, J = 9.1 Hz, 1H, Ar-8-H), 7.79−7.76 (d, J = 9.1 Hz, 1H, Ar-6′-H), 7.35−7.32 (d, J = 9.1 Hz, 1H, Ar-5′-H), 7.24−7.19 (m, 1H, Ar-2″), 7.12−7.07 (t, J = 7.4 Hz, 1H, Ar-5″-H), 7.00−6.97 (d, J = 7.7 Hz, 1H, Ar-6″-H), 6.80−6.78 (d, J = 7.5 Hz, 1H, Ar-4″-H), 2.25 (s, 3H, CH_3). ^{13}C DEPT (75 MHz, DMSO-d_6): δ 158.03 (1C, Ar-2-CH), 132.02 (1C, Ar-8-CH), 130.03 (1C, Ar-5″-CH), 127.93 (1C, Ar-7-CH), 127.17 (1C, Ar-4″-CH), 124.88 (1C, Ar-5′-CH), 124.38 (1C, Ar-6′-CH), 123.24 (1C, Ar-5-CH), 121.20 (1C, Ar-2′-CH), 119.92 (1C, Ar-2″-CH), 117.83 (1C, Ar-6″-CH). MS (ESI$^+$): m/z 407.1 [M + 1]$^+$.

General Procedure for the Synthesis of Compounds (13a−c). A mixture of the 6-nitro quinazoline derivatives (**12a−c**) (5 mmol) and stannous chloride (25 mmol) in methanol (20 mL) was stirred at reflux for 1.5 h, under a nitrogen atmosphere. Excess methanol was removed under reduced pressure, the remaining residue was dissolved in ethyl acetate (200 mL), and the resulting solution was neutralized with an aqueous saturated solution of $NaHCO_3$ and stirred for 1 h. The resulting gelatinous precipitate was centrifuged for 45 min and then discarded by filtration. The clear filtrate was transferred into a separating funnel, and the organic layer was

https://dx.doi.org/10.1021/acs.jmedchem.0c01647
J. Med. Chem. XXXX, XXX, XXX−XXX

separated from the aqueous one. The aqueous phase was extracted with ethyl acetate (2 × 20 mL), and the organic fractions were combined, dried over anhydrous sodium sulfate, and concentrated under vacuum to afford the corresponding 6-amino quinazoline derivatives **13a−c**.

*N-4-(3-Chloro-4-(3-fluorophenoxy)phenyl)quinazoline-4,6-diamine (**13a**).* Brown oil, (1.63 g, yield; 86%), ^{1}H NMR (300 MHz, DMSO-d_6): δ 9.54 (s, 1H, NH, exchanged with D_2O), 8.38 (s, 1H, Ar-2-H), 8.27 (s, 1H, Ar-2″-H), 7.91−7.88 (d, J = 8.7 Hz, 1H, Ar-8-H), 7.57−7.54 (d, J = 8.8 Hz, 1H, Ar-7-H), 7.43−7.38 (m, 1H, AR-5-H), 7.34 (s, 1H, Ar-2′-H), 7.28−7.25 (d, J = 8.5 Hz, 2H, Ar-4″, 6′-H), 6.96−6.91 (t, J = 8.1 Hz, 1H, Ar-5″-H), 6.82−6.79 (d, J = 10.5 Hz, 1H, Ar-5′-H), 6.75−6.73 (d, J = 8.2 Hz, 1H, Ar-6″-H), 5.65 (s, 2H, NH_2, exchanged with D_2O). MS (APCI$^+$): m/z 381.2 $[M + 1]^+$.

*N-4-(3-Chloro-4-(3-(trifluoromethyl)phenoxy)phenyl)-quinazoline-4,6-diamine (**13b**).* Yellow solid, 1.97 g, yield; 86%, mp 104−106 °C, as reported.[110]

*N-4-(3-Chloro-4-(m-tolyloxy)phenyl)quinazoline-4,6-diamine (**13c**).* Brown solid, (1.77 g, yield; 94%), ^{1}H NMR (300 MHz, DMSO-d_6):δ 9.46 (s, 1H, NH, exchanged with D_2O), 8.37 (s, 1H, Ar-2-H), 8.23 (s, 1H, Ar-2′-H), 7.81−7.78 (d, J = 8.6 Hz, 1H, Ar-8-H), 7.57−7.54 (d, J = 8.8 Hz, 1H, Ar-7-H), 7.34 (s, 1H, Ar-5-H), 7.31−7.25 (m, 2H, Ar-6″, 6′), 7.20−7.15 (m, 1H, Ar-2″-H), 7.07−7.02 (t, J = 7.3 Hz, 1H, Ar-5″-H), 7.00−6.97 (d, J = 8.9 Hz, 1H, Ar-5′-H), 6.73−6.70 (d, J = 7.5 Hz, 1H, Ar-4″-H), 5.61 (s, 2H, NH_2, exchanged with D_2O), 2.26 (s, 3H, CH_3). ^{13}C DEPT (75 MHz, DMSO-d_6): δ 150.10 (1C, Ar-2-CH), 131.89 (1C, Ar-8-CH), 129.17 (1C, Ar-5″-CH), 127.78 (1C, Ar-7-CH), 124.23 (1C, Ar-4″-CH), 123.90 (1C, Ar-5′-CH), 123.49 (1C, Ar-6′-CH), 122.05 (1C, Ar-2′-CH), 120.53 (1C, Ar-2″-CH), 117.07 (1C, Ar-6″-CH), 101.34 (1C, Ar-5-CH), 16.21 (1C, CH_3). MS (APCI$^+$): m/z 377.1 $[M + 1]^+$.

General Procedure for the Synthesis of Compounds 14a−c. To the solution of intermediate **13a−c** (5 mmol) in acetone (20 mL), $NaHCO_3$ (0.44 g, 5.2 mmol) was added. The reaction mixture was stirred under nitrogen at 0 °C, followed by the dropwise addition of 2-choroacetyl chloride (0.4 mL, 5.2 mmol) and stirring was continued for 1 h at 0 °C. Excess solvent was then removed under reduced pressure.

Cold water was added (20 mL) to the remaining residue and the resulting suspension was neutralized with a solution of $NaHCO_3$, if necessary (if pH still acidic). The formed solid was then filtered and purified by column chromatography with EtOAc as an eluent to afford compounds **14a−c** as a yellow solid.

*2-Chloro-N-(4-((3-chloro-4-(3-fluorophenoxy)phenyl)amino)-quinazolin-6-yl)acetamide (**14a**).* (1.41 g, yield; 62%), ^{1}H NMR (300 MHz, DMSO-d_6): δ 10.93 (s, 2H, 2NH, exchanged with D_2O), 8.83 (s, 1H, Ar-2-H), 8.69 (s, 1H, Ar-5-H), 8.14 (s, 1H, Ar-2″-H), 7.9−7.94 (d, J = 8.9 Hz, 1H, Ar-8-H), 7.87−7.80 (m, 2H, Ar-7, 6′-H), 7.45−7.38 (dd, 1H, Ar-4″-H), 7.30−7.28 (d, J = 8.8 Hz, 1H, Ar-5′-H), 6.99−6.93 (t, J = 7.7 Hz, 1H, Ar-5″-H), 6.86−6.76 (m, 2H, Ar-2′,6″-H), 4.40 (s, 2H, CH_2). ^{13}C DEPT (75 MHz, DMSO-d_6): δ 152.59 (1C, Ar-2-CH), 131.90 (1C, Ar-5″-CH), 128.40 (1C, Ar-8-CH), 126.65 (1C, Ar-7-CH), 125.12 (1C, Ar-5′-CH), 123.76 (1C, Ar-6′-CH), 122.55 (1C, Ar-2′-CH), 113.11 (1C, Ar-6″-CH), 112.99 (1C, Ar-4″-CH), 110.19 (1C, Ar-2″-CH), 104.71 (1C, Ar-5-CH), 43.90 (1C, CH_2). MS (APCI$^+$): m/z 457.2 $[M + 1]^+$.

*2-Chloro-N-(4-((3-chloro-4-(3-(trifluoromethyl) phenoxy)-phenyl)amino)quinazolin-6-yl)acetamide (**14b**).* 1.36 g, yield; 54%, ^{1}H NMR (300 MHz, DMSO-d_6): δ 10.94 (s, 2H, NH, exchanged with D_2O), 8.87 (s, 1H, Ar-2-H), 8.73 (s, 1H, Ar-5-H), 8.17−8.18 (d (m-coupling), J = 1.2 Hz, 1H, Ar-2′-H), 7.97−7.94 (d, J = 9 Hz, 1H, Ar-8-H), 7.89−7.82 (m, 2H, Ar-7, 6′-H), 7.66−7.61 (t, J = 7.8 Hz, 1H, Ar-5″-H), 7.51−7.48 (d, J = 7.7 Hz, 1H, Ar-4″-H), 7.36−7.33 (d, J = 7.7 Hz, 1H, Ar-6″-H), 7.28−7.24 (m, 2H, Ar-2″, 5′), 4.41 (s, 2H, CH_2); ^{13}C DEPT (75 MHz, DMSO-d_6): δ 152.40 (1C, Ar-2-CH), 131.98 (1C, Ar-5″-CH), 128.60 (1C, Ar-8-CH), 126.16 (1C, Ar-7-CH), 125.40 (1C, Ar-6″-CH), 124.10 (1C, Ar-5′-CH), 122.74 (1C, Ar-6′-CH), 120.96 (1C, Ar-4″-CH), 120.16 (1C, Ar-2′-CH), 113.56 (1C, Ar-2″-CH), 113.12 (1C, Ar-5-CH), 43.90 (1C, CH_2); MS (ESI$^+$): m/z 507.1 $[M + 1]^+$.

*2-Chloro-N-(4-((3-chloro-4-(m-tolyloxy)phenyl)amino)-quinazolin-6-yl) Acetamide (**14c**).* (2.01 g, yield; 89%); ^{1}H NMR (300 MHz, DMSO-d_6): δ 11.22 (s, 2H, 2NH, exchanged with D_2O), 8.97 (s, 1H, Ar-2-H), 8.83 (s, 1H, Ar-5-H), 8.08−7.95 (m, 3H, Ar-Ar-2′,8,7-H), 7.65−7.62 (d, J = 8.8 Hz, 1H, Ar-6′-H), 7.36−7.34 (d, J = 7.8 Hz, 1H, Ar-6″-CH), 7.26−7.21 (m, 1H, Ar-2″-CH), 7.14−7.09 (t, J = 7.8 Hz, 1H, Ar-5″-CH), 6.97−6.94 (d, J = 8.8 Hz, 1H, Ar-5′-H), 6.86−6.83 (d, J = 7.9 Hz, 1H, Ar-4″-CH), 4.44 (s, 2H, CH_2), 2.24 (s, 3H, CH_3); ^{13}C DEPT (75 MHz, DMSO-d_6): δ 150.93 (1C, Ar-2-CH), 132.10 (1C, Ar-8-CH), 129.47 (1C, Ar-5″-CH), 128.01 (1C, Ar-7-CH), 126.71 (1C, Ar-4″-CH), 124.98 (1C, Ar-5′-CH), 124.7 (1C, Ar-6′-CH)$_3$, 122.94 (1C, Ar-2′-CH), 119.29 (1C, Ar-2″-CH), 118.40 (1C, Ar-6″-CH), 113.44 (1C, Ar-5-CH), 43.86 (1C, CH_2), 16.12 (1C, CH_3); MS (APCI$^+$): m/z 453.6 $[M + 1]^+$.

General Procedure for the Synthesis of Compounds (15a−l). A mixture of appropriate 6-chloro-acetamido-quinazoline derivative (**14a−c**) (1 mmol) and the appropriate secondary amine, 1-methyl piperazine or morpholine (50 mmol), was placed into a 25 mL round-bottomed flask or into a capped vial in the case of low boiling point secondary amine including dimethylamine or diethylamine (50 mmol). The reaction mixture was heated under reflux temperature and monitored by TLC. After 2 h, the TLC of reaction mass indicated the absence of intermediate (**14a−c**). The reaction mixture was cooled to room temperature and poured onto iced-water (30 mL) portion wise while stirring, and the resultant precipitate was collected by filtration, washed with water, dried, and purified by flash column chromatography using DCM/methanol (95:5%) as an eluent to afford the desired products (**15a-1**).

*N-(4-((3-Chloro-4-(3-fluorophenoxy)phenyl)amino)quinazolin-6-yl)-2-morpholino Acetamide (**15a**).* Yellow solid, 0.39 g, yield; 77%, mp 122−125 °C; ^{1}H NMR (300 MHz, DMSO-d_6): δ 10.05 (s, 1H, NH, exchanged with D_2O), 9.95 (s, 1H, NH, exchanged with D_2O), 8.68 (s, 1H, Ar-2-H), 8.59 (s, 1H, Ar-5-H), 8.22 (s, 1H, Ar-2″-H), 8.03−8.00 (d, J = 9 Hz, 1H, Ar-8-H), 7.90−7.87 (d, 1H, J = 8.5, Ar-6′-H), 7.81−7.78 (d, J = 9 Hz, 1H, Ar-7-H), 7.44, 7.37 (dd, 1H, Ar-4″-H), 7.30−7.27 (d, 1H, J = 8.7, Ar-5′-H), 6.97−6.92 (t, J = 7.1 Hz, 1H, Ar-5″-H), 6.84−6.74 (m, 2H, Ar-2′, 6″-H), 3.67 (br s, 4H, $2CH_2$, morpholino), 3.22 (s, 2H, CH_2, acetamido), 2.57 (br s, 4H, $2CH_2$, morpholino); ^{13}C DEPT (75 MHz, DMSO-d_6): δ 153.58 (1C, Ar-2-CH), 131.86 (1C, Ar-5″-CH), 128.84 (1C, Ar-8-CH), 128.00 (1C, Ar-7-CH), 124.08 (1C, Ar-5′-CH), 122.83 (1C, Ar-6′-CH), 112.78 (1C, Ar-2′-CH), 110.28 (1C, Ar-6″-CH), 110.00 (1C, Ar-4″-CH), 104.80 (1C, Ar-2″-CH), 104.47 (1C, Ar-5-CH), 66.57 (2C, $2CH_2$, morpholine), 62.40 (1C, CH_2, acetamido), 53.72 (2C, $2CH_2$, morpholine); ^{13}C NMR (75 MHz, DMSO-d_6): δ 173.77 (1C, C═O), 163.85 (1C, Ar-4-C), 162.42 (1C, Ar-3″-C), 158.34 (1C, Ar-1″-C), 151.81 (1C, Ar-2-CH), 150.97 (1C, Ar-6-C), 142.58 (1C, Ar-8a-C), 141.52 (1C, Ar-4′-C), 136.62 (1C, Ar-1′-C), 136.49 (1C, Ar-5″-CH), 133.54 (1C, Ar-8-CH), 132.73 (1C, Ar-3′-C), 130.09 (1C, Ar-7-CH), 128.90 (1C, Ar-5′-CH), 127.66 (1C, Ar-6′-CH), 120.45 (1C, Ar-2′-C), 117.52 (1C, Ar-4a-C), 115.03 (1C, Ar-6″-CH), 114.75 (1C, Ar-4″-CH), 109.49 (1C, Ar-2″-CH), 109.16 (1C, Ar-5-CH), 71.29 (2C, $2CH_2$, morpholino), 67.10 (2C, $2CH_2$, morpholino), 58.42 (2C, $2CH_2$, morpholino); HRMS (ES$^+$): m/z calcd for $C_{26}H_{24}ClFN_5O_3$ $[M + 1]^+$, 508.1552; found, 508.1559.

*N-(4-((3-Chloro-4-(3-fluorophenoxy)phenyl)amino)quinazolin-6-yl)-2-(4-methylpiperazin-1-yl)acetamide (**15b**).* Light-brown solid, 0.35 g, yield; 68%, mp 163−165 °C; ^{1}H NMR (300 MHz, DMSO-d_6): δ 9.97 (s, 1H, NH, exchanged with D_2O), 9.95 (s, 1H, NH, exchanged with D_2O), 8.65 (s, 1H, Ar-2-H), 8.59 (s, 1H, Ar-5-H), 8.22 (s, 1H, Ar-2′-H), 8.05−8.02 (d, J = 8.7 Hz, 1H, Ar-8-H), 7.90−7.89, 7.87−7.86 (dd, J = 8.8, 1.07 Hz, 1H, Ar-7-H), 7.81−7.78 (d, 1H, J = 9, Ar-6′-H), 7.45−7.37 (m, 1H, Ar-2″-H), 7.30−7.28 (d, 1H, J = 8.9, Ar-5′-H), 6.98−6.92 (t, J = 8.3 Hz, 1H, Ar-5″-H), 6.84−6.81 (d, J = 8.5 Hz, 1H, Ar-4″-H), 6.78−6.75 (d, J = 8.2 Hz, 1H, Ar-6″-H), 3.20 (s, 2H, CH_2, acetamido), 2.57 (br s, 4H, $2CH_2$, piperazino), 2.41 (br s, 4H, $2CH_2$, piperazino), 2.18 (s, 3H, CH_3); ^{13}C DEPT (75 MHz, DMSO-d_6): δ 153.54 (1C, Ar-2-CH), 131.75 (1C, Ar-5″-CH), 128.86 (1C, Ar-8-CH), 127.84 (1C, Ar-7-CH), 125.01 (1C, Ar-5′-CH), 124.07 (1C, Ar-6′-CH), 122.79 (1C, Ar-2′-CH), 112.75 (1C, Ar-6″-

https://dx.doi.org/10.1021/acs.jmedchem.0c01647
J. Med. Chem. XXXX, XXX, XXX−XXX

CH), 112.58 (1C, Ar-4″-CH), 110.01 (1C, Ar-2″-CH), 104.46 (1C, Ar-5-CH), 62.17 (1C, CH_2, acetamido), 54.99 (2C, $2CH_2$, piperazine), 53.29 (2C, $2CH_2$, piperazino), 46.23 (1C, CH_3); ^{13}C NMR (75 MHz, DMSO-d_6): δ 169.09 (1C, C═O), 159.12 (1C, Ar-4-C), 157.63 (1C, Ar-1″-C), 153.57 (1C, Ar-2-CH), 147.12 (1C, Ar-6-C), 146.17 (1C, Ar-8a-C), 137.91 (1C, Ar-4′-C), 136.84 (2C, Ar-1′, 3″-C), 131.74 (1C, Ar-5″-CH), 128.87 (1C, Ar-8-CH), 127.86 (1C, Ar-7-CH), 125.29 (2C, Ar-3′-C, Ar-6″-CH), 125.00 (1C, Ar-5′-CH), 124.10 (2C, Ar-6′, 4″-CH), 122.86 (1C, Ar-2′-CH), 115.76 (1C, Ar-4a-C), 110.00 (1C, Ar-2″-CH), 104.46 (1C, Ar-5-CH), 62.15 (1C, CH_2, acetamido), 54.98 (2C, $2CH_2$, piperazino), 53.28 (2C, $2CH_2$, piperazino), 46.21 (1C, CH_3); HRMS (ES^+): m/z calcd for $C_{27}H_{27}ClFN_6O_2$ $[M + 1]^+$, 521.1868; found, 521.1868.

*N-(4-((3-Chloro-4-(3-fluorophenoxy)phenyl)amino)quinazolin-6-yl)-2-(diethylamino) Acetamide (**15c**).* Brown solid, 0.4 g, yield; 86%, mp 110−115 °C; ^1H NMR (300 MHz, DMSO-d_6): δ 9.95 (s, 2H, 2NH, exchanged with D_2O), 8.62 (s, 1H, Ar-2-H), 8.59 (s, 1H, Ar-5-H), 8.24 (s, 1H, Ar-2″-H), 8.21−8.18 (d, J = 9 Hz, 1H, Ar-8-H), 7.92−7.89 (d, 1H, J = 9 Hz, Ar-7-H), 7.81−7.78 (d, 1H, J = 9, Ar-5′-H), 7.45−7.37 (dd, 1H, Ar-6′-H), 7.30−7.27 (d, 1H, J = 8.8, Ar-2′-H), 6.98−6.92 (t, J = 9 Hz, 1H, Ar-5″-H), 6.84−6.81 (d, J = 9 Hz, 1H, Ar-4″-H), 6.77−6.74 (d, 1H, J = 9 Hz, Ar-6″-H), 3.23 (s, 2H, CH_2, acetamido), 2.68−2.61 (q, J = 7 Hz, 4H, $2CH_2$, $(CH_3\mathbf{C}\boldsymbol{H}_2)_2N-$), 1.09−1.04 (t, J = 7 Hz, 6H, $2CH_3$, $(\mathbf{C}\boldsymbol{H}_3CH_2)_2N-$); ^{13}C DEPT (75 MHz, DMSO-d_6): δ 153.53 (1C, Ar-2-CH), 131.85 (1C, Ar-8-CH), 128.92 (1C, Ar-5″-CH), 127.38 (1C, Ar-7-CH), 124.04 (1C, Ar-5′-CH), 122.79 (1C, Ar-6′-CH), 112.77 (1C, Ar-2′-CH), 112.18 (1C, Ar-6″-CH), 110.28 (1C, Ar-4″-CH), 104.81 (1C, Ar-2″-CH), 104.46 (1C, Ar-5-CH), 57.78 (1C, CH_2, acetamido), 48.48 (2C, $2CH_2$, $(CH_3\mathbf{C}\boldsymbol{H}_2)_2N-$), 12.44 (2C, $2CH_3$, $(\mathbf{C}\boldsymbol{H}_3CH_2)_2N-$); ^{13}C NMR (75 MHz, DMSO-d_6): δ 170.98 (1C, C═O), 159.06 (1C, Ar-4-C), 158.92 (1C, Ar-3″-C), 157.65 (1C, Ar-1″-C), 153.55 (1C, Ar-2-CH), 146.86 (1C, Ar-6-C), 146.29 (1C, Ar-8a-C), 137.69 (1C, Ar-4′-C), 136.69 (1C, Ar-1′-C), 131.89 (1C, Ar-8-CH), 128.80 (1C, Ar-5″-CH), 127.51 (1C, Ar-7-CH), 125.38 (1C, Ar-3′-C), 124.20 (1C, Ar-5′-CH), 122.83 (1C, Ar-6′-CH), 115.68 (1C, Ar-4a-C), 112.72 (1C, Ar-2′-CH), 112.05 (1C, Ar-6″-CH), 110.29 (1C, Ar-4″-CH), 104.67 (1C, Ar-2″-CH), 104.34 (1C, Ar-5-CH), 57.68 (1C, CH_2, acetamido), 48.47 (2C, $2CH_2$, $(CH_3\mathbf{C}\boldsymbol{H}_2)_2N-$), 12.35 (2C, $2CH_3$, $(\mathbf{C}\boldsymbol{H}_3CH_2)_2N-$); HRMS ($ES^+$): m/z calcd for $C_{26}H_{26}ClFN_5O_2$ $[M + 1]^+$, 494.1759; found, 494.1756.

*N-(4-((3-Chloro-4-(3-fluorophenoxy)phenyl)amino)quinazolin-6-yl)-2-(dimethylamino)acetamide (**15d**).* Brown solid, 0.3 g, yield: 72%; ^1H NMR (300 MHz, DMSO-d_6): δ 10.00 (s, 1H, NH, exchanged with D_2O), 9.91 (s, 1H, NH, exchanged with D_2O), 8.65 (s, 1H, Ar-2-H), 8.58 (s, 1H, Ar-5-H), 8.23 (s, 1H, Ar-2″-H), 8.13−8.10 (d, J = 9 Hz, 1H, Ar-8-H), 7.90−7.87 (d, 1H, J = 8.6, Ar-6′-H), 7.80−7.77 (d, J = 9 Hz, 1H, Ar-7-H), 7.44−7.37 (dd, 1H, Ar-4″-H), 7.30−7.27 (d, 1H, J = 8.8, Ar-5′-H), 6.98−6.92 (t, J = 8.5 Hz, 1H, Ar-5″-H), 6.85−6.75 (m, 2H, Ar-2′,6″-H), 3.16 (s, 2H, CH_2, acetamido), 2.33 (s, 6H, $2CH_3$); ^{13}C DEPT (75 MHz, DMSO-d_6): δ 153.46 (1C, Ar-2-CH), 131.73 (1C, Ar-5″-CH), 128.82 (1C, Ar-8-CH), 127.64 (1C, Ar-7-CH), 123.93 (1C, Ar-5′-CH), 122.79 (1C, Ar-6′-CH), 112.77 (1C, Ar-2′-CH), 110.27 (1C, Ar-6″-CH), 109.98 (1C, Ar-4″-CH), 104.80 (1C, Ar-2″-CH), 104.46 (1C, Ar-5-CH), 63.69 (1C, CH_2), 45.95 (2C, $2CH_3$); ^{13}C NMR (75 MHz, DMSO-d_6): δ 169.44 (1C, C═O), 165.00 (1C, Ar-4-C), 161.76 (1C, Ar-3″-C), 159.14 (1C, Ar-1″-C), 153.50 (1C, Ar-2-CH), 146.11 (1C, Ar-6-C), 136.96 (1C, Ar-8a-C), 131.86 (1C, Ar-4′-C), 131.73 (1C, Ar-5″-CH), 128.82 (1C, Ar-8-CH), 127.65 (1C, Ar-7-CH), 125.31 (1C, Ar-1′-C), 123.94 (1C, Ar-5′-CH), 122.80 (1C, Ar-6′-CH), 122.69 (1C, Ar-3′-C), 112.75 (1C, Ar-2′-CH), 112.45 (1C, Ar-4a-C), 110.27 (1C, Ar-6″-CH), 109.99 (1C, Ar-4″-CH), 104.79 (1C, Ar-2″-CH), 104.46 (1C, Ar-5-CH), 63.68 (1C, CH_2), 45.94 (2C, $2CH_3$); HRMS (ES^+): m/z calcd for $C_{24}H_{22}ClFN_5O_2$ $[M + 1]^+$, 466.1446; found, 466.1441.

*N-(4-((3-Chloro-4-(3-(trifluoromethyl)phenoxy)phenyl)amino)-quinazolin-6-yl)-2-morpholino-acetamide (**15e**).* Yellow solid, 0.42 g, yield; 77%, mp 105−108; ^1H NMR (300 MHz, DMSO-d_6): δ 10.05 (s, H, NH, exchanged with D_2O), 9.96 (s, H, NH, exchanged with D_2O), 8.67 (s, 1H, Ar-2-H), 8.60 (s, 1H, Ar-5-H), 8.25 (s, 1H, Ar-2′-H), 8.03−8.00 (d, J = 9 Hz, 1H, Ar-8-H), 7.92−7.89 (d, 1H, J = 9 Hz, Ar-7-H), 7.81−7.78 (d, 1H, J = 9, Ar-6′-H), 7.65−7.59 (t, J = 9 Hz, 1H, Ar-5″-H), 7.49−7.46 (d, 1H, J = 9 Hz, Ar-4″-H), 7.35−7.32 (d, 1H, J = 9 Hz, Ar-6″-H), 7.25−7.21 (m, 2H, Ar-2″, 5′), 3.67 (br s, 4H, $2CH_2$, morpholino) 3.22 (s, 2H, CH_2), 2.57 (br s, 4H, $2CH_2$, morpholino); ^{13}C DEPT (75 MHz, DMSO-d_6): δ 153.58 (1C, Ar-2-CH), 131.91 (1C, Ar-5″-CH), 128.87 (1C, Ar-8-CH), 128.02 (1C, Ar-7-CH), 124.12 (1C, Ar-6″-CH), 122.83 (2C, Ar-5′, 6′-CH), 120.67 (1C, Ar-4″-CH), 119.90 (1C, Ar-2′-CH), 113.27 (1C, Ar-2″-CH), 112.74 (1C, Ar-5-CH), 66.57 (2C, $2CH_2$, morpholino), 62.41 (1C, CH_2), 53.72 (2C, $2CH_2$, morpholino); ^{13}C NMR (75 MHz, DMSO-d_6): δ 168.90 (1C, C═O), 158.12 (1C, Ar-4-C), 157.63 (1C, Ar-1″-C), 153.57 (1C, Ar-2-CH), 147.16 (1C, Ar-6-C), 145.84 (1C, Ar-8a-C), 138.15 (1C, Ar-4′-C), 136.83 (2C, Ar-1′, 3″-C), 131.91 (1C, Ar-5″-CH), 128.85 (1C, Ar-8-CH), 128.01 (1C, Ar-7-CH), 125.37 (1C, Ar-3′-C), 125.22 (1C, CF_3), 124.12 (1C, Ar-6″-CH), 122.95 (2C, Ar-5′, 6′-CH), 120.69 (1C, Ar-4″-CH), 119.91 (1C, Ar-2′-CH), 115.76 (1C, Ar-4a-C), 113.26 (1C, Ar-2″-CH), 112.75 (1C, Ar-5-CH), 66.56 (2C, $2CH_2$, morpholino), 62.40 (1C, CH_2), 53.72 (2C, $2CH_2$, morpholino); HRMS (ES^+): m/z calcd for $C_{27}H_{24}ClF_3N_5O_3$ $[M + 1]^+$, 558.1520; found, 558.1528.

*N-(4-((3-Chloro-4-(3-(trifluoromethyl)phenoxy)phenyl)amino)-quinazolin-6-yl)-2-(4-methylpiperazin-1-yl)acetamide (**15f**).* Brown oil solidifies when kept in the fridge overnight, 0.27 g, yield; 48%: ^1H NMR (300 MHz, DMSO-d_6): δ 9.96 (s, 2H, 2NH, exchanged with D_2O), 8.65 (s, 1H, Ar-2-H), 8.59 (s, 1H, Ar-5-H), 8.25 (s, 1H, Ar-2′-H), 8.06−8.03 (d, J = 9 Hz, 1H, Ar-8-H), 7.92−7.89 (d, 1H, J = 9 Hz, Ar-7-H), 7.81−7.78 (d, 1H, J = 9, Ar-6′-H), 7.64−7.59 (t, J = 6 Hz, 1H, Ar-5″-H), 7.48−7.46 (d, 1H, J = 6 Hz, Ar-4″-H), 7.34−7.32 (d, 1H, J = 6 Hz, Ar-6″-H), 7.25−7.21 (m, 2H, Ar-2″, 5′), 3.20 (s, 2H, CH_2, acetamido), 2.57 (br s, 4H, $2CH_2$, piperazino), 2.41 (br s, 4H, $2CH_2$, piperazine), 2.18 (s, 3H, CH_3); ^{13}C DEPT (75 MHz, DMSO-d_6): δ 153.54 (1C, Ar-2-CH), 131.90 (1C, Ar-5″-CH), 128.87 (1C, Ar-8-CH), 127.85 (1C, Ar-7-CH), 124.12 (1C, Ar-6″-CH), 122.94 (2C, Ar-5′, 6′-CH), 120.66 (1C, Ar-4″-CH), 119.90 (1C, Ar-2′-CH), 113.31 (1C, Ar-2″-CH), 112.54 (1C, Ar-5-CH), 62.15 (1C, CH_2, acetamido), 54.97 (2C, $2CH_2$, piperazino), 53.26 (2C, $2CH_2$, piperazino), 46.18 (1C, CH_3); ^{13}C NMR (75 MHz, DMSO-d_6): δ 169.08 (1C, C═O), 158.12 (1C, Ar-4-C), 157.62 (1C, Ar-1″-C), 153.54 (1C, Ar-2-CH), 147.14 (1C, Ar-6-C), 145.84 (1C, Ar-8a-C), 138.15 (1C, Ar-4′-C), 136.85 (2C, Ar-1′, 3″-C), 131.90 (1C, Ar-5″-CH), 128.87 (1C, Ar-8-CH), 127.85 (1C, Ar-7-CH), 125.81 (1C, Ar-3′-C), 125.40 (1C, CF_3), 124.12 (1C, Ar-6″-CH), 122.94 (2C, Ar-5′, 6′-CH), 120.67 (1C, Ar-4″-CH), 119.95 (1C, Ar-2′-CH), 115.78 (1C, Ar-4a-C), 113.32 (1C, Ar-2″-CH), 112.54 (1C, Ar-5-CH), 62.15 (1C, CH_2, acetamido), 54.97 (2C, $2CH_2$, piperazino), 53.26 (2C, $2CH_2$, piperazino), 46.18 (1C, CH_3); HRMS (ES^+): m/z calcd for $C_{28}H_{27}ClF_3N_6O_2$ $[M + 1]^+$, 571.1836; found, 571.1837.

*N-(4-((3-Chloro-4-(3-(trifluoromethyl)phenoxy)phenyl)amino)-quinazolin-6-yl)-2-(dimethylamino)acetamide (**15g**).* Brown solid, 0.42 g, yield; 83%; ^1H NMR (300 MHz, DMSO-d_6): δ 9.99 (s, 2H, 2NH, exchanged with D_2O), 8.65 (s, 1H, Ar-2-H), 8.59 (s, 1H, Ar-5-H), 8.25 (s, 1H, Ar-2′-H), 8.13−8.10 (d, J = 9 Hz, 1H, Ar-8-H), 7.92−7.89 (d, 1H, J = 9 Hz, Ar-7-H), 7.80−7.77 (d, 1H, J = 9 Hz, Ar-6′-H), 7.64−7.59 (t, J = 6 Hz, 1H, Ar-5″-H), 7.48−7.46 (d, 1H, J = 6 Hz, Ar-4″-H), 7.34−7.32 (d, 1H, J = 6 Hz, Ar-6″-H), 7.25−7.21 (m, 2H, Ar-2″, 5′), 3.15 (s, 2H, CH_2), 2.33 (s, 6H, $2CH_3$); ^{13}C DEPT (75 MHz, DMSO-d_6): δ 153.45 (1C, Ar-2-CH), 131.89 (1C, Ar-5″-CH), 128.82 (1C, Ar-8-CH), 127.66 (1C, Ar-7-CH), 123.97 (1C, Ar-6″-CH), 122.95 (1C, Ar-5′-CH), 122.77 (1C, Ar-6′-CH), 120.69 (1C, Ar-4″-CH), 119.94 (1C, Ar-2′-CH), 113.29 (1C, Ar-2″-CH), 112.44 (1C, Ar-5-CH), 63.68 (1C, CH_2), 45.93 (2C, $2CH_3$); ^{13}C NMR (75 MHz, DMSO): δ 169.41 (1C, C═O), 158.13 (1C, Ar-4-C), 157.51 (1C, Ar-1″-C), 153.44 (1C, Ar-2-CH), 147.02 (1C, Ar-6-C), 145.82 (1C, Ar-8a-C), 138.27 (1C, Ar-4′-C), 136.98 (1C, Ar-1′-C), 131.88 (1C, Ar-5″-CH), 131.40 (1C, Ar-3″-C), 130.99 (1C, Ar-3′-C), 128.82 (1C, Ar-8-CH), 127.64 (1C, Ar-7-CH), 125.41 (1C, CF_3), 123.97 (1C, Ar-6″-CH), 122.92 (1C, Ar-5′-CH), 122.77 (1C, Ar-6′-CH), 120.69 (1C, Ar-4″-CH), 119.88 (1C, Ar-2′-CH), 115.82 (1C, Ar-4a-C), 113.28 (1C, Ar-2″-CH), 112.44 (1C, Ar-5-CH), 63.68 (1C,

https://dx.doi.org/10.1021/acs.jmedchem.0c01647
J. Med. Chem. XXXX, XXX, XXX−XXX

CH_2), 45.93 (2C, $2CH_3$); HRMS (ES^+): m/z calcd for $C_{25}H_{22}ClF_3N_5O_2$ $[M + 1]^+$, 516.1414; found, 516.1424.

*N-(4-((3-Chloro-4-(m-tolyloxy)phenyl)amino)quinazolin-6-yl)-2-morpholino Acetamide (**15h**).* Off-white solid, 0.42 g, yield; 84%; ^1H NMR (300 MHz, DMSO-d_6): δ 10.04 (s, 1H, NH, exchanged with D_2O), 9.89 (s, 1H, NH, exchanged with D_2O), 8.64 (s, 1H, Ar-2-H), 8.55 (s, 1H, Ar-5-H), 8.16 (s, 1H, Ar-2′-H), 8.03−8.00 (d, J = 8.7 Hz, 1H, Ar-8-H), 7.79−7.76 (d, J = 8.8 Hz, 1H, Ar-7-H), 7.75 (s, 1H, Ar-2″-H), 7.32−7.30 (d, 1H, J = 7.1 Hz, Ar-6′-H), 7.21−7.19 (d, 1H, J = 7.3 Hz, Ar-5′-H), 7.09−7.04 (t, J = 8.8 Hz, 1H, Ar-5″-H), 6.99−6.96 (d, J = 8.9 Hz, 1H, Ar-6″-H), 6.76−6.73 (d, J = 8.8 Hz, 1H, Ar-4″-H), 3.67 (br s, 4H, $2CH_2$, morpholino), 3.21 (s, 2H, CH_2, acetamido), 2.56 (br s, 4H, $2CH_2$, morpholino), 2.26 (s, 3H, CH_3); ^{13}C DEPT (75 MHz, DMSO-d_6): δ 153.66 (1C, Ar-2-CH), 131.95 (1C, Ar-8-CH), 128.78 (1C, Ar-5″-CH), 127.85 (2C, Ar-7, 4″-CH), 124.40 (1C, Ar-5′-CH), 124.12 (1C, Ar-6′-CH), 122.90 (1C, Ar-2′-CH), 120.22 (1C, Ar-2″-CH), 117.39 (1C, Ar-6″-CH), 112.78 (1C, Ar-5-CH), 66.57 (2C, $2CH_2$, morpholino), 62.38 (1C, CH_2, acetamido), 53.70 (2C, $2CH_2$, morpholino), 16.19 (1C, CH_3); ^{13}C NMR (75 MHz, DMSO-d_6): δ 168.92 (1C, C═O), 157.73 (1C, Ar-4-C), 155.01 (1C, Ar-1″-C), 153.66 (1C, Ar-2-CH), 148.08 (1C, Ar-6-C), 147.09 (1C, Ar-8a-C), 136.73 (1C, Ar-4′-C), 136.37 (1C, Ar-3″-C), 131.95 (1C, Ar-8-CH), 128.77 (1C, Ar-5″-CH), 128.26 (1C, Ar-1′-C), 127.84 (2C, Ar-7, 4″-CH), 124.41 (1C, Ar-5′-CH), 124.11 (1C, Ar-6′-CH), 123.79 (1C, Ar-3′-C), 122.90 (1C, Ar-2′-CH), 120.20 (1C, Ar-2″-CH), 117.41 (1C, Ar-6″-CH), 115.70 (1C, Ar-4a-C), 112.78 (1C, Ar-5-CH), 66.57 (2C, $2CH_2$, morpholino), 62.38 (1C, CH_2, acetamido), 53.71 (2C, $2CH_2$, morpholino), 16.18 (1C, CH_3); HRMS (ES^+): m/z calcd for $C_{27}H_{27}ClN_5O_3$ $[M + 1]^+$, 504.1802; found, 504.1799.

*N-(4-((3-Chloro-4-(m-tolyloxy)phenyl)amino)quinazolin-6-yl)-2-(4-methylpiperazin-1-yl)acetamide (**15i**).* Light-brown solid, 0.47 g, yield; 92%; ^1H NMR (300 MHz, DMSO-d_6): δ 9.94 (s, 1H, 1NH, exchanged with D_2O), 9.87 (s, 1H, 1NH, exchanged with D_2O), 8.62 (s, 1H, Ar-2-H), 8.56 (s, 1H, Ar-5-H), 8.17−8.16 (d (m-coupling), J = 2.1 Hz, 1H, Ar-2′-H), 8.04−8.01 (d, J = 9 Hz, 1H, Ar-8-H), 7.79−7.76 (d, J = 9 Hz, 1H, Ar-7-H), 7.78−7.74 (dd, J = 9 Hz, 2.1 Hz, 1H, Ar-6′-H), 7.34−7.31 (d, J = 7.3 Hz, 1H, Ar-6″-H), 7.22−7.17 (m, 1H, Ar-2″-H), 7.10−7.05 (t, J = 7.3 Hz, 1H, Ar-5″-H), 7.00−6.97 (d, J = 8.9 Hz, 1H, Ar-5′-H), 6.77−6.74 (d, J = 7.4 Hz, 1H, Ar-4″-H), 3.19 (s, 2H, CH_2, acetamido), 2.57 (br s, 4H, 2-CH_2, piperazino), 2.41 (br s, 4H, 2-CH_2, piperazino), 2.26 (s, 3H, CH_3, piperazino), 2.18 (s, 3H, CH_3, tolyl); ^{13}C DEPT (75 MHz, DMSO-d_6): δ 153.63 (1C, Ar-2-CH), 131.94 (1C, Ar-8-CH), 128.82 (1C, Ar-5″-CH), 127.82 (2C, Ar-7, 4″-CH), 124.39 (1C, Ar-5′-CH), 124.10 (1C, Ar-6′-CH), 122.89 (1C, Ar-2′-CH), 120.23 (1C, Ar-2″-CH), 117.39 (1C, Ar-6″-CH), 112.61 (1C, Ar-5-CH), 62.15 (1C, CH_2, acetamido), 54.99 (2C, 2-CH_2, piperazino), 53.29 (2C, 2-CH_2, piperazino), 46.21 (1C, CH_3, piperazino), 16.21 (1C, CH_3, tolyl); ^{13}C NMR (75 MHz, DMSO-d_6): δ 169.05 (1C, C═O), 157.72 (1C, Ar-4-C), 155.03 (1C, Ar-1″-C), 153.63 (1C, Ar-2-CH), 148.06 (1C, Ar-6-C), 147.12 (1C, Ar-8a-C), 136.77 (1C, Ar-4′-C), 136.41 (1C, Ar-3″-C), 131.95 (1C, Ar-8-CH), 128.83 (1C, Ar-5″-CH), 128.27 (1C, Ar-1′-C), 127.84 (2C, Ar-7, 4″-CH), 124.40 (1C, Ar-5′-CH), 124.11 (1C, Ar-6′-CH), 123.78 (1C, Ar-3′-C), 122.90 (1C, Ar-2′-CH), 120.21 (1C, Ar-2″-CH), 117.42 (1C, Ar-6″-CH), 115.73 (1C, Ar-4a-C), 112.62 (1C, Ar-5-CH), 62.15 (1C, CH_2, acetamido), 55.00 (2C, 2-CH_2, piperazino), 53.29 (2C, 2-CH_2, piperazino), 46.20 (1C, CH_3, piperazino), 16.18 (1C, CH_3, tolyl); HRMS (ES^+): m/z calcd for $C_{28}H_{30}ClN_6O_2$ $[M + 1]^+$, 517.2119; found, 517.2120.

*N-(4-((3-Chloro-4-(m-tolyloxy)phenyl)amino)quinazolin-6-yl)-2-(diethylamino) Acetamide (**15j**).* Yellow solid, 0.37 g, yield; 77%; ^1H NMR (300 MHz, DMSO-d_6): δ 9.92 (s, 1H, NH, exchanged with D_2O), 9.86 (s, 1H, NH, exchanged with D_2O), 8.57 (s, 1H, Ar-2-H), 8.56 (s, 1H, Ar-5-H), 8.20−8.17 (m, 2H, Ar-8, 2′-H), 7.80−7.77 (d, J = 9 Hz, 2H, Ar-7, 2″-H), 7.33−7.31 (d, 1H, J = 7.4, Ar-6′-H), 7.19−7.17 (d, 1H, J = 7.3, Ar-5′-H), 7.09−7.05 (t, J = 8.9 Hz, 1H, Ar-5″-H), 7.00−6.97 (d, J = 8.9 Hz, 1H, Ar-6″-H), 6.77−6.74 (d, J = 8.8 Hz, 1H, Ar-4″-H), 3.23 (s, 2H, CH_2, acetamido), 2.68−2.61 (q, J = 7.1 Hz, 4H, 2-CH_2, $(CH_3\mathbf{CH_2})_2N$−), 2.26 (s, 3H, CH_3, tolyl), 1.08−1.04 (t, J = 7.1 Hz, 6H, 2-CH_3, $(\mathbf{CH_3}CH_2)_2N$−); ^{13}C DEPT (75 MHz, DMSO-d_6): δ 153.60 (1C, Ar-2-CH), 131.95 (1C, Ar-8-CH), 128.89 (1C, Ar-5″-CH), 127.84 (1C, Ar-7-CH), 127.32 (1C, Ar-4″-CH), 124.34 (1C, Ar-5′-CH), 124.10 (1C, Ar-6′-CH), 122.82 (1C, Ar-2′-CH), 120.24 (1C, Ar-2″-CH), 117.40 (1C, Ar-6″-CH), 112.16 (1C, Ar-5-CH), 57.82 (1C, CH_2, acetamido), 48.50 (2C, 2-CH_2, $(CH_3\mathbf{CH_2})_2N$−) 16.20 (1C, CH_3, tolyl), 12.44 (2C, 2-CH_3, $(\mathbf{CH_3}CH_2)_2N$−); ^{13}C NMR (75 MHz, DMSO-d_6): δ 170.60 (1C, C═O), 157.64 (1C, Ar-4-C), 155.03 (1C, Ar-1″-C), 153.59 (1C, Ar-2-CH), 148.05 (1C, Ar-6-C), 147.01 (1C, Ar-8a-C), 136.74 (1C, Ar-4′-C), 136.41 (1C, Ar-3″-C), 131.94 (1C, Ar-8-CH), 128.88 (1C, Ar-5″-CH), 128.26 (1C, Ar-1′-C), 127.84 (1C, Ar-7-CH), 127.31 (1C, Ar-4″-CH), 124.34 (1C, Ar-5′-CH), 124.10 (1C, Ar-6′-CH), 123.80 (1C, Ar-3′-C), 122.83 (1C, Ar-2′-CH), 120.23 (1C, Ar-2″-CH), 117.41 (1C, Ar-6″-CH), 115.79 (1C, Ar-4a-C), 112.17 (1C, Ar-5-CH), 57.83 (1C, CH_2, acetamido), 48.51 (2C, 2-CH_2, $(CH_3\mathbf{CH_2})_2N$−), 16.19 (1C, CH_3, tolyl), 12.44 (2C, 2-CH_3, $(\mathbf{CH_3}CH_2)_2N$); HRMS (ES^+): m/z calcd for $C_{27}H_{29}ClN_5O_2$ $[M + 1]^+$, 490.2010; found, 490.2015.

*N-(4-((3-Chloro-4-(m-tolyloxy)phenyl)amino)quinazolin-6-yl)-2-(dimethylamino) Acetamide (**15k**).* Yellow solid, 0.22 g, yield; 84%; ^1H NMR (300 MHz, DMSO-d_6): δ 9.96 (s, 2H, 2NH, exchanged with D_2O), 8.62 (s, 1H, Ar-2-H), 8.55 (s, 1H, Ar-5-H), 8.17 (s, 1H, Ar-2′-H), 8.13−8.10 (d, J = 8.9 Hz, 1H, Ar-8-H), 7.79−7.76 (d, J = 8.9 Hz, 2H, Ar-7, 6′-H), 7.33−7.30 (d, J = 7.1 Hz, 1H, Ar-6″-H), 7.21−7.16 (m, 1H, Ar-2″-H), 7.09−7.04 (t, J = 7.1 Hz, 1H, Ar-5″-H), 7.00−6.97 (d, J = 8.9 Hz, 1H, Ar-5′-H), 6.77−6.74 (d, J = 7.2 Hz, 1H, Ar-4″-H), 3.15 (s, 2H, CH_2), 2.33 (s, 6H, $2CH_3$), 2.26 (s, 3H, CH_3, tolyl); ^{13}C DEPT 135 (75 MHz, DMSO-d_6): δ 153.52 (1C, Ar-2-CH), 131.93 (1C, Ar-8-CH), 128.78 (1C, Ar-5″-CH), 127.83 (1C, Ar-7-CH), 127.56 (1C, Ar-4″-CH), 124.21 (1C, Ar-5′-CH), 124.08 (1C, Ar-6′-CH), 122.69 (1C, Ar-2′-CH), 120.24 (1C, Ar-2″-CH), 117.39 (1C, Ar-6″-CH), 112.49 (1C, Ar-5-CH), 63.68 (1C, CH_2), 45.93 (2C, 2-CH_3), 16.19 (1C, CH_3, tolyl); ^{13}C NMR (75 MHz, DMSO-d_6): δ 169.39 (1C, C═O), 157.59 (1C, Ar-4-C), 155.05 (1C, Ar-1″-C), 153.52 (1C, Ar-2-CH), 148.00 (1C, Ar-6-C), 146.99 (1C, Ar-8a-C), 136.89 (1C, Ar-4′-C), 136.55 (1C, Ar-3″-C), 131.93 (1C, Ar-8-CH), 128.78 (1C, Ar-5″-CH), 128.26 (1C, Ar-1′-C), 127.82 (1C, Ar-7-CH), 127.56 (1C, Ar-4″-CH), 124.22 (1C, Ar-5′-CH), 124.08 (1C, Ar-6′-CH), 123.82 (1C, Ar-3′-C), 122.69 (1C, Ar-2′-CH), 120.23 (1C, Ar-2″-CH), 117.40 (1C, Ar-6″-CH), 115.80 (1C, Ar-4a-C), 112.49 (1C, Ar-5-CH), 63.69 (1C, CH_2), 45.93 (2C, 2-CH_3), 16.18 (1C, CH_3, tolyl); HRMS (ES^+): m/z calcd for $C_{25}H_{25}ClN_5O_2$ $[M + 1]^+$, 462.1697; found, 462.1693.

*N-(4-((3-Chloro-4-(m-tolyloxy)phenyl)amino)quinazolin-6-yl)-2-((2-hydroxyethyl)amino)acetamide (**15l**).* A mixture of intermediate **14c** (0.45 g, 1 mmol) and 2-aminoethanol (0.25 g, 0.3 mL, 5 mmol) in methanol (20 mL) was held at reflux for 6 h in the presence of triethylamine (15 drops). Methanol was then removed under reduced pressure, and the remaining residue was recrystallized from acetone to yield compound **15l**.

White solid, 0.2 g, yield: 43%; ^1H NMR (300 MHz, DMSO-d_6): δ 9.88 (s, 2H, 2NH, exchanged with D_2O), 8.63 (s, 1H, Ar-2-H), 8.56 (s, 1H, Ar-5-H), 8.18 (s, 1H, Ar-2′-H), 8.09−8.05 (d, J = 9.1 Hz, 1H, Ar-8-H), 7.80−7.77 (dd, J = 9.1 Hz, 3.1 Hz, 2H, Ar-7, 6′-H), 7.33−7.31 (d, J = 6 Hz, 1H, Ar-6″-H), 7.19−7.17 (d, J = 6 Hz, 1H, Ar-4″-H), 7.10−7.05 (t, J = 6 Hz, 1H, Ar-5″), 7.00−6.97 (d, J = 9 Hz, 1H, Ar-5′-H), 6.76−6.74 (s, 1H, Ar-2″-H), 4.67 (s, 1H, OH, exchanged with D_2O), 4.66 (s, 1H, 1NH, exchanged with D_2O), 3.51 (br s, 2H, CH_2, $OH\mathbf{CH_2}CH_2NH$), 3.38 (s, 2H, CH_2, acetamido), 2.68 (br s, 2H, CH_2, $OHCH_2\mathbf{CH_2}NH$), 2.27 (s, 3H, CH_3); ^{13}C DEPT (75 MHz, DMSO-d_6): δ 153.55 (1C, Ar-2-CH), 131.94 (1C, Ar-8-CH), 128.89 (1C, Ar-5″-CH), 127.85 (1C, Ar-7-CH), 127.36 (1C, Ar-4″-CH), 124.26 (1C, Ar-5′-CH), 124.09 (1C, Ar-6′-CH), 122.76 (1C, Ar-2′-CH), 120.26 (1C, Ar-2″-CH), 117.37 (1C, Ar-6″-CH), 112.11 (1C, Ar-5-CH), 60.85 (1C, CH_2, $OH\mathbf{CH_2}CH_2NH$), 53.17 (1C, CH_2, acetamido), 52.18 (1C, CH_2, $OHCH_2\mathbf{CH_2}NH$), 16.20 (1C, CH_3); ^{13}C NMR (75 MHz, DMSO-d_6): δ 171.18 (1C, C═O), 157.66 (1C, Ar-4-C), 155.04 (1C, Ar-1″-C), 153.55 (1C, Ar-2-CH), 147.97 (1C, Ar-6-C), 146.98 (1C, Ar-8a-C), 136.91 (1C, Ar-4′-C), 136.47 (1C,

https://dx.doi.org/10.1021/acs.jmedchem.0c01647
J. Med. Chem. XXXX, XXX, XXX−XXX

Ar-3″-C), 131.94 (1C, Ar-8-CH), 128.90 (1C, Ar-5″-CH), 128.24 (1C, Ar-1′-C), 127.84 (1C, Ar-7-CH), 127.37 (1C, Ar-4″-CH), 124.27 (1C, Ar-5′-CH), 124.09 (1C, Ar-6′-CH), 122.76 (1C, Ar-2′-CH), 120.26 (1C, Ar-2″-CH), 117.37 (1C, Ar-6″-CH), 115.80 (1C, Ar-4a-C), 112.11 (1C, Ar-5-CH), 60.81 (1C, CH_2, OH$\mathbf{CH_2}CH_2NH$), 53.14 (1C, CH_2, acetamido), 52.15 (1C, CH_2, $OHCH_2\mathbf{CH_2}NH$), 16.21 (1C, CH_3); HRMS (ES^+): m/z calcd for $C_{25}H_{25}ClN_5O_3$ $[M + 1]^+$, 478.1646; found, 478.1642.

***N*-(4-((3-Chloro-4-(3-fluorophenoxy)phenyl)amino)-quinazolin-6-yl)-4-(chloromethyl)benzamide (16).** To the solution of intermediate **13a** (1.5 g, 4 mmol) in acetone (20 mL), $NaHCO_3$ (0.35 g, 4.2 mmol) was added. The reaction mixture was stirred under nitrogen at 0 °C, followed by the dropwise addition of a solution of 4(choromethyl) benzoyl chloride (0.8 g, 4.2 mmol) in acetone (2 mL). The reaction mixture was stirred for 30 min at 0 °C. Excess solvent was removed under reduced pressure. Cold water (20 mL) was added to the remaining residue and the resulting suspension was neutralized with a saturated solution of $NaHCO_3$, if necessary. The solid obtained was filtered, dried, and washed with DCM and diethylether to afford compound **16** as pure greenish-yellow solid. 1.1 g, yield: 51%.

^{1}H NMR (300 MHz, DMSO-d_6): δ 10.81 (s, 2H, 2NH, exchanged with D_2O), 9.05 (s, 1H, Ar-2′-H), 8.74 (s, 1H, Ar-5′-H), 8.18 (s, 1H, Ar-2‴-H), 8.15−8.12 (d, J = 9 Hz, 1H, Ar-8′-H), 8.10−8.07 (d, J = 7.9 Hz, 2H, Ar-2,6-H), 7.92−7.89 (d, J = 9 Hz, 1H, Ar-7′-H), 7.86−7.83 (d, J = 9 Hz, 1H, Ar-6″-H), 7.65−7.62 (d, J = 7.8 Hz, 2H, Ar-3,5-H), 7.46−7.38 (m, 1H, Ar-2″-H), 7.32−7.29 (d, J = 9 Hz, 1H, Ar-5″-H), 7.00−6.94 (t, J = 8.4 Hz, 1H, Ar-5‴-H), 6.88−6.85 (d, J = 8.4, 1H, Ar-4‴-H), 6.80−6.77 (d, J = 8.3 Hz, 1H, Ar-6‴-H), 4.87 (s, 2H, CH_2); ^{13}C DEPT (75 MHz, DMSO-d_6): δ 152.37 (1C, Ar-2′-CH), 131.92 (1C, Ar-5‴-CH), 129.76 (1C, Ar-8′-CH), 129.37 (2C, Ar-2, 6-CH), 128.63 (2C, Ar-3,5-CH), 125.92 (1C, Ar-7′-CH), 125.20 (1C, Ar-5″-CH), 123.81 (1C, Ar-6″-CH), 122.54 (1C, Ar-2″-CH), 114.35 (1C, Ar-6‴-CH), 113.07 (1C, Ar-4‴-CH), 110.24 (1C, Ar-2‴-CH), 104.78 (1C, Ar-5′-CH), 45.83 (1C, CH_2). MS ($APCI^+$): m/z 533.2 $[M + 1]^+$.

General Procedure for the Synthesis of Compounds (17a−c). A mixture of intermediate **16** (0.53 g, 1 mmol) and the appropriate secondary amine, 1-methyl piperazine or morpholine (50 mmol), was placed into a 25 mL round-bottomed flask or into a capped vial in the case of low boiling point secondary amine, dimethylamine (100 mmol). The reaction mixture was heated under reflux and monitored by TLC. After 2 h, the TLC of the reaction mass indicated the absence of intermediate **16**. The reaction mixture was cooled to room temperature and poured onto iced-water (30 mL) portion wise with stirring. The resultant precipitate was filtered, washed with water, and dried. The obtained product was purified by flash column chromatography using hexane/ethylacetate (90:10%) as an eluent to afford the desired products (**17a−c**).

*N-(4-((3-Chloro-4-(3-fluorophenoxy)phenyl)amino)quinazolin-6-yl)-4-(morpholinomethyl)benzamide (**17a**).* Light-yellow solid, 0.27 g, yield; 48%, mp 134−137 °C; ^{1}H NMR (300 MHz, DMSO-d_6): δ 10.59 (s, 1H, NH, exchanged with D_2O), 10.01 (s, 1H, NH, exchanged with D_2O), 8.94 (s, 1H, Ar-2′-H), 8.62 (s, 1H, Ar-5′-H), 8.26 (s, 1H, Ar-2‴-H), 8.03−8.01 (ds, J = 7.5 Hz, 3H, Ar-2″,2,6-H), 7.93−7.90 (d, J = 9 Hz, 1H, Ar-8′-H), 7.85−7.82 (d, J = 9 Hz, 1H, Ar-7′-H), 7.51−7.49 (d, J = 7.8 Hz, 2H, Ar-3,5-H), 7.44−7.36 (dd, J = 8.1 Hz, 1.2 Hz, 1H, Ar-6″-H), 7.30−7.27 (d, J = 9 Hz, 1H, Ar-4‴-H), 6.97−6.92 (t, J = 9 Hz, 1H, Ar-5‴-H), 6.85−6.81 (d, J = 8.4 Hz, 1H, Ar-5″-H), 6.78−6.75 (d, J = 9 Hz, 1H, Ar-6‴-H), 3.59 (br s, 4H, $2CH_2$, morpholino), 3.55 (s, 2H, CH_2, $-\mathbf{CH_2}C_6H_4$), 2.38 (br s, 4H, $2CH_2$, morpholino); ^{13}C DEPT (75 MHz, DMSO-d_6): δ 153.67 (1C, Ar-2′-CH), 131.84 (1C, Ar-5‴-CH), 129.34 (2C, Ar-2, 6-CH), 128.76 (1C, Ar-8′-CH), 128.15 (2C, Ar-3,5-CH), 123.99 (1C, Ar-7′-CH), 122.74 (1C, Ar-5″-CH), 113.91 (1C, Ar-6″-CH), 112.76 (1C, Ar-2″-CH), 110.26 (1C, Ar-6‴-CH), 109.98 (1C, Ar-4‴-CH), 104.80 (1C, Ar-2‴-CH), 104.47 (1C, Ar-5′-CH), 66.65 (2C, $2CH_2$, morpholino), 62.43 (1C, CH_2, $-\mathbf{CH_2}C_6H_4$), 53.66 (2C, $2CH_2$, morpholino); ^{13}C NMR (75 MHz, DMSO-d_6): δ 165.93 (1C, Ar-4′-C), 165.01 (1C, C═O), 161.77 (1C, Ar-3‴-C), 159.15 (1C, Ar-1‴-C), 159.00 (1C, Ar-4″-C), 157.73 (1C, Ar-8′a-C), 153.68 (1C, Ar-2′-CH), 147.34 (1C, Ar-4-C), 146.12 (1C, Ar-6′-C), 142.57 (1C, Ar-1″-C), 138.02 (1C, Ar-1-C), 137.36 (1C, Ar-4′a-C), 131.84 (1C, Ar-5‴-CH), 129.34 (2C, Ar-2, 6-CH), 128.84 (1C, Ar-8′-CH), 128.14 (2C, Ar-3,5-CH), 125.29 (1C, Ar-3″-C), 124.00 (1C, Ar-7′-CH), 122.74 (1C, Ar-5″-CH), 113.91 (1C, Ar-6″-CH), 112.76 (1C, Ar-2″-CH), 110.26 (1C, Ar-6‴-CH), 109.98 (1C, Ar-4‴-CH), 104.81 (1C, Ar-2‴-CH), 104.47 (1C, Ar-5′-CH), 66.65 (2C, $2CH_2$, morpholino), 62.43 (1C, CH_2, $-\mathbf{CH_2}C_6H_4$), 53.66 (2C, $2CH_2$, morpholino); HRMS (ES^+): m/z calcd for $C_{32}H_{28}ClFN_5O_3$ $[M + 1]^+$, 584.1865; found, 584.1869.

*N-(4-((3-Chloro-4-(3-fluorophenoxy)phenyl)amino)quinazolin-6-yl)-4-((4-methylpip erazin-1-yl)methyl)benzamide (**17b**).* Brown solid, 0.39 g, yield; 67%; ^{1}H NMR (300 MHz, DMSO-d_6): δ 10.58 (s, 1H, NH, exchanged with D_2O), 10.00 (s, 1H, NH, exchanged with D_2O), 8.93 (s, 1H, Ar-2′-H), 8.61 (s, 1H, Ar-5′-H), 8.25 (s, 1H, Ar-2‴-H), 8.02−8.00 (ds, J = 7.1 Hz, 3H, Ar-2″,2,6-H), 7.92−7.90 (d, J = 8.4 Hz, 1H, Ar-8′-H), 7.84−7.81 (d, J = 8.5 Hz, 1H, Ar-7′-H), 7.48−7.46 (d, J = 7.0 Hz, 2H, Ar-3,5-H), 7.41−7.36 (m, 1H, Ar-6″-H), 7.29−7.26 (d, J = 7.6 Hz, 1H, Ar-4‴-H), 6.97−6.92 (t, J = 7.7 Hz, 1H, Ar-5‴-H), 6.84−6.80 (d, J = 10.4 Hz, 1H, Ar-5″-H), 6.77−6.75 (d, J = 7.7 Hz, 1H, Ar-6‴-H), 3.54 (s, 2H, CH_2, $-\mathbf{CH_2}C_6H_4$), 2.38 (br s, 8H, 4-CH_2, piperazino), 2.17 (s, 3H, CH_3); ^{13}C DEPT (75 MHz, DMSO-d_6): δ 153.66 (1C, Ar-2′-CH), 131.84 (1C, Ar-5‴-CH), 129.22 (2C, Ar-2, 6-CH), 128.73 (1C, Ar-8′-CH), 128.13 (2C, Ar-3,5-CH), 124.00 (1C, Ar-7′-CH), 122.74 (1C, Ar-5″-CH), 113.93 (1C, Ar-6″-CH), 112.79 (1C, Ar-2″-CH), 110.27 (1C, Ar-6‴-CH), 109.99 (1C, Ar-4‴-CH), 104.81 (1C, Ar-2‴-CH), 104.47 (1C, Ar-5′-CH), 62.00 (1C, CH_2, $-\mathbf{CH_2}C_6H_4$), 55.06 (2C, $2CH_2$, piperazino), 52.89 (2C, $2CH_2$, piperazino), 46.01 (1C, CH_3); ^{13}C NMR (75 MHz, DMSO-d_6): δ 165.96 (1C, Ar-4′-C), 165.01 (1C, C═O), 161.77 (1C, Ar-3‴-C), 159.14 (1C, Ar-1‴-C), 159.00 (1C, Ar-4″-C), 157.74 (1C, Ar-8′a-C), 153.65 (1C, Ar-2′-CH), 147.32 (1C, Ar-4-C), 146.15 (1C, Ar-6′-C), 142.99 (1C, Ar-1″-C), 138.02 (1C, Ar-1-C), 137.39 (1C, Ar-4′a-C), 131.71 (1C, Ar-5‴-CH), 129.22 (2C, Ar-2, 6-CH), 128.72 (1C, Ar-8′-CH), 128.12 (2C, Ar-3,5-CH), 125.29 (1C, Ar-3″-C), 124.01 (1C, Ar-7′-CH), 122.73 (1C, Ar-5″-CH), 113.93 (1C, Ar-6″-CH), 112.79 (1C, Ar-2″-CH), 110.27 (1C, Ar-6‴-CH), 109.99 (1C, Ar-4‴-CH), 104.81 (1C, Ar-2‴-CH), 104.48 (1C, Ar-5′-CH), 62.01 (1C, CH_2, $-\mathbf{CH_2}C_6H_4$), 55.06 (2C, $2CH_2$, piperazino), 52.89 (2C, $2CH_2$, piperazino), 46.01 (1C, CH_3); HRMS (ES^+): m/z calcd for $C_{33}H_{31}ClFN_6O_2$ $[M + 1]^+$, 597.2181; found, 597.2184.

*N-(4-((3-Chloro-4-(3-fluorophenoxy)phenyl)amino)quinazolin-6-yl)-4-((dimethyl amino)methyl) Benzamide (**17c**).* Yellow solid, 0.42 g, yield; 78%, mp 135−138 °C (dec); ^{1}H NMR (300 MHz, DMSO-d_6): δ 10.60 (s, 1H, NH, exchanged with D_2O), 10.01 (s, 1H, NH, exchanged with D_2O), 8.94 (s, 1H, Ar-2′-H), 8.62 (s, 1H, Ar-5′-H), 8.25 (s, 1H, Ar-2‴-H), 8.03−8.00 (ds, J = 7.4 Hz, 3H, Ar-2″,2,6H), 7.93−7.90 (d, J = 8.8 Hz, 1H, Ar-8′-H), 7.85−7.82 (d, J = 8.9 Hz, 1H, Ar-7′-H), 7.50−7.47 (d, J = 7.6 Hz, 2H, Ar-3,5-H), 7.42−7.39 (d, J = 9 Hz, 1H, Ar-6″-H), 7.31−7.28 (d, J = 8.5 Hz, 1H, Ar-4‴-H), 6.98−6.92 (t, J = 8.4 Hz, 1H, Ar-5‴-H), 6.85−6.82 (d, J = 9 Hz, 1H, Ar-5″-H), 6.78−6.75 (d, J = 8.4 Hz, 1H, Ar-6‴-H), 3.48 (s, 2H, CH_2), 2.17 (s, 6H, $2CH_3$); ^{13}C DEPT (75 MHz, DMSO-d_6): δ 153.68 (1C, Ar-2′-CH), 131.86 (1C, Ar-5‴-CH), 129.17 (2C, Ar-2, 6-CH), 128.74 (1C, Ar-8′-CH), 128.12 (2C, Ar-3,5-CH), 124.01 (1C, Ar-7′-CH), 122.77 (1C, Ar-5″-CH), 113.91 (1C, Ar-6″-CH), 112.77 (1C, Ar-2″-CH), 110.27 (1C, Ar-6‴-CH), 109.99 (1C, Ar-4‴-CH), 104.79 (1C, Ar-2‴-CH), 104.46 (1C, Ar-5′-CH), 63.42 (1C, CH_2), 45.48 (2C, $2CH_3$); ^{13}C NMR (75 MHz, DMSO-d_6): δ 165.97 (1C, Ar-4′-C), 165.00 (1C, C═O), 161.76 (1C, Ar-3‴-C), 159.14 (1C, Ar-1‴-C), 158.99 (1C, Ar-4″-C), 157.73 (1C, Ar-8′a-C), 153.68 (1C, Ar-2′-CH), 147.30 (1C, Ar-4-C), 146.13 (1C, Ar-6′-C), 143.65 (1C, Ar-1″-C), 138.00 (1C, Ar-1-C), 137.37 (1C, Ar-4′a-C), 131.86 (1C, Ar-5‴-CH), 129.17 (2C, Ar-2, 6-CH), 128.74 (1C, Ar-8′-CH), 128.11 (2C, Ar-3,5-CH), 125.30 (1C, Ar-3″-C), 124.01 (1C, Ar-7′-CH), 122.77 (1C, Ar-5″-CH), 113.92 (1C, Ar-6″-CH), 112.77 (1C, Ar-2″-CH), 110.27 (1C, Ar-6‴-CH), 110.00 (1C, Ar-4‴-CH), 104.80 (1C, Ar-2‴-CH), 104.46 (1C, Ar-5′-CH), 63.43 (1C, CH_2), 45.48 (2C, $2CH_3$);

https://dx.doi.org/10.1021/acs.jmedchem.0c01647
J. Med. Chem. XXXX, XXX, XXX−XXX

HRMS (ES$^+$): m/z calcd for $C_{30}H_{26}ClFN_5O_2$ [M + 1]$^+$, 542.1759; found, 542.1755.

*N-(4-((3-Chloro-4-((3-fluorobenzyl)oxy)phenyl)amino)-quinazolin-6-yl)-2-((2-hydroxyethyl)amino) Acetamide (**17d**).* A mixture of intermediate **17** (0.53 g, 1 mmol) and 2-aminoethanol (0.25 g, 0.3 mL, 5 mmol) in methanol (20 mL) was held at reflux for 4 h in the presence of triethylamine (15 drops). Methanol was removed under reduced pressure, and the remaining residue was dissolved in DCM and purified by flash column chromatography with ethylacetate/MeOH (90:10%) as an eluent to afford compound **17d**.

Brown solid, 0.37 g, yield: 68%; ^{1}H NMR (300 MHz, DMSO): δ 10.59 (s, 2H, 2NH, exchanged with D_2O), 10.03 (s, 1H, NH, exchanged with D_2O), 8.95 (s, 1H, Ar-2′-H), 8.61 (s, 1H, Ar-5′-H), 8.26 (s, 1H, Ar-2‴-H), 8.06 (s, 1H, Ar-2″-H), 8.03−8.00 (d, J = 8 Hz, 2H, Ar-2,6-H), 7.93−7.90 (d, J = 8.4 Hz, 1H Ar-4‴-H), 7.85−7.82 (d, J = 8.9 Hz, 1H, Ar-8′-H), 7.54−7.51 (d, J = 7.9 Hz, 2H, Ar-3,5-H), 7.45−7.37 (m, 1H, Ar-6″-H), 7.30−7.28 (d, J = 8.9 Hz, 1H, Ar-7′-H), 6.98−6.92 (t, J = 8.4 Hz,, 1H, Ar-5‴), 6.85−6.82 (d, J = 9 Hz, 1H, Ar-5″-H), 6.78−6.75 (d, J = 8.3 Hz, 1H, Ar-6‴-H), 4.50 (s, 1H, OH, exchanged with D_2O), 3.81 (s, 2H, CH_2, −NH**C*H*$_2$**C_6H_4), 3.51−3.48 (t, J = 5.6 Hz, 2H, CH_2, OH**C*H*$_2$**CH_2NH−), 2.61−2.58 (t, J = 5.7 Hz, 2H, CH_2, $OHCH_2$**C*H*$_2$**NH−); ^{13}C DEPT (75 MHz, DMSO-d_6): δ 153.65 (1C, Ar-2′-CH), 131.86 (1C, Ar-5‴-CH), 128.85 (1C, Ar-8′-CH), 128.32 (2C, Ar-2,6-CH), 128.07 (2C, Ar-3,5-CH), 123.98 (1C, Ar-7′-CH), 122.72 (1C, Ar-5″-CH), 113.97 (1C, Ar-6″-CH), 112.77 (1C, Ar-2″-CH), 110.27 (1C, Ar-6‴-CH), 109.99 (1C, Ar-4‴-CH), 104.81 (1C, Ar-2‴-CH), 104.48 (1C, Ar-5′-CH), 60.87 (1C, CH_2, OH**C*H*$_2$**CH_2NH−), 52.97 (1C, CH_2, NH**C*H*$_2$**C6H4), 51.57 (1C, CH_2, $OHCH_2$**C*H*$_2$**NH−); ^{13}C NMR (75 MHz, DMSO-d_6): δ 165.96 (1C, Ar-4′-C), 165.01 (1C, C═O), 161.77 (1C, Ar-3‴-C), 159.15 (1C, Ar-1‴-C), 159.01 (1C, Ar-4″-C), 157.69 (1C, Ar-8′a-C), 153.64 (1C, Ar-2′-CH), 147.27 (1C, Ar-4-C), 146.10 (1C, Ar-6′-C), 145.82 (1C, Ar-1″-C), 137.42 (1C, Ar-1-C), 133.07 (1C, Ar-4′a-C), 131.85 (1C, Ar-5‴-CH), 128.87 (1C, Ar-8′-CH), 128.32 (2C, Ar-2, 6-CH), 128.06 (2C, Ar-3,5-CH), 125.30 (1C, Ar-3″-C), 123.98 (1C, Ar-7′-CH), 122.72 (1C, Ar-5″-CH), 113.98 (1C, Ar-6″-CH), 112.80 (1C, Ar-2″-CH), 110.27 (1C, Ar-6‴-CH), 109.99 (1C, Ar-4‴-CH), 104.81 (1C, Ar-2‴-CH),,104.48 (1C, Ar-5′-CH), 60.87 (1C, CH_2, OH**C*H*$_2$**CH_2NH−), 52.97 (1C, CH_2, NH**C*H*$_2$**C_6H_4), 51.57 (1C, CH_2, $OHCH_2$**C*H*$_2$**NH−). HRMS (ES$^+$): m/z calcd for $C_{30}H_{26}ClFN_5O_3$ [M + 1]$^+$, 558.1708; found, 558.1703.

Quinazoline-4,6-diol (19). 2-Amino-5-hydroxybenzoic acid (**18**; 2.00 g, 13.1 mmol) and formamide (9.37 mL, 235 mmol) were mixed and stirred for 1 h at 190 °C, a precipitate was formed while hot, and then, the reaction mixture was cooled to room temperature. The solid was filtered, triturated with H_2O, and washed with diethyl ether to afford quinazoline-4,6-diol (**19**).

Brown solid, mp >300 (dec),[109,115] 1.5 g, yield: 71%; ^{1}H NMR (300 MHz, DMSO-d_6): δ 12.02 (s, 1H, OH, exchanged with D_2O), 10.05 (s, 1H, OH, exchanged with D_2O), 7.90 (s, 1H, Ar-2-H), 7.54−7.51 (d, J = 8.8 Hz, 1H, Ar-8-H), 7.41−7.40 (d (m-coupling), J = 2.3 Hz, 1H, Ar-5-H), 7.27−7.23 (dd, J = 8.7, 2.5 Hz, 1H, Ar-7-H).

4-Hydroxyquinazolin-6-yl Acetate (20). A mixture of (**19**) (2.00 g, 12.3 mmol) and pyridine (2.5 mL) in acetic anhydride (18 mL) was stirred at 100 °C for 2 h. The reaction mixture was poured into ice-cold water (100 mL). The formed precipitate was filtered, washed with water, and dried to obtain the product (**20**).[109,115]

Off-white solid, 1.5 g, yield: 60%, mp >300 °C; ^{1}H NMR (300 MHz, DMSO-d_6): δ 12.34 (s, 1H, OH, exchanged with D_2O), 8.10 (s, 1H, Ar-2-H), 7.83−7.82 (d (m-coupling), J = 1.8 Hz, 1H, Ar-5-H), 7.74−7.71 (d, J = 8.8 Hz, 1H, Ar-8-H), 7.60−7.57(dd, J = 8.8, 1.8 Hz, 1H, Ar-7-H), 2.31 (s, 3H, CH_3).

General Procedure for the Synthesis of Compounds (22a−c). A mixture of (**20**) (2.00 g, 9.8 mmol), $SOCl_2$ (15 mL), and DMF (0.5 mL) was heated under reflux (95 °C) for 5 h. Excess $SOCl_2$ was removed under reduced pressure. The residue was treated with toluene (10 mL) and the solvent was evaporated under reduced pressure to yield 4-chloroquinazolin-6-yl acetate (**21**) in a pure form. Immediately, to a mixture of intermediate **21** and the appropriate aniline derivative (**4a−c**) (9.8 mmol) dissolved in acetonitrile (25 mL), K_2CO_3 (1.4 g, 9.8 mmol) was added. For compound **22a**, the reaction mixture was stirred at room temperature under a nitrogen atmosphere for 8 h, and the formed precipitate was filtered and washed with acetonitrile, water, and ether in order and dried to provide product (**22a**) in a pure form. For compounds **22b**,**c**, the reaction mixture was refluxed under a nitrogen atmosphere for 12 h, cooled to room temperature, and filtered. The filtrate was evaporated under reduced pressure, and the produced oily mass was dissolved in DCM and purified by flash column chromatography using hexane/ethyl acetate (80:20%) as an eluent to afford compound **22b** or using DCM/methanol (90:10%) to afford compound **22c** in a pure form.

*4-(3-Chloro-4-(3-fluorobenzyloxy)phenylamino)quinazolin-6-yl Acetate (**22a**).* Yellow solid, 3.8 g, yield: 90%, mp 290−292 °C, as reported.[115]

*4-((3-Chloro-4-(3-fluorophenoxy)phenyl)amino)quinazolin-6-yl Acetate (**22b**).* Brown solid, 3.1 g, yield: 76%; ^{1}H NMR (300 MHz, DMSO-d_6): δ 9.88 (s, 1H, NH, exchanged with D_2O), 8.68 (s, 1H, Ar-2-H), 8.35−8.36 (d (m-coupling), J = 2.2 Hz, 1H, Ar-5-H), 8.30−8.29 (d (m-coupling), J = 2.5 Hz, 1H, Ar-2′-H), 7.93−7.90 (dd, J = 8.9, 2.5 Hz, 1H, Ar-6′-H), 7.89−7.86 (d, J = 9 Hz, 1H, Ar-8-H), 7.72−7.69 (dd, J = 9.0, 2.2 Hz, 1H, Ar-7-H), 7.44−7.36 (m, 1H, Ar-2″-H), 7.31−7.28 (d, J = 8.9 Hz, 1H, Ar-5′-H), 6.97−6.92 (t, J = 8.3 Hz, 1H, Ar-5″-H), 6.85−6.81 (dd, J = 8.3, 2.1 Hz, 1H, Ar-4″-H), 6.77−6.74 (dd, J = 8.3 Hz, 1.9 Hz, 1H, Ar-6″-H), 2.38 (s, 3H, CH_3); ^{13}C DEPT (75 MHz, DMSO-d_6): δ 154.59 (1C, Ar-2-CH), 131.85 (1C, Ar-8-CH), 129.88 (1C, Ar-7-CH), 129.06 (1C, Ar-5″-CH), 123.83 (1C, Ar-5′-CH), 122.80 (1C, Ar-6′-CH), 122.50 (1C, Ar-2′-CH), 115.10 (1C, Ar-6″-CH), 112.85 (1C, Ar-5-CH), 110.32 (1C, Ar-4″-CH), 104.87 (1C, Ar-2″-CH), 21.22 (1C, CH_3); MS (APCI$^+$): m/z 424.1 [M + 1]$^+$.

*4-((3-Chloro-4-(3-(trifluoromethyl)phenoxy)phenyl)amino)-quinazolin-6-ylacetate (**22c**).* Yellow solid, 2.7 g, yield: 60%; ^{1}H NMR (300 MHz, DMSO-d_6): δ 9.89 (s, 1H, NH, exchanged with D_2O), 8.69 (s, 1H, Ar-2-H), 8.35−8.32 (d, J = 8.3 Hz, 2H, Ar-5,8-H), 7.95−7.92 (d, J = 8.5 Hz, 1H, Ar-7-H), 7.89−7.86 (d, J = 8.9 Hz, 1H, Ar-6′-H), 7.72−7.69 (d, J = 8.9 Hz, 1H, Ar-5′-H), 7.64−7.59 (t, J = 7.9 Hz, 1H, Ar-5″-H), 7.48−7.46 (d, J = 7.8 Hz, 1H, Ar-4″-H), 7.35−7.32 (d, J = 8 Hz, 1H, Ar-6″-H), 7.25−7.2 (m, 2H, Ar-2′,2″-H), 2.38 (s, 3H, CH_3); ^{13}C DEPT (75 MHz, DMSO-d_6): δ 154.57 (1C, Ar-2-CH), 131.89 (1C, Ar-8-CH), 129.87 (1C, Ar-7-CH), 129.07 (1C, Ar-5″-CH), 123.86 (1C, Ar-6″-CH), 122.97 (1C, Ar-5′-CH), 122.59 (1C, Ar-6′-CH), 120.71 (1C, Ar-4″-CH), 119.93 (1C, Ar-2′-CH), 115.10 (1C, Ar-2″-CH), 113.35 (1C, Ar-5-CH), 21.2 (1C, CH_3); MS (APCI$^+$): m/z 474.1 [M + 1]$^+$.

General Procedure for the Synthesis of Compounds (23a−c). A mixture of compound **22a**, **22b**, or **22c** (5 mmol) and ammonium hydroxide (20 mL) in methanol (60 mL) was stirred at room temperature for 3−12 h. The clear solution formed was evaporated under reduced pressure, and the residue was diluted with water (30 mL) and stirred for 30 min. The resulting solid was filtered, washed with water, and dried at 50 °C to afford compounds **23a−c**.

*4-(3-Chloro-4-(3-fluorobenzyloxy)phenylamino)quinazolin-6-ol (**23a**).* Reaction time: 12 h, yellow solid, 1.9 g, yield 71%; mp >300 °C, as reported.[115]

*4-((3-Chloro-4-(3-fluorophenoxy)phenyl)amino)quinazolin-6-ol (**23b**).* Reaction time: 4 h, yellow solid, 1.75 g, yield: 92%; ^{1}H NMR (300 MHz, DMSO-d_6): δ 10.14 (s, 1H, OH, exchanged with D_2O), 9.65 (s, 1H, NH, exchanged with D_2O), 8.5 (s, 1H, Ar-2-H), 8.31 (s, 1H, Ar-2″-H), 7.95−7.93 (d, J = 8.2 Hz, 1H, Ar-8-H), 7.80 (s, 1H, Ar-2′-H), 7.72−7.69 (d, J = 8.9 Hz, 1H, Ar-6′-H), 7.47−7.43 (m, 1H, Ar-6″-H), 7.41−7.38 (d, J = 7.5 Hz, 1H, Ar-4″-H), 7.29−7.26 (d, J = 8.8 Hz, 1H, Ar-5′-H), 6.96−6.91 (t, J = 7.7 Hz, 1H, Ar-5″-H), 6.82−6.81 (d (m-coupling), J = 2.3 Hz, 1H, Ar-5-H), 6.76−6.73 (d, J = 8.3 Hz, 1H, Ar-7-H); ^{13}C DEPT (75 MHz, DMSO-d_6): δ 151.74 (1C, Ar-2-CH), 131.69 (1C, Ar-8-CH), 129.87 (1C, Ar-5″-CH), 124.81 (1C, Ar-7-CH), 123.49 (1C, Ar-5′-CH), 122.86 (1C, Ar-6′-CH), 122.28 (1C, Ar-2′-CH), 112.68 (1C, Ar-6″-CH), 110.19 (1C, Ar-4″-CH), 105.43 (1C, Ar-2″-CH), 104.71 (1C, Ar-5-CH); MS (APCI$^+$): m/z 382.1 [M + 1]$^+$.

https://dx.doi.org/10.1021/acs.jmedchem.0c01647
J. Med. Chem. XXXX, XXX, XXX−XXX

*4-((3-Chloro-4-(3-(trifluoromethyl)phenoxy)phenyl)amino)-quinazolin-6-ol (**23c**).* Reaction time: 3 h, yellowish white solid, 1.89 g, yield: 88%; ^{1}H NMR (300 MHz, DMSO-d_6): δ 10.14 (s, 1H, OH, exchanged with D_2O), 9.67 (s, 1H, NH, exchanged with D_2O), 8.52 (s, 1H, Ar-2-H), 8.34−8.33 (d (m-coupling), J = 1.8 Hz, 1H, Ar-2′-H), 7.98−7.95 (dd, J = 8.8 Hz, 1.9 Hz, 1H, Ar-6′-H), 7.80 (s, 1H, Ar-5-H), 7.73−7.70 (d, J = 8.9 Hz, 1H, Ar-8-H), 7.64−7.59 (t, J = 7.9 Hz, 1H, Ar-5″-H), 7.48−7.45 (d, J = 8.8 Hz, 2H, Ar-7, 5′-H), 7.34−7.32 (d, J = 7.9 Hz, 1H, Ar-4″-H), 7.24−7.20 (m, 2H, Ar-6″, 2″-H); ^{13}C DEPT (75 MHz, DMSO-d_6): δ 151.72 (1C, Ar-2-CH), 131.88 (1C, Ar-8-CH), 129.88 (1C, Ar-5″-CH), 124.83 (1C, Ar-7-CH), 123.04 (1C, Ar-6″-CH), 122.37 (1C, Ar-5′-CH), 120.60 (1C, Ar-6′-CH), 119.89 (1C, Ar-4″-CH), 119.84 (1C, Ar-2′-CH), 113.18 (1C, Ar-2″-CH), 105.42 (1C, Ar-5-CH); MS (APCI$^+$): m/z 432.1 [M + 1]$^+$.

General Procedure for the Synthesis of Compounds (24a−c). A mixture of compound **24a**, **24b**, or **24c** (5 mmol), K_2CO_3 (1.4 g, 10 mmol), and catalytic amount of TBAB (81 mg, 0.25 mmol, 0.05 equiv) in acetonitrile (30 mL) was stirred at room temperature for 30 min, and then, 1-bromo-3-chloropropane (3.14 g, 2mL, 20 mmol) was added. The reaction mixture was refluxed at 85 °C for 2 h and then cooled to room temperature and filtered. The filtrate was evaporated under reduced pressure, and the residue obtained was dissolved in ethyl acetate and loaded on silica gel 60 (230−450 mesh) to be purified by flash column chromatography (DCM/methanol = 97:3%) to afford pure products (**24a−c**).

*N-(3-Chloro-4-(3-fluorobenzyloxy)phenyl)-6-(3-chloropropoxy)-quinazolin-4-amine (**24a**).* Yellow solid, 0.9 g, yield: 42%; mp 144−146 °C, as reported.[115]

*N-(3-Chloro-4-(3-fluorophenoxy)phenyl)-6-(3-chloropropoxy)-quinazolin-4-amine (**24b**).* Yellowish white solid, 2 g, yield: 88%; ^{1}H NMR (300 MHz, DMSO-d_6): δ 9.73 (s, 1H, NH, exchanged with D_2O), 8.57 (s, 1H, Ar-2-H), 8.24 (d (m-coupling), J = 2.3 Hz, 1H, Ar-5-H), 7.95−7.94 (d (m-coupling), J = 2.1 Hz, 1H, Ar-2′-H), 7.93−7.89 (dd, J = 9.0, 2.3 Hz, 1H, Ar-7-H), 7.78−7.75 (d, J = 9.0 Hz, 1H, Ar-8-H), 7.57−7.53 (dd, J = 9.1, 2.1 Hz, 1H, Ar-6′-H), 7.45−7.37 (m, 1H, Ar-2″-H), 7.32−7.29 (d, J = 9 Hz, 1H, Ar-5′-H), 6.98−6.93 (t, J = 8.4 Hz, 1H, Ar-5″-H), 6.85−6.82 (d, J = 8.4 Hz, 1H, Ar-4″-H), 6.78−6.75 (dd, J = 8.4, 1.7 Hz, 1H, Ar-6″-H), 4.31−4.28 (t, J = 5.8 Hz, 2H, CH_2, Cl(CH$_2$)$_2$**C*H*$_2$**O), 3.89−3.85 (t, J = 6.4 Hz, 2H, CH_2, Cl**C*H*$_2$**(CH$_2$)$_2$O), 2.33−2.25 (p, 2H, CH_2, ClCH$_2$**C*H*$_2$**CH$_2$O); ^{13}C DEPT (75 MHz, DMSO-d_6): δ 152.66 (1C, Ar-2-CH), 131.75 (1C, Ar-8-CH), 130.07 (1C, Ar-5″-CH), 124.90 (1C, Ar-7-CH), 124.01 (1C, Ar-5′-CH), 122.81 (1C, Ar-6′-CH), 122.73 (1C, Ar-2′-CH), 112.84 (1C, Ar-6″-CH), 110.31 (1C, Ar-4″-CH), 104.84 (1C, Ar-2″-CH), 103.49 (1C, Ar-5-CH), 65.61 (1C, CH_2, Cl(CH$_2$)$_2$**C*H*$_2$**O), 42.46 (1C, CH_2, Cl**C*H*$_2$**(CH$_2$)$_2$O), 32.13 (1C, CH_2, ClCH$_2$**C*H*$_2$**CH$_2$O); MS (APCI$^+$): m/z 458.1 [M + 1]$^+$.

*N-(3-Chloro-4-(3-(trifluoromethyl)phenoxy)phenyl)-6-(3-chloropropoxy)quinazolin-4-amine (**24c**).* Yellow solid, 1.55 g, yield: 62%; ^{1}H NMR (300 MHz, DMSO-d_6): δ 9.72 (s, 1H, NH, exchanged with D_2O), 8.57 (s, 1H, Ar-2-H), 8.27−8.26 (d (m-coupling), J = 1.8 Hz, 1H, Ar-5-H), 7.92 (m, 2H, Ar-2′, 7-H), 7.77−7.74 (d, J = 9.1 Hz, 1H, Ar-8-H), 7.64−7.59 (t, J = 7.8 Hz, 1H, Ar-5″-H), 7.54−7.51 (dd, J = 9.1, 1.7 Hz, 1H, Ar-6′-H), 7.48−7.45 (d, J = 7.7 Hz, 1H, Ar-4″-H), 7.36−7.33 (d, J = 9 Hz, 1H, Ar-5′-H), 7.25−7.22 (m, 2H, Ar-2″, 6″-H), 4.30−4.26 (t, J = 5.8 Hz, 2H, CH_2, Cl(CH$_2$)$_2$**C*H*$_2$**O), 3.89−3.85 (t, J = 6.3 Hz, 2H, CH_2, Cl**C*H*$_2$**(CH$_2$)$_2$O), 2.33−2.25 (p, 2H, CH_2, ClCH$_2$**C*H*$_2$**CH$_2$O); ^{13}C DEPT (75 MHz, DMSO-d_6): δ 152.61 (1C, Ar-2-CH), 131.87 (1C, Ar-8-CH), 130.04 (1C, Ar-5″-CH), 124.84 (1C, Ar-7-CH), 123.99 (1C, Ar-6″-CH), 122.95 (1C, Ar-5′-CH), 122.75 (1C, Ar-6′-CH), 120.70 (1C, Ar-4″-CH), 119.89 (1C, Ar-2′-CH), 113.27 (1C, Ar-2″-CH), 103.45 (1C, Ar-5-CH), 65.59 (1C, CH_2, Cl(CH$_2$)$_2$**C*H*$_2$**O), 42.43 (1C, CH_2, Cl**C*H*$_2$**(CH$_2$)$_2$O), 32.15 (1C, CH_2, ClCH$_2$**C*H*$_2$**CH$_2$O); MS (APCI$^+$): m/z 508.2 [M + 1]$^+$.

General Procedure for the Synthesis of Compounds (25a−h). A mixture of **24a**, **24b**, or **24c** (1 mmol) and the appropriate secondary amine, 1-methyl piperazine or morpholine (100 mmol), was placed in a 25 mL round-bottomed flask or in a capped vial in the case of secondary amine of low boiling point as diethylamine (100 mmol). The reaction mixture was heated under reflux and monitored by TLC. After 2−4 h, the TLC of the reaction mass indicated the absence of the 6-chloropropoxy quinazoline intermediate (**24a−c**). The reaction mixture was cooled to room temperature and poured onto iced-water (30 mL). The resultant precipitate was filtered, washed with water, and dried. Trituration of the dried precipitate with diethyl ether yielded the desired products in a pure form.

*N-(3-Chloro-4-((3-fluorobenzyl)oxy)phenyl)-6-(3-morpholinopropoxy)quinazolin-4-amine (**25a**).* Reaction time: 2 h, yellowish white solid, 0.4 g, yield: 92%; ^{1}H NMR (300 MHz, $CDCl_3$): δ 8.67 (s, 1H, Ar-2-H), 7.86−7.83 (d, J = 9 Hz, 1H, Ar-8-H), 7.79 (s, 1H, Ar-5-H), 7.57 (s, 1H, NH), 7.55−7.52 (d, J = 9 Hz, 1H, Ar-7-H), 7.46−7.43 (d, J = 8.9 Hz, 1H, Ar-6′-H), 7.40−7.33 (m, 1H, Ar-4″-H), 7.25−7.23 (d, J = 8.6 Hz, 1H, Ar-6″-H), 7.18 (br s, 2H, Ar-2′, 2″-H), 7.06−7.00 (t, J = 8.6 Hz, 1H, Ar-5″-H), 6.97−6.94 (d, J = 8.8 Hz, 1H, Ar-5′-H), 5.14 (s, 2H, CH_2, O**C*H*$_2$**C$_6$H$_4$F), 4.14−4.09 (t, J = 6.2 Hz, 2H, CH_2, *N*-(CH$_2$)$_2$-**C*H*$_2$**-O), 3.74 (br s, 4H, 2-CH_2, O(**C*H*$_2$**)$_2$, morpholino), 2.57−2.52 (t, J = 7.1 Hz, *N*-**C*H*$_2$**CH$_2$CH$_2$O), 2.48 (br s, 4H, 2-CH_2, N(**C*H*$_2$**)$_2$, morpholino), 2.08−2.01 (m, 2H, CH_2, *N*-CH$_2$-**C*H*$_2$**-CH$_2$-O); ^{13}C DEPT (75 MHz, $CDCl_3$): δ 152.83 (1C, Ar-2-CH), 130.39 (1C, Ar-8-CH), 130.14 (1C, Ar-5″-CH), 124.75 (1C, Ar-7-CH), 124.54 (1C, Ar-6″-CH), 122.44 (1C, Ar-6′-CH), 121.83 (1C, Ar-2′-CH), 115.24 (1C, Ar-5′-CH), 114.43 (1C, Ar-4″-CH), 113.83 (1C, Ar-2″-CH), 100.59 (1C, Ar-5-CH), 70.45 (1C, CH_2, O**C*H*$_2$**C$_6$H$_4$F), 66.94 (2C, 2-CH_2, O(**C*H*$_2$**)$_2$, morpholino), 66.74 (1C, CH_2, *N*-(CH$_2$)$_2$-**C*H*$_2$**-O), 55.39 (1C, CH_2, *N*-**C*H*$_2$**-(CH$_2$)$_2$-O), 53.75 (2C, 2-CH_2, N(**C*H*$_2$**)$_2$, morpholino), 26.28 (1C, CH_2, *N*-CH$_2$-**C*H*$_2$**-CH$_2$-O); ^{13}C NMR (75 MHz, $CDCl_3$): δ 157.44 (1C, Ar-4-C), 156.90 (1C, Ar-6-C), 152.83 (1C, Ar-2-CH), 150.97 (1C, Ar-3″-C), 145.43 (1C, Ar-8a-C), 139.10 (1C, Ar-4′-C), 132.46 (2C, Ar-1″, 1′-C), 130.26 (2C, Ar-8, 5″-CH), 124.74 (1C, Ar-7-CH), 124.53 (1C, Ar-6″-CH), 123.55 (1C, Ar-3′-C), 122.45 (1C, Ar-6′-CH), 121.83 (1C, Ar-2′-CH), 115.50 (1C, Ar-5′-CH), 114.79 (1C, Ar-4a-C), 114.44 (1C, Ar-4″-CH), 113.84 (1C, Ar-2″-CH), 100.60 (1C, Ar-5-CH), 70.46 (1C, CH_2, O**C*H*$_2$**C$_6$H$_4$F), 66.93 (2C, 2-CH_2, O(**C*H*$_2$**)$_2$, morpholino), 66.76 (1C, CH_2, *N*-(CH$_2$)$_2$-**C*H*$_2$**-O), 55.38 (1C, CH_2, *N*-**C*H*$_2$**-(CH$_2$)$_2$-O), 53.75 (2C, 2-CH_2, N(**C*H*$_2$**)$_2$, morpholino), 26.28 (1C, CH_2, *N*-CH$_2$-**C*H*$_2$**-CH$_2$-O); HRMS (ES$^+$): m/z calcd for $C_{28}H_{29}ClFN_4O_3$ [M + 1]$^+$, 523.1912; found, 523.1912.

*N-(3-Chloro-4-((3-fluorobenzyl)oxy)phenyl)-6-(3-(4-methylpiperazin-1-yl)propoxy)quinazolin-4-amine (**25b**).* Reaction time; 3 h, light-brown solid, 0.4 g, yield: 77%; ^{1}H NMR (300 MHz, DMSO-d_6): δ 9.61 (s, 1H, NH, exchanged with D_2O), 8.48 (s, 1H, Ar-2-H), 8.00 (d, 1H, Ar-8-H), 7.88 (s, 1H, Ar-5-H), 7.75−7.69 (m, 2H, Ar-7, 6′-H), 7.48 (s, 1H, Ar-2′-H), 7.45−7.43 (d, J = 8.8 Hz, 1H, Ar-4″-H), 7.34 (s, 1H, Ar-2″-H), 7.32−7.29 (d, J = 7.5 Hz, 1H, Ar-5′-H), 7.28−7.25 (d, J = 9 Hz, 1H, Ar-6″-H), 7.20−7.15 (t, J = 9 Hz, 1H, Ar-5″-H), 5.25 (s, 2H, CH_2, O**C*H*$_2$**C$_6$H$_4$F), 4.18−4.14 (t, J = 6 Hz, 2H, CH_2, *N*-(CH$_2$)$_2$-**C*H*$_2$**-O), 2.47−2.43 (t, J = 6.1 Hz, *N*-**C*H*$_2$**CH$_2$CH$_2$O), 2.38 (br s, 4H, 2-**C*H*$_2$**, piperazino), 2.30 (br s, 4H, 2-**C*H*$_2$**, piperazino), 2.13 (s, 3H, **C*H*$_3$**), 1.98−1.90 (p, 2H, CH_2, *N*-CH$_2$-**C*H*$_2$**-CH$_2$-O); ^{13}C DEPT (75 MHz, DMSO): δ 152.71 (1C, Ar-2-CH), 131.06 (1C, Ar-8-CH), 129.85 (1C, Ar-5″-CH), 124.69 (1C, Ar-7-CH), 124.54 (1C, Ar-6″-CH), 123.76 (1C, Ar-6′-CH), 122.72 (1C, Ar-2′-CH), 115.28 (1C, Ar-5′-CH), 114.73 (1C, Ar-4″-CH), 114.33 (1C, Ar-2″-CH), 103.36 (1C, Ar-5-CH), 69.8 4 (1C, CH_2, O**C*H*$_2$**C$_6$H$_4$F), 67.12 (1C, CH_2, *N*-(CH$_2$)$_2$-**C*H*$_2$**-O), 55.19 (2C, 2-**C*H*$_2$**, piperazino), 54.91 (1C, CH_2, *N*-**C*H*$_2$**-(CH$_2$)$_2$-O), 53.25 (2C, 2-**C*H*$_2$**, piperazino), 46.20 (1C, CH_3), 26.70 (1C, CH_2, *N*-CH$_2$-**C*H*$_2$**-CH$_2$-O); ^{13}C NMR (75 MHz, DMSO): δ 157.28 (1C, Ar-4-C), 157.20 (1C, Ar-6-C), 152.71 (1C, Ar-2-CH), 150.01 (1C, Ar-3″-C), 145.38 (1C, Ar-8a-C), 140.18 (1C, Ar-4′-C), 140.08 (1C, Ar-1″-C), 133.81 (1C, Ar-1′-C), 131.05 (1C, Ar-8-CH), 129.85 (1C, Ar-5″-CH), 124.68 (1C, Ar-7-CH), 124.53 (1C, Ar-6″-CH), 123.78 (1C, Ar-6′-CH), 122.71 (1C, Ar-2′-CH), 121.50 (1C, Ar-3′-C), 116.03 (1C, Ar-4a-C), 115.27 (1C, Ar-5′-CH), 114.76 (1C, Ar-4″-CH), 114.33 (1C, Ar-2″-CH), 103.39 (1C, Ar-5-CH), 69.87 (1C, CH_2, O**C*H*$_2$**C$_6$H$_4$F), 67.13 (1C, CH_2, CH_2, *N*-(CH$_2$)$_2$-**C*H*$_2$**-O), 55.18 (2C, 2-**C*H*$_2$**, piperazino), 54.91 (1C, CH_2, *N*-CH$_2$-**C*H*$_2$**-CH$_2$-O), 53.24 (2C, 2-**C*H*$_2$**, piperazino), 46.18 (1C, CH_3), 26.70 (1C, CH_2, *N*-CH$_2$-

https://dx.doi.org/10.1021/acs.jmedchem.0c01647
J. Med. Chem. XXXX, XXX, XXX−XXX

CH_2-CH_2-O); HRMS (ES$^+$): m/z calcd for $C_{29}H_{32}ClFN_5O_2$ [M + 1]$^+$, 536.2229; found, 536.2226.

*N-(3-Chloro-4-(3-fluorophenoxy)phenyl)-6-(3-morpholinopropoxy)quinazolin-4-amine (**25c**).* Reaction time; 3 h, white solid, mp 172−175 °C, 0.4 g, yield: 94%; ^{1}H NMR (300 MHz, $CDCl_3$): δ 8.70 (s, 1H, NH), 8.34 (s, 1H, Ar-2-H), 8.00 (s, 1H, Ar-5-H), 7.84−7.81 (d, J = 8.9 Hz, 1H, Ar-8-H), 7.68−7.65 (d, J = 8.9 Hz, 1H, Ar-7-H), 7.43−7.38 (m, 2H, Ar-6′, 2′-H), 7.27−7.21 (m, 1H, Ar-4″-H), 7.07−7.04 (d, J = 8.8 Hz, 1H, Ar-5′-H), 6.77−6.71 (m, 2H, Ar-2″, 5″-H), 6.67−6.63 (dd, 1H, Ar-6″-H), 4.08−4.04 (t, J = 6.0 Hz, 2H, CH_2, N-$(CH_2)_2$-**CH_2**-O), 3.72 (br s, 4H, O(**CH_2**)$_2$, morpholino), 2.52−2.46 (m, 6H, 3-CH_2, 2-CH_2 of N(**CH_2**)$_2$, morpholino, &N-**CH_2**$(CH_2)_2$O), 2.03−1.95 (p, J = 6.0 Hz, 2H, CH_2, N-CH_2-**CH_2**-CH_2-O); ^{13}C DEPT (75 MHz, $CDCl_3$): δ 152.63 (1C, Ar-2-CH), 130.58 (1C, Ar-8-CH), 130.08 (1C, Ar-5″-CH), 124.81 (1C, Ar-7-CH), 124.06 (1C, Ar-5′-CH), 122.01 (1C, Ar-6′-CH), 121.59 (1C, Ar-2′-CH), 112.66 (1C, Ar-6″-CH), 109.95 (1C, Ar-4″-CH), 104.96 (1C, Ar-2″-CH), 101.07 (1C, Ar-5-CH), 66.86 (2C, 2-CH_2, O(**CH_2**)$_2$, morpholino), 66.74 (1C, CH_2, N-$(CH_2)_2$-**CH_2**-O), 55.38 (1C, CH_2, N-**CH_2**-$(CH_2)_2$-O), 53.71 (2C, 2-CH_2, N(**CH_2**)$_2$, morpholino), 26.18 (1C, CH_2, N-CH_2-**CH_2**-CH_2-O); ^{13}C NMR (75 MHz, $CDCl_3$): δ 157.54 (1C, Ar-4-C), 156.71 (1C, Ar-6-C), 152.64 (1C, Ar-2-CH), 147.48 (1C, Ar-3″-C), 145.49 (1C, Ar-1″-C), 136.11 (1C, Ar-8a-C), 130.59 (1C, Ar-8-CH), 130.46 (1C, Ar-4′-C), 130.28 (1C, Ar-5″-CH), 126.66 (1C, Ar-1′-C), 124.74 (1C, Ar-7-CH), 123.98 (1C, Ar-5′-CH), 122.07 (2C, Ar-6′, 3′-CH), 121.49 (1C, Ar-2′-CH), 115.70 (1C, Ar-4a-C), 112.63 (1C, Ar-6″-CH), 109.97 (1C, Ar-4″-CH), 104.97 (1C, Ar-2″-CH), 100.86 (1C, Ar-5-CH), 66.89 (2C, 2-CH_2, O(**CH_2**)$_2$ morpholino), 66.76 (1C, CH_2, N-$(CH_2)_2$-**CH_2**-O), 55.39 (1C, CH_2, N-**CH_2**-$(CH_2)_2$-O), 53.74 (2C, 2-CH_2, N(**CH_2**)$_2$, morpholino), 26.22 (1C, CH_2, N-CH_2-**CH_2**-CH_2-O); HRMS (ES$^+$): m/z calcd for $C_{27}H_{27}ClFN_4O_3$ [M + 1]$^+$, 509.1756; found, 509.1755.

*N-(3-Chloro-4-(3-fluorophenoxy)phenyl)-6-(3-(4-methylpiperazin-1-yl)propoxy)quinazolin-4-amine (**25d**).* Reaction time: 4 h, brown solid, 0.39 g, yield: 76%; ^{1}H NMR (300 MHz, DMSO-d_6): δ 9.73 (s, 1H, NH, exchanged with D_2O), 8.54 (s, 1H, Ar-2-H), 8.24 (s, 1H, Ar-2″-H), 7.90 (br s, 2H, Ar-2′,5-H), 7.75−7.72 (d, J = 9.1 Hz, 1H, Ar-8-H), 7.52−7.49 (d, J = 9 Hz, 1H, Ar-7-H), 7.44−7.36 (m, 1H, Ar-4″-H), 7.31−7.28 (d, J = 8.9 Hz, 1H, Ar-6′-H), 6.97−6.92 (t, J = 8.1 Hz, 1H, Ar-5″-H), 6.83−6.80 (d, J = 8.9 Hz, 1H, Ar-5′-H), 6.77−6.74 (d, J = 8.2 Hz, 1H, Ar-6″-H), 4.19−4.15 (t, J = 5.4 Hz, 2H, CH_2, N-$(CH_2)_2$-**CH_2**-O), 2.45−2.31 (m, 10H, 4-CH_2 of piperazine & N-**CH_2**$(CH_2)_2$O), 1.97−1.93 (m, 2H, CH_2, N-CH_2-**CH_2**-CH_2-O); ^{13}C DEPT (75 MHz, DMSO): δ 152.50 (1C, Ar-2-CH), 131.73 (1C, Ar-8-CH), 129.96 (1C, Ar-5″-CH), 124.83 (1C, Ar-7-CH), 123.93 (1C, Ar-5′-CH), 122.80 (1C, Ar-6′-CH), 122.66 (1C, Ar-2′-CH), 112.74 (1C, Ar-6″-CH), 110.27 (1C, Ar-4″-CH), 104.78 (1C, Ar-2″-CH), 103.43 (1C, Ar-5-CH), 67.15 (1C, CH_2, N-$(CH_2)_2$-**CH_2**-O), 55.18 (2C, 2-CH_2, piperazino), 54.89 (1C, CH_2, N-**CH_2**-$(CH_2)_2$-O), 53.24 (2C, 2-CH_2, piperazino), 46.18 (1C, CH_3), 26.70 (1C, CH_2, N-CH_2-**CH_2**-CH_2-O); ^{13}C NMR (75 MHz, DMSO): δ 161.76 (1C, Ar-4-C), 159.13 (1C, Ar-3″-CH), 157.34 (1C, Ar-1″-C), 157.09 (1C, Ar-6-C), 152.50 (1C, Ar-2-CH), 146.16 (1C, Ar-8a-C), 145.50 (1C, Ar-4′-C), 137.91 (1C, Ar-1′-C), 131.72 (1C, Ar-8-CH), 129.95 (1C, Ar-5″-CH), 125.35 (1C, Ar-3′-C), 124.84 (1C, Ar-7-CH), 123.96 (1C, Ar-5′-CH), 122.78 (1C, Ar-6′-CH), 122.68 (1C, Ar-2′-CH), 116.13 (1C, Ar-4a-C), 112.81 (1C, Ar-6″-CH), 110.27 (1C, Ar-4″-CH), 104.78 (1C, Ar-2″-CH), 103.49 (1C, Ar-5-CH), 67.18 (1C, CH_2, N-$(CH_2)_2$-**CH_2**-O), 55.17 (2C, 2-CH_2, piperazino), 54.89 (1C, CH_2, N-$(CH_2)_2$-**CH_2**-O), 53.22 (2C, 2-CH_2, piperazino), 46.15 (1C, CH_3), 26.70 (1C, CH_2, N-CH_2-**CH_2**-CH_2-O); HRMS (ES$^+$): m/z calcd for $C_{28}H_{30}ClFN_5O_2$ [M + 1]$^+$, 522.2072; found, 522.2071.

*N-(3-Chloro-4-(3-(trifluoromethyl)phenoxy)phenyl)-6-(3-morpholinopropoxy)quinazolin-4-amine (**25e**).* Reaction time, yellow solid, 3 h, mp 95−100 °C, 0.46 g, yield: 84%; ^{1}H NMR (300 MHz, $CDCl_3$): δ 8.71 (s, 1H, NH), 8.20 (s, 1H, Ar-2-H), 8.04 (s, 1H, Ar-5-H), 7.86−7.83 (d, J = 9 Hz, 1H, Ar-8-H), 7.69−7.67 (d, J = 8.8 Hz, 1H, Ar-7-H), 7.45−7.40 (m, 2H, Ar-6′, 2′-H), 7.34 (br s, 2H, Ar-4″,5′-H), 7.20 (s, 1H, Ar-2″-H), 7.12−7.05 (m, 2H, Ar-6″, 5″-H), 4.08−4.05 (t, J = 5.6 Hz, 2H, CH_2, N-$(CH_2)_2$-**CH_2**-O), 3.74 (br s, 4H, O(**CH_2**)$_2$, morpholino), 2.59−2.48 (m, 6H, 3-CH_2, 2-CH_2 of N(**CH_2**)$_2$ morpholino, &N-**CH_2**$(CH_2)_2$O), 2.02−1.98 (p, J = 5.6 Hz, 2H, CH_2, N-CH_2-**CH_2**-CH_2-O); ^{13}C DEPT (75 MHz, $CDCl_3$): δ 152.61 (1C, Ar-2-CH), 130.32 (1C, Ar-8-CH), 130.19 (1C, Ar-5″-CH), 124.85 (1C, Ar-7-CH), 124.04 (1C, Ar-6″-CH), 121.98 (1C, Ar-5′-CH), 121.55 (1C, Ar-6′-CH), 120.17 (1C, Ar-4″-CH), 119.61 (1C, Ar-2′-CH), 113.95 (1C, Ar-2″-CH), 100.83 (1C, Ar-5-CH), 66.85 (3C, 3-CH_2, 2-CH_2 of O(**CH_2**)$_2$, morpholino, N-$(CH_2)_2$-**CH_2**-O), 55.37 (1C, CH_2, N-**CH_2**$(CH_2)_2$O), 53.70 (2C, 2-CH_2 of N(**CH_2**)$_2$ morpholino), 26.14 (1C, CH_2, N-CH_2-**CH_2**-CH_2-O); ^{13}C NMR (75 MHz, $CDCl_3$): δ 157.64 (1C, Ar-4-C), 157.58 (1C, Ar-6-C), 156.75 (1C, Ar-1″-C), 152.61 (1C, Ar-2-CH), 147.24 (1C, Ar-8a-C), 145.45 (1C, Ar-4′-C), 136.31 (1C, Ar-1′-C), 130.33 (2C, Ar-8-CH, CF_3), 130.20 (2C, Ar-5″-CH, Ar-3″-C), 126.68 (1C, Ar-3′-C), 124.85 (1C, Ar-7-CH), 124.04 (1C, Ar-6″-CH), 121.98 (1C, Ar-5′-CH), 121.54 (1C, Ar-6′-CH), 120.17 (1C, Ar-4″-CH), 119.64 (1C, Ar-2′-CH), 115.73 (1C, Ar-4a-C), 113.96 (1C, Ar-2″-CH), 100.83 (1C, Ar-5-CH), 66.86 (2C, 2-CH_2 of O(**CH_2**)$_2$, morpholino), 66.74 (1C, CH_2, N-$(CH_2)_2$-**CH_2**-O), 55.37 (1C, CH_2, N-**CH_2**$(CH_2)_2$O), 53.71 (2C, 2-CH_2 of N(**CH_2**)$_2$ morpholino), 26.16 (1C, CH_2, N-CH_2-**CH_2**-CH_2-O); HRMS (ES$^+$): m/z calcd for $C_{28}H_{27}ClF_3N_4O_3$ [M + 1]$^+$, 559.1724; found, 559.1726.

*N-(3-Chloro-4-(3-(trifluoromethyl)phenoxy)phenyl)-6-(3-(4-methylpiperazin-1-yl)propoxy)quinazolin-4-amine (**25f**).* Reaction time: 4 h, brown solid, 0.46 g, yield: 82%, ^{1}H NMR (300 MHz, $CHCl_3$): δ 8.71 (s, 1H, NH), 8.49 (s, 1H, Ar-2-H), 8.09 (s, 1H, Ar-5-H), 7.84−7.81 (d, J = 8.9 Hz, 1H, Ar-8-H), 7.76−7.73 (d, J = 8.8 Hz, 1H, Ar-7-H), 7.43−7.40 (m, 3H, Ar-6′, 2′,4″-H), 7.34−7.32 (d, 1H, Ar-5′-H), 7.20 (s, 1H, Ar-2″-H), 7.12−7.06 (m, 2H, Ar-6″, 5″-H), 4.05 (br s, 2H, CH_2, N-$(CH_2)_2$-**CH_2**-O), 2.83 (br s, 2H, CH_2, N-**CH_2**$(CH_2)_2$O), 2.49 (br s, 8H, 4CH_2, piperazino), 2.29 (s, 3H, CH_3), 2.00 (br s, 2H, CH_2, N-CH_2-**CH_2**-CH_2-O). ^{13}C DEPT (75 MHz, $CHCl_3$): δ 152.61 (1C, Ar-2-CH), 130.31 (1C, Ar-8-CH), 130.07 (1C, Ar-5″-CH), 125.85 (1C, Ar-7-CH), 124.85 (1C, Ar-6″-CH), 122.00 (1C, Ar-5′-CH), 121.56 (1C, Ar-6′-CH), 120.11 (1C, Ar-4″-CH), 119.54 (1C, Ar-2′-CH), 113.88 (1C, Ar-2″-CH), 101.26 (1C, Ar-5-CH), 66.89 (1C, CH_2, N-$(CH_2)_2$-**CH_2**-O), 54.89 (3C, 3-CH_2, 2-CH_2 of piperazino, N-**CH_2**$(CH_2)_2$O), 53.08 (2C, 2-CH_2, piperazino), 45.89 (1C, CH_3), 26.37 (1C, CH_2, N-CH_2-**CH_2**-CH_2-O). ^{13}C NMR (75 MHz, $CHCl_3$): δ 157.73 (1C, Ar-4-C), 157.44 (1C, Ar-6-C), 156.86 (1C, Ar-1″-C), 152.64 (1C, Ar-2-CH), 147.03 (1C, Ar-8a-C), 145.48 (1C, Ar-4′-C), 136.62 (1C, Ar-1′-C), 130.31 (2C, Ar-8-CH, CF_3), 130.10 (2C, Ar-5″-CH, Ar-3″-C), 126.63 (1C, Ar-3′-C), 124.81 (1C, Ar-7-CH), 123.99 (1C, Ar-6″-CH), 122.01 (1C, Ar-5′-CH), 121.54 (1C, Ar-6′-CH), 120.12 (1C, Ar-4″-CH), 119.52 (1C, Ar-2′-CH), 115.86 (1C, Ar-4a-C), 113.90 (1C, Ar-2″-CH), 101.31 (1C, Ar-5-CH), 66.78 (1C, CH_2, N-$(CH_2)_2$-**CH_2**-O), 54.87 (1C, CH_2, N-**CH_2**$(CH_2)_2$O), 54.72 (2C, 2-CH_2, piperazine), 52.89 (2C, 2-CH_2, piperazine), 45.75 (1C, CH_3), 26.33 (1C, CH_2, N-CH_2-**CH_2**-CH_2-O); HRMS (ES$^+$): m/z calcd for $C_{29}H_{30}ClF_3N_5O_2$ [M + 1]$^+$, 572.2040; found, 572.2042.

*N-(3-Chloro-4-(3-(trifluoromethyl)phenoxy)phenyl)-6-(3-(diethylamino)propoxy)quinazolin-4-amine (**25g**).* Reaction time; 2 h, yellow solid, 0.41 g, yield: 76%; ^{1}H NMR (300 MHz, $CDCl_3$): δ 8.72 (s, 1H, NH), 8.56 (s, 1H, Ar-2-H), 8.12 (s, 1H, Ar-5-H), 7.85−7.82 (d, J = 8.8 Hz, 1H, Ar-8-H), 7.74−7.72 (d, J = 8.8 Hz, 1H, Ar-7-H), 7.44−7.40 (m, 3H, Ar-6′, 2′,4″-H), 7.34−7.32 (d, 1H, Ar-5′-H), 7.21 (s, 1H, Ar-2″-H), 7.12−7.05 (m, 2H, Ar-6″, 5″-H), 4.04−4.00 (t, J = 6.3 Hz, 2H, CH_2, N-$(CH_2)_2$-**CH_2**-O), 2.61−2.54 (m, 6H, 3(CH_2)), 1.99−1.91 (p, 2H, CH_2, N-CH_2-**CH_2**-CH_2-O), 1.07−1.02 (t, J = 7.1 Hz, 6H, 2(CH_3)); ^{13}C DEPT (75 MHz, $CDCl_3$): δ 152.61 (1C, Ar-2-CH), 130.30 (1C, Ar-8-CH), 130.02 (1C, Ar-5″-CH), 125.10 (1C, Ar-7-CH), 124.05 (1C, Ar-6″-CH), 121.97 (1C, Ar-5′-CH), 121.56 (1C, Ar-6′-CH), 120.11 (1C, Ar-4″-CH), 119.57 (1C, Ar-2′-CH), 113.97 (1C, Ar-2″-CH), 101.04 (1C, Ar-5-CH), 66.91 (1C, CH_2, **CH_2**O), 49.13 (1C, CH_2, NH **CH_2**$(CH_2)_2$O), 46.89 (2C, 2CH_2, (CH_3**CH_2**-)$_2$), 26.46 (1C, CH_2, NHCH$_2$**CH_2**CH$_2$O), 11.28 (2C, 2CH_3); ^{13}C NMR (75 MHz, $CDCl_3$): δ 157.72 (1C, Ar-4-C), 157.52 (1C, Ar-6-C), 156.89 (1C, Ar-1″-C), 152.61 (1C, Ar-2-CH),

https://dx.doi.org/10.1021/acs.jmedchem.0c01647
J. Med. Chem. XXXX, XXX, XXX−XXX

147.09 (1C, Ar-8a-C), 145.43 (1C, Ar-4′-C), 136.54 (1C, Ar-1′-C), 130.29 (2C, Ar-8-CH, CF_3), 130.03 (2C, Ar-5″-CH, Ar-3″-C), 126.64 (1C, Ar-3′-C), 125.09 (1C, Ar-7-CH), 124.04 (1C, Ar-6″-CH), 121.96 (1C, Ar-5′-CH), 121.56 (1C, Ar-6′-CH), 120.11 (1C, Ar-4″-CH), 119.57 (1C, Ar-2′-CH), 115.84 (1C, Ar-4a-C), 113.97 (1C, Ar-2″-CH), 101.03 (1C, Ar-5-CH), 66.91 (1C, CH_2, $\mathbf{CH_2}O$), 49.14 (1C, CH_2, NH $\mathbf{CH_2}(CH_2)_2O$), 46.90 (2C, $2CH_2$, $2(CH_3\mathbf{CH_2}\text{-})_2$), 26.49 (1C, CH_2, $NHCH_2\mathbf{CH_2}CH_2O$), 11.29 (2C, $2CH_3$); HRMS (ES^+): m/z calcd for $C_{28}H_{29}ClF_3N_4O_2$ $[M + 1]^+$, 545.1931; found, 545.1933.

*2-((3-((4-((3-Chloro-4-(3-(trifluoromethyl)phenoxy)phenyl)-amino)quinazolin-6-yl)oxy)propyl) amino)ethan-1-ol (**25h**).* A mixture of intermediate **24c** (0.5 g, 1 mmol) and 2-aminoethanol (0.5 g, 0.6 mL, 10 mmol) in methanol (25 mL) was held at reflux for 8 h in the presence of triethylamine (15 drops). Methanol was removed under reduced pressure, and the remaining residue was dissolved in DCM and purified by flash column chromatography with DCM/MeOH (95:5%) as an eluent to yield compound **25h**.

Yellow semisolid mass, 0.22 g, yield: 42%; ^{1}H NMR (300 MHz, DMSO-d_6): δ 9.76 (1H, NH, exchanged with D_2O), 8.56 (s, 1H, Ar-2-H), 8.27−8.26 (d (m-coupling), J = 2.1, 1H, Ar-5-H), 7.96−7.92 (dd, J = 8.7 Hz, 2 Hz, 2H, Ar-7, 8-H), 7.77−7.74 (d, J = 9 Hz, Ar-5′-H), 7.65−7.60 (t, J = 7.8 Hz, 1H, Ar-5″-H), 7.54−7.50 (dd, J = 9 Hz, 2.1 Hz, 1H, Ar-6′-H), 7.49−7.46 (d, J = 7.9 Hz, 1H, Ar-4″-H), 7.36−7.33 (d (m-coupling), J = 2.1 Hz, 1H, Ar-2′-H), 7.25−7.22 (m, 2H, Ar-6″, 2″), 4.24−4.20 (t, J = 6.2 Hz, 2H, NH + OH, exchanged with D_2O), 3.49−3.45 (t, J = 5.7 Hz, 2H, CH_2, $-CH_2O$), 3.37−3.33 (t, J = 6.7 Hz, 2H, CH_2, $OHCH_2CH_2NH-$), 2.76−2.71 (t, J = 6.7 Hz, 2H, CH_2, $OHCH_2CH_2NH-$), 2.62−2.56 (m, 2H, CH_2, $NHCH_2(CH_2)_2O$), 2.00−1.92 (p, 2H, CH_2, $NHCH_2CH_2CH_2O$); ^{13}C DEPT (75 MHz, DMSO-d_6): δ 152.47 (1C, Ar-2-CH), 131.92 (1C, Ar-8-CH), 129.96 (1C, Ar-5″-CH), 124.92 (1C, Ar-7-CH), 123.98 (1C, Ar-6″-CH), 123.00 (1C, Ar-5′-CH), 122.78 (1C, Ar-6′-CH), 120.70 (1C, Ar-4″-CH), 119.91 (1C, Ar-2′-CH), 113.30 (1C, Ar-2″-CH), 103.35 (1C, Ar-5-CH), 67.25 (1C, CH_2, $-CH_2O-$), 60.84 (1C, CH_2, $OHCH_2-$), 52.29 (1C, CH_2, $OHCH_2CH_2NH-$), 46.41 (1C, CH_2, $-NHCH_2(CH_2)_2O$), 29.82 (1C, CH_2, $NHCH_2CH_2CH_2O$); ^{13}C NMR (75 MHz, DMSO-d_6): δ 158.14 (1C, Ar-4-C), 157.42 (1C, Ar-6-C), 157.04 (1C, Ar-1″-C), 152.47 (1C, Ar-2-CH), 145.81 (1C, Ar-8a-C), 145.51 (1C, Ar-4′-C), 138.20 (1C, Ar-1′-C), 131.92 (1C, Ar-8-CH), 131.39 (1C, CF_3), 130.97 (1C, Ar-3″-C), 129.97 (1C, Ar-5″-CH), 125.46 (1C, Ar-3′-C), 124.91 (1C, Ar-7-CH), 123.98 (1C, Ar-6″-CH), 123.00 (1C, Ar-5′-CH), 122.78 (1C, Ar-6′-CH), 120.70 (2C, Ar-2′,4″-CH), 116.17 (1C, Ar-4a-C), 113.31 (1C, Ar-2″-CH), 103.36 (1C, Ar-5-CH), 67.25 (1C, CH_2, CH_2O), 60.84 (1C, CH_2, $OHCH_2$-), 52.29 (1C, CH_2, $OHCH_2CH_2NH$), 46.41 (1C, CH_2, NH $CH_2(CH_2)_2O$), 29.83 (1C, CH_2, $NHCH_2CH_2CH_2O$); HRMS (ES^+): m/z calcd for $C_{26}H_{25}ClF_3N_4O_3$ $[M + 1]^+$, 533.1567; found, 533.1563.

Pharmacology. *Material Quality Control and Reagents.* The recombinant protein kinases employed in the compound profiling process were cloned, expressed, and purified using proprietary methods. Quality control testing is routinely performed to ensure compliance to acceptable standards. The [γ-^{32}P]ATP was purchased from PerkinElmer. All other materials were of standard laboratory grade. The stock solutions of the tested compounds were prepared and 5 μL were incorporated into each assay and tested against the protein kinase panel selected. Quality control testing is routinely performed to ensure compliance with acceptable standards. The ADP-GloTM assay kit was purchased from Promega, and all other materials were of standard laboratory grade.

[γ-^{32}P]ATP Radiometric Protein Kinase Assay Method. The protein kinase profiling was conducted by Kinexus Bioinformatics Corporation, Vancouver, British Columbia, Canada, according to the following protocols. The kinase profiling of 7 test compounds, namely, **10a**, **10b**, **15a**, **15e**, **15l**, **17d**, and **25f** by [γ-^{32}P]ATP radioisotope was carried out in a single measurement at 10 μM concentration against a panel of 20 protein kinases. Sorafenib and lapatinib were used as positive references at a final concentration of 10 μM. All experiments have been conducted in a designated radioactive environment and at ambient temperature for 30 min in a total volume of 25 μL according to the following protocol. Component 1: 5.0 μL of the active kinase (∼10−50 nM final concentration), component 2: 5.0 μL of the substrate solution, component 3: 5.0 μL of buffer, component 4: 5.0 μL of test and reference at various concentrations or 10% DMSO for the blank control, and component 5: 5.0 μL of [γ-^{32}P]ATP (from 50 μM stock solution, 0.8 μCi). The research was launched by adding [γ-^{32}P]ATP to a mixture of other components and incubating for 30 min. Then, the assay was terminated by adding 10 μL of the mixture onto a MultiScreen phosphocellulose P81 plate, which was then washed 3× with 1% solution of phosphoric acid solution. Using a Trilux scintillation counter, the radioactivity was measured for the test samples in comparison with the blank control which contains all components except replacing the kinase substrate by an equal volume of assay buffer. The protein kinase activity was corrected by removing the value of the blank control. The protocol of these assays was optimized to afford a high signal-to-noise ratio.

ADP-Glo Protein Kinase Assay Method. This assay was conducted using the ADP-GloTM assay kit, to check the generated ADP by specific kinase to be detected through the increase in the luminescence signal. All experiments have been conducted at 30 °C temperature for 30 min in a total volume of 25 μL according to the formula: Component 1: 5.0 μL of active kinase, component 2: 5.0 μL of substrate solution (from 125 μM stock), component 3: 5.0 μL of buffer, component 4: 5.0 μL of test and reference at various concentrations or 10% DMSO for the blank control, and component 5: 5.0 μL of ATP stock solution. The research was launched by mixing all the 5 components in a 96-well plate and incubating it for 30 min. Then, the assay was terminated by adding 25 μL of ADP-Glo (Promega) and then was shaken at 30 °C for 40 min. A total of 50 μL of Kinase Detection Reagent was added and then the 96-well plate was shaken and then incubated for an additional 0.5 h at 30 °C. A GloMax plate reader (Promega; Cat# E7031) was used to read the 96-well reaction plate compared with the blank control which contains all components except replacing the kinase substrate by an equal volume of assay buffer. The protein kinase activity was corrected by removing the value of the blank control. The protocol of these assays was optimized to afford a high signal-to-noise ratio.

In Vitro HER2 Kinase Inhibitory Activity (IC_{50}) against Wild and L755S Mutant Types. The recombinant protein kinases employed in the compound profiling process were cloned, expressed, and purified using proprietary methods. The stock solutions of the test compounds were prepared and tested against HER2 kinases. The assay was carried out as described in detail under the ADP-Glo protein kinase assay method, where the intra-assay variability of each experiment was determined to be less than 10%.

Cell Culture. Four human BC cell lines were utilized in this study to carry out cell proliferation assay, including luminal HER2-positive AU565 cell line, triple-positive BT474 cells, (ER/PR)-positive MCF7 cells, and triple-negative (MDA-MB-231) cells. The four BC cell lines have been purchased from ATCC (Manassas, VA). The cell culture was conducted at 37 °C, at 5% CO_2, 95% air, and 100% relative humidity. 10% heat-inactivated fetal bovine serum, L-glutamine, and 1% penicillin/streptomycin were added to RPMI-1640 media and RPMI/DMEM. The use of the BC cells was limited to 20 passages and was checked regularly (every 6 months) for mycoplasma by detecting the bioluminescence using a MycoWarning sample detection kit (Lonza, Switzerland).

Cell Proliferation Assay. The *in vitro* cell viability assay was used to determine cellular proliferation, inhibitory activity, and cytotoxicity of 27 test compounds using a WST-8 reagent as per manufacturer's instructions (Cell Counting Kit-8, Dojindo Molecular Technologies, Inc., Rockville, MD). About 70−80% of cell confluency was used in all experiments. Cells were seeded in 96-well plates (Nalgene−Nunc, Thermo Fisher Scientific, USA) at a density of 5×10^3 cells per each well in 100 μL of culture medium. Cells were incubated at 37 °C overnight to allow cell attachment. The final concentrations of each compound in wells were 0.0, 0.005, 0.05, 0.5, 5, 25, and 50 μM/mL in 100 μL of media (0.1% DMSO for the blank control). After incubation for 72 h, 10 μL of the WST-8 reagent was added into each well and then the plates were incubated for 3 h. Plates were shaken for

https://dx.doi.org/10.1021/acs.jmedchem.0c01647
J. Med. Chem. XXXX, XXX, XXX−XXX

1 min and the absorbance was examined using a multiplate reader at λ_{450} nm. The IC_{50} (50% growth inhibition) for the test compounds against each BC cell was determined using GraphPad Prism version 5.00 for Windows (GraphPad Software, San Diego, CA, www.graphpad.com).

NCI-60 Screening Assay. The screening methodology is described in detail at http://dtp.nci.nih.gov/branches/btb/ivclsp.html.

*NCI **60 Cell One-Dose Screen**.*[116] All compounds submitted to the NCI 60 cell screen were initially evaluated at a single high dose (10 μM) in the full NCI 60 cell panel including 9 subpanels (hematopoietic system, lung cancer, colon, brain, skin melanoma, ovary, kidney, prostate, and BCs) as described in detail.[116] Briefly, different cancer cells (100 μL) were inoculated into 96-well microtiter plates at plating densities varying from 5000 to 40,000 cells/well depending on the replication time of each cell line. In the case of suspension cells, the protocol was the same except that 50 μL of 80% TCA (final concentration, 16% TCA) was added to terminate the experiment with fixing the settled cells at the bottom of the wells. The % growth was calculated at each of the drug concentrations levels using the absorbance measurements [time zero, T_z, control growth, C, and test growth in the presence of drugs at 10 μM concentration (T_i)].

$$\%\ \text{growth inhibition} = \frac{T_i - T_z}{C - T_z} \times 100$$

for concentrations for which $T_i \geq T_z$

$$\%\ \text{growth inhibition} = \frac{T_i - T_z}{T_z} \times 100$$

for concentrations for which $T_i < T_z$

NCI 60 Cell Five-Dose Screen.[116] Out of 20 compounds tested by one-dose screen, namely, **10a,b**, **15a,c,e,f,g,i,k**, **17a,c,d**, and **25b,c,d,e,f,g,h**, 13 compounds were selected to be screened by five-dose concentration. These compounds, namely, **15f**, **15g**, **15i**, **15k**, **17a**, **17c**, **17d**, **25b**, **25d**, **25e**, **25f**, **25g**, and **25h** exhibited significant growth inhibition and further screened at five concentration levels (0.01, 0.1, 1.0, 10, and 100 μM) against the full NCI 60 cell panel. Five-dose NCI 60 cell screening was conducted as described under one-dose screen but at different concentrations.[116] Three dose–response parameters were calculated for each experimental agent. Growth inhibition of 50% (GI_{50}) was calculated by $\frac{T_i - T_z}{C - T_z} \times 100 = 50$, which is the drug concentration resulting in a 50% reduction in the net protein increase in control cells during the drug incubation. The drug concentration resulting in total growth inhibition (**TGI**) was calculated by $T_i = T_z$. The **LC_{50}** (concentration of the drug resulting in a 50% reduction in the measured protein at the end of the drug treatment as compared to that at the beginning) indicating a net loss of cells following treatment was calculated by $\frac{T_i - T_z}{T_z} \times 100 = -50$.

Effect of the Optimized compounds in Inducing Cell Apoptosis in BT474 cells. Cell apoptosis assay was conducted by flow cytometry using BT474 breast cell lines as described.[117] Briefly, BT474 cells were harvested and then washed twice and resuspended in ice-cold phosphate-buffered saline (PBS). The cells were stained by Guava Nexin (Millipore) reagent (Annexin V-PE and 7-AAD), followed by incubation for 20 min in the dark at room temperature. Samples were acquired using Guava easyCyte 5 flow cytometer. The dot plots were generated using CellQuest software (BD Biosciences, San Jose, CA, USA).[118] Data represented the mean of duplicates ± SD.

Apoptosis Assay Using MCF7 and MDA-MB-231 Cells. Cell apoptosis assay using MCF7 and MDA-MB-231 BC cells was conducted by flow cytometry as described.[3−5] Annexin V-FITC apoptosis detection kit (Abcam Inc., Cambridge Science Park, Cambridge, UK) was used to determine the apoptosis and necrosis of the cell populations. Briefly, after treatment with test compounds for 72 h, BC cells (MCF7 and MDA-MB231; 10^5 cells) were harvested by trypsinization and washed twice with ice-cold PBS (pH 7.4). Then, cells were incubated with 0.5 mL of Annexin V-FITC/PI (1.0 mg/mL) solution for 30 min in the dark at room temperature following the manufacturer's protocol.[119] The stained cells were injected via ACEA Novocyte flow cytometer (ACEA Biosciences Inc., San Diego, CA, USA) and analyzed for FITC and PI fluorescent signals using an FL1 and FL2 signal detector, respectively ($\lambda_{ex/em}$ 488/530 nm for FITC and $\lambda_{ex/em}$ 535/617 nm for PI). For each sample, 12,000 events were acquired and positive FITC and/or PI cells were quantified by quadrant analysis and calculated using ACEA NovoExpress software (ACEA Biosciences Inc., San Diego, CA, USA).

Western Blot Analysis. Immunoblotting was used to determine the antitumor effects of the optimized compounds on the molecular level through the detection of downstream signaling targets of the HER2 pathway. The analysis was conducted according to which we previously described.[101,120] Briefly, about 25 μg of cellular protein lysates prepared from the control and the treated AU565 and BT474 cells were resolved onto a 4–20% SDS-PAGE gel (Bio-Rad, Hercules, CA) under reducing conditions. The fractionated proteins are transferred onto a nitrocellulose membrane (Bio-Rad, Hercules, CA) and subsequently blocked with 3% bovine serum albumin for 1 h at room temperature. The blocked membranes were incubated overnight at 4 °C with appropriate primary antibodies raised against HER2, total and phosphorylated Akt, and ERK1/2 (Cell Signaling, Beverly, USA). Lapatinib was used as an authenticated control for the tested compounds and GAPDH was used as a reference loading control (Santa Cruz Biotechnology, Dallas, TX). Cells were treated with different concentrations at IC_{50}, 0.5 IC_{50}, and 0.1 IC_{50} for each compound at two different time points (24 and 72 h). After serial washing, the membranes were incubated with the appropriate secondary antibodies for 1 h at room temperature, and the signal was developed by Amersham ECL Prime WB Detection Reagent (GE Healthcare Life Sciences, Pittsburgh, PA) using C-Digit and Odyssey CLX Imaging System (LI-COR Biosciences, Lincoln, NE).

Antitumor Effects of the Most Potent Optimized Scaffolds Using the Preclinical BC Model. All animal experiments, surgical and dosing procedures, were approved by Texas A&M University, Rangel College of Pharmacy, and consistent with the Institutional Animal Care and Use Committee (IACUC#091604). Two of the most active compounds with the lowest IC_{50} against BT474 cell lines were subjected to preclinical studies. Approximately 21 female athymic nude mice ($Foxn^{1nu}/Foxn^{1+}$) of 6-week old were obtained from Envigo (Indianapolis, IN, USA); code: 069(nu)/070(nu/+) and maintained with sterilized food and water. These nude mice were used to assess the *in vivo* anticancer activities as described.[25,100] Briefly, 2×10^6 triple-positive BT474 cells in a 1:1 serum-free medium were mixed with an equal amount of Matrigel on ice and were subcutaneously inoculated into dorsal flanks of each athymic nude mouse. Then, mice were randomly divided into three groups (n = 7); group I received the vehicle, group II and III received compounds **17d** and **25b**, respectively, in sterile saline, 50 mg/kg, by oral gavage 5×/week. Based on an overall statistical significance level of 5%, the power of 80% and effect size of 1.06284, a balanced one-way ANOVA, comparing these three groups would require at least 5 animals per group as previously described.[104] Tumor volume was measured with digital calipers every other day and calculated using the formula: (length × width × depth × 0.5236) and body weight daily. The experiment was terminated, and the animal was sacrificed when the tumor volume reached the maximum allowed size. Treatments were started after the tumor reached 100–150 mm^3 and continued for 55 days. Each animal received about 50 doses.[80,81] Animals were then sacrificed, and tumors were collected. H&E and Ki67 immunostaining in tumor sections was performed to assess the effect of the most active candidate.

CD-1 Mouse Microsomal Stability Assay. The assay was conducted using liver microsomes of CD-1 Mouse Cat no. M1000 Xenotech MLM and according to the protocol of creative bioarray, as shown in detail in the Supporting Information. Briefly, compounds **17d** and **25b**, 5 μL at a final concentration of 100 μM, were incubated with pooled mouse liver microsomes (final concentration 0.56 mg/mL) in phosphate buffer 0.1 M (pH 7.4) in a 37 °C water bath and

https://dx.doi.org/10.1021/acs.jmedchem.0c01647
J. Med. Chem. XXXX, XXX, XXX−XXX

the reaction was initiated by the addition of an NADPH cofactor. The reaction was allowed for different time points, 5, 15, 30, 45, and 60 min and after quenching of the reactions, each bioanalysis plate was sealed and shaken for 10 min prior to LC−MS/MS analysis. The equation of first-order kinetics was used to calculate $T_{1/2}$ and $CL_{int(mic)}$ (μL/min/mg).

Confirmation of the Compounds' Purity by the UHPLC/MS Method. The UHPLC/MS method was developed for the evaluation of final compounds' purity, using an UltiMate 3000 UHPLC system by Thermo Fisher Scientific. UHPLC-grade methanol and acetonitrile (Thermo Scientific) were used. The mobile phase was filtered through a 0.45 μm membrane filter and then used. Chromatography was carried out on an Accucore C-18 RP column (4.6 mm diameter, 50 mm length, 2.6 μm bead size, Thermo Scientific) using a mixture of methanol and acetonitrile in the ratio of 50:50 (v/v) as mobile phase at a rate of 0.3 mL/min. The detection was carried out at a wavelength of 240 and 254 nm with a run time of 8 min. Stock solutions of the analyzed compounds were prepared by dissolving 10 mg of each in 1 mL of methanol and filtered through a Whatman Syringe Filter (PVDF membrane, pore size 0.45 μm) to get 10 mg/mL solutions. These stock solutions were diluted with methanol to get the working solutions of a concentration of 1 mg/mL. 0.5−2 μL of each working solution was injected into the UPLC system to obtain the chromatogram, and the injection volume used for each sample was selected with consideration of the linear region of relatively uniform response. The area under curve (AUC) value for each analyte was measured, and the relative area percentage was considered as an indicator for sample purity.

■ ASSOCIATED CONTENT

Supporting Information

The Supporting Information is available free of charge at https://pubs.acs.org/doi/10.1021/acs.jmedchem.0c01647.

Molecular formula strings for the target compounds: **10a−25h**, additional discussion of *in vitro* single-dose and five-dose screening against the NCI 60 cell panel and the selectivity ratio, Annexin V FITC/PI apoptosis assays, average tumor growth rate for mice groups that received the vehicle, compound **17d**, and **25b**, the structural optimization using CADD and the docking results into HER2 kinase, and the spectra of ^{1}H NMR, ^{13}C DEPT, ^{13}C NMR, and HRMS for compounds **4c−25h** and UPLC/MS chromatograms and final analytical reports of compounds (**10a−c,15a,b,c,e,f,i,k,l**, **17d**, **and 25a,b,c,e,f,g**) (PDF)

Antiproliferative activity of compounds (CSV)

3PP0 dimer (PDB)

3PP0 monomer (PDB)

Optimization of docking validation (PDB)

Analysis of 27 compounds (PDB)

■ AUTHOR INFORMATION

Corresponding Authors

Zakaria Y. Abd Elmageed − *Department of Pharmaceutical Sciences, Irma Lerma Rangel College of Pharmacy, Texas A&M University, Kingsville, Texas 78363, United States; Department of Pharmacology, Edward Via College of Osteopathic Medicine, University of Louisiana at Monroe, Monroe, Louisiana 71203, United States*; Phone: (318) 342-7185; Email: Zelmageed@ulm.vcom.edu; Fax: (318) 342-7280

Hamed I. Ali − *Department of Pharmaceutical Sciences, Irma Lerma Rangel College of Pharmacy, Texas A&M University, Kingsville, Texas 78363, United States;* orcid.org/0000-0002-6939-8462; Phone: (361) 221-0758; Email: alyismail@tamu.edu; Fax: (361) 221-0793

Authors

Tamer A. Elwaie − *Department of Pharmaceutical Sciences, Irma Lerma Rangel College of Pharmacy, Texas A&M University, Kingsville, Texas 78363, United States; Department of Pharmaceutical Chemistry, Faculty of Pharmacy, Cairo University, Cairo 11562, Egypt*

Safinaz E. Abbas − *Department of Pharmaceutical Chemistry, Faculty of Pharmacy, Cairo University, Cairo 11562, Egypt*

Enayat I. Aly − *Department of Pharmaceutical Chemistry, Faculty of Pharmacy, Cairo University, Cairo 11562, Egypt*

Riham F. George − *Department of Pharmaceutical Chemistry, Faculty of Pharmacy, Cairo University, Cairo 11562, Egypt*

Hamdy Ali − *Department of Pharmaceutical Sciences, Irma Lerma Rangel College of Pharmacy, Texas A&M University, Kingsville, Texas 78363, United States*

Nikolai Kraiouchkine − *Department of Physical and Environmental Sciences, Texas A&M University, Corpus Christi, Texas 78412, United States*

Khaldoun S. Abdelwahed − *School of Basic Pharmaceutical and Toxicological Sciences, College of Pharmacy, University of Louisiana at Monroe, Monroe, Louisiana 71201, United States*

Tamer E. Fandy − *Department of Pharmaceutical & Administrative Sciences, School of Pharmacy, University of Charleston, Charleston, West Virginia 25304, United States*

Khalid A. El Sayed − *School of Basic Pharmaceutical and Toxicological Sciences, College of Pharmacy, University of Louisiana at Monroe, Monroe, Louisiana 71201, United States;* orcid.org/0000-0002-1456-4064

Complete contact information is available at: https://pubs.acs.org/10.1021/acs.jmedchem.0c01647

Author Contributions

Participated in research design: H.I.A. and S.E.A. Conducted experiments: T.A.E., Z.Y.A.E., T.E.F., H.A., and N.K. Performed data analysis: H.I.A., S.E.A., Z.Y.A.E., T.A.E., R.F.G., N.K., Z.Y.A.E., T.E.F., and H.A. Wrote or contributed to the writing of the manuscript: H.I.A., S.E.A., Z.Y.A.E., T.A.E., E.I.A., T.E.F., and H.A.

Notes

The authors declare no competing financial interest.

■ ACKNOWLEDGMENTS

This work was supported by the Start-up Fund by Texas A&M Health Sciences Center (to H.I.A. grant number 121500-35558). It was also supported in part by the scholarship offered to T.A.E. by the Department of Missions, Ministry of higher education in Egypt. The authors wish to offer their deep gratitude to Mohamed Gaballah and Rofaida Gaballa for their generous help in conducting the antiproliferative and Western blot assays. We would also like to thank the staff at the vivarium of Texas A&M-Rangel College of pharmacy with special gratitude to Jennifer Santos (Veterinary Technician IV). Special gratitude to Mr. Daniel Freeman, Multimedia Project Coordinator for improving the quality of the figures in this manuscript.

■ ABBREVIATIONS

BC, breast cancer; EGFR, epidermal growth factor receptor-2; HER2, human epidermal growth factor receptor-2; TKIs, tyrosine kinase inhibitors; NSCLC, nonsmall-cell lung carcinoma; RTKs, receptor tyrosine kinases; ADP-Glo, adenosine diphosphate assay using ADP-Glo kits (ADP-Glo, Promega Corp.); [γ-^{32}P]ATP, adenosine 5′-triphosphate-gamma-^{32}P; TBAB, tetra-*n*-butylammonium bromide; ^{13}C DEPT, ^{13}C distortionless enhancement by polarization transfer; HRMS, high-resolution mass spectrometry; SAR, structure−activity relationship; rmsd, root-mean-square deviation; CADD, computer-aided drug design

■ REFERENCES

(1) Fitzmaurice, C.; Dicker, D.; Pain, A.; Hamavid, H.; Moradi-Lakeh, M.; MacIntyre, M. F.; Allen, C.; Hansen, G.; Woodbrook, R.; Wolfe, C.; Hamadeh, R. R.; Moore, A.; Werdecker, A.; Gessner, B. D.; Te Ao, B.; McMahon, B.; Karimkhani, C.; Yu, C.; Cooke, G. S.; Schwebel, D. C.; Carpenter, D. O.; Pereira, D. M.; Nash, D.; Kazi, D. S.; De Leo, D.; Plass, D.; Ukwaja, K. N.; Thurston, G. D.; Yun Jin, K.; Simard, E. P.; Mills, E.; Park, E.-K.; Catalá-López, F.; deVeber, G.; Gotay, C.; Khan, G.; Hosgood, H. D., 3rd; Santos, I. S.; Leasher, J. L.; Singh, J.; Leigh, J.; Jonas, J. B.; Sanabria, J.; Beardsley, J.; Jacobsen, K. H.; Takahashi, K.; Franklin, R. C.; Ronfani, L.; Montico, M.; Naldi, L.; Tonelli, M.; Geleijnse, J.; Petzold, M.; Shrime, M. G.; Younis, M.; Yonemoto, N.; Breitborde, N.; Yip, P.; Pourmalek, F.; Lotufo, P. A.; Esteghamati, A.; Hankey, G. J.; Ali, R.; Lunevicius, R.; Malekzadeh, R.; Dellavalle, R.; Weintraub, R.; Lucas, R.; Hay, R.; Rojas-Rueda, D.; Westerman, R.; Sepanlou, S. G.; Nolte, S.; Patten, S.; Weichenthal, S.; Abera, S. F.; Fereshtehnejad, S.-M.; Shiue, I.; Driscoll, T.; Vasankari, T.; Alsharif, U.; Rahimi-Movaghar, V.; Vlassov, V. V.; Marcenes, W. S.; Mekonnen, W.; Melaku, Y. A.; Yano, Y.; Artaman, A.; Campos, I.; MacLachlan, J.; Mueller, U.; Kim, D.; Trillini, M.; Eshrati, B.; Williams, H. C.; Shibuya, K.; Dandona, R.; Murthy, K.; Cowie, B.; Amare, A. T.; Antonio, C. A.; Castañeda-Orjuela, C.; van Gool, C. H.; Violante, F.; Oh, I.-H.; Deribe, K.; Soreide, K.; Knibbs, L.; Kereselidze, M.; Green, M.; Cardenas, R.; Roy, N.; Tillmann, T.; Li, Y.; Krueger, H.; Monasta, L.; Dey, S.; Sheikhbahaei, S.; Hafezi-Nejad, N.; Kumar, G. A.; Sreeramareddy, C. T.; Dandona, L.; Wang, H.; Vollset, S. E.; Mokdad, A.; Salomon, J. A.; Lozano, R.; Vos, T.; Forouzanfar, M.; Lopez, A.; Murray, C.; Naghavi, M. The global burden of cancer 2013. *JAMA Oncol.* **2015**, *1*, 505−527.

(2) Heron, M. Deaths : leading causes for 2008. *Natl. Vital Stat. Rep.* **2012**, *60*, 1−94.

(3) Fekry, M. I.; Ezzat, S. M.; Salama, M. M.; Alshehri, O. Y.; Al-Abd, A. M. Bioactive glycoalkaloides isolated from Solanum melongena fruit peels with potential anticancer properties against hepatocellular carcinoma cells. *Sci. Rep.* **2019**, *9*, 1746−1756.

(4) Bashmail, H. A.; Alamoudi, A. A.; Noorwali, A.; Hegazy, G. A.; Choudhry, H.; Al-Abd, A. M. Thymoquinone synergizes gemcitabine anti-breast cancer activity via modulating its apoptotic and autophagic activities. *Sci. Rep.* **2018**, *8*, 11674−11684.

(5) Mohamed, G. A.; Al-Abd, A. M.; El-Halawany, A. M.; Abdallah, H. M.; Ibrahim, S. R. M. New xanthones and cytotoxic constituents from Garcinia mangostana fruit hulls against human hepatocellular, breast, and colorectal cancer cell lines. *J. Ethnopharmacol.* **2017**, *198*, 302−312.

(6) Hunt, M.; Bradley, P.; Lapierre, S. G.; Heys, S.; Thomsit, M.; Hall, M. B.; Malone, K. M.; Wintringer, P.; Walker, T. M.; Cirillo, D. M.; Comas, I.; Farhat, M. R.; Fowler, P.; Gardy, J.; Ismail, N.; Kohl, T. A.; Mathys, V.; Merker, M.; Niemann, S.; Omar, S. V.; Sintchenko, V.; Smith, G.; Soolingen, D. v.; Supply, P.; Tahseen, S.; Wilcox, M.; Arandjelovic, I.; Peto, T. E. A.; Crook, D. W.; Iqbal, Z. Antibiotic resistance prediction for Mycobacterium tuberculosis from genome sequence data with Mykrobe. *Wellcome Open Res.* **2019**, *4*, 191−222.

(7) Bray, F.; Ferlay, J.; Soerjomataram, I.; Siegel, R. L.; Torre, L. A.; Jemal, A. Global cancer statistics 2018: GLOBOCAN estimates of incidence and mortality worldwide for 36 cancers in 185 countries. *Ca-Cancer J. Clin.* **2018**, *68*, 394−424.

(8) National Cancer Institute. *Cancer Stat Facts: Female Breast Cancer*, 2020.

(9) Olayioye, M. A.; Neve, R. M.; Lane, H. A.; Hynes, N. E. The ErbB signaling network : receptor heterodimerization in development and cancer. *EMBO J.* **2000**, *19*, 3159−3167.

(10) Burgess, A. W.; Cho, H.-s.; Eigenbrot, C.; Ferguson, K. M.; Garrett, T. P. J.; Leahy, D. J.; Lemmon, M. A.; Sliwkowski, M. X.; Ward, C. W.; Yokoyama, S.; Parade, R.; Parade, R. An open-and-shut case ? recent insights into the activation of EGF / ErbB receptors csiro health science and nutrition. *Mol. Cell* **2003**, *12*, 541−552.

(11) Roskoski, R. ErbB/HER protein-tyrosine kinases: structures and small molecule inhibitors. *Pharmacol. Res.* **2014**, *87*, 42−59.

(12) Yarden, Y. Biology of HER2 and its importance in breast cancer. *Oncology* **2001**, *61*, 1−13.

(13) Sliwkowski, M. X.; Lofgren, J. A.; Lewis, G. D.; Hotaling, T. E.; Fendly, B. M.; Fox, J. A. Nonclinical studies addressing the mechanism of action of trastuzumab (Herceptin). *Semin. Oncol.* **1999**, *26*, 60−70.

(14) Brennan, P. J.; Kumagai, T.; Berezov, A.; Murali, R.; Greene, M. I. Erratum: HER2/Neu: mechanisms of dimerization/oligomerization. *Oncogene* **2002**, *21*, 328.

(15) Pohlmann, P. R.; Mayer, I. A.; Mernaugh, R. Resistance to trastuzumab in breast cancer. *Clin. Cancer Res.* **2009**, *15*, 7479−7491.

(16) Hung, M. C.; Schechter, A. L.; Chevray, P. Y.; Stern, D. F.; Weinberg, R. A. Molecular cloning of the neu gene: Absence of gross structural alteration in oncogenic alleles. *Proc. Natl. Acad. Sci. U.S.A.* **1986**, *83*, 261−264.

(17) Funkhouser, W. K.; Kaiser-Rogers, K. Review: Significance of, and optimal screening for, HER-2 gene amplification and protein overexpression in breast carcinoma. *Ann. Clin. Lab. Sci.* **2001**, *31*, 349.

(18) Brabender, J.; Danenberg, K. D.; Metzger, R.; Schneider, P. M.; Park, J.; Salonga, D.; Hölscher, A. H.; Danenberg, P. V. Epidermal growth factor receptor and HER2-neu mRNA expression in non-small cell lung cancer is correlated with survival. *Clin. Cancer Res.* **2001**, *7*, 1850.

(19) Hou, L.; Shi, D.; Tu, S.-M.; Zhang, H.-Z.; Hung, M.-C.; Ling, D. Oral cancer progression and c-erbB-2/neu proto-oncogene expression. *Cancer Lett.* **1992**, *65*, 215−220.

(20) Ma, J.; Han, H.; Liu, D.; li, W.; Feng, H.; Xue, X.; Wu, X.; Niu, G.; Zhang, G.; Zhao, Y.; Liu, C.; Tao, H.; Gao, B. HER2 as a promising target for cytotoxicity T cells in human melanoma therapy. *PLoS One* **2013**, *8*, e73261.

(21) Musolino, A.; Ciccolallo, L.; Panebianco, M.; Fontana, E.; Zanoni, D.; Bozzetti, C.; Michiara, M.; Silini, E. M.; Ardizzoni, A. Multifactorial central nervous system recurrence susceptibility in patients with HER2-positive breast cancer. *Cancer* **2011**, *117*, 1837−1846.

(22) Loibl, S.; Gianni, L. HER2-positive breast cancer. *Lancet* **2017**, *389*, 2415−2429.

(23) Escrivá-de-Romaní, S.; Arumí, M.; Bellet, M.; Saura, C. HER2-positive breast cancer: Current and new therapeutic strategies. *Breast* **2018**, *39*, 80−88.

(24) Oh, D.-Y.; Bang, Y.-J. HER2-targeted therapies - a role beyond breast cancer. *Nat. Rev. Clin. Oncol.* **2020**, *17*, 33−48.

(25) Arribas, J.; Baselga, J.; Pedersen, K.; Parra-Palau, J. L. p95HER2 and breast cancer. *Cancer Res.* **2011**, *71*, 1515−1519.

(26) Mohan, N.; Jiang, J.; Dokmanovic, M.; Wu, W. J. Trastuzumab-mediated cardiotoxicity: current understanding, challenges, and frontiers. *Antibody Ther.* **2018**, *1*, 13−17.

(27) Diéras, V.; Miles, D.; Verma, S.; Pegram, M.; Welslau, M.; Baselga, J.; Krop, I. E.; Blackwell, K.; Hoersch, S.; Xu, J.; Green, M.; Gianni, L. Trastuzumab emtansine versus capecitabine plus lapatinib in patients with previously treated HER2-positive advanced breast cancer (EMILIA): a descriptive analysis of final overall survival results from a randomised, open-label, phase 3 trial. *Lancet Oncol.* **2017**, *18*, 732−742.

https://dx.doi.org/10.1021/acs.jmedchem.0c01647
J. Med. Chem. XXXX, XXX, XXX−XXX

(28) Schneeweiss, A.; Chia, S.; Hickish, T.; Harvey, V.; Eniu, A.; Hegg, R.; Tausch, C.; Seo, J. H.; Tsai, Y.-F.; Ratnayake, J.; McNally, V.; Ross, G.; Cortés, J. Pertuzumab plus trastuzumab in combination with standard neoadjuvant anthracycline-containing and anthracycline-free chemotherapy regimens in patients with HER2-positive early breast cancer: A randomized phase II cardiac safety study (TRYPHAENA). *Ann. Oncol.* **2013**, *24*, 2278−2284.
(29) Nahta, R.; Yuan, L. X. H.; Du, Y.; Esteva, F. J. Lapatinib induces apoptosis in trastuzumab-resistant breast cancer cells: effects on insulin-like growth factor I signaling. *Mol. Cancer Ther.* **2007**, *6*, 667−674.
(30) Collins, D. M.; Conlon, N. T.; Kannan, S.; Verma, C. S.; Eli, L. D.; Lalani, A. S.; Crown, J. Preclinical characteristics of the irreversible pan- her kinase inhibitor neratinib compared with lapatinib: implications for the treatment of HER2- positive and HER2-mutated breast cancer. *Cancers* **2019**, *11*, 737.
(31) https://www.fda.gov/drugs/new-drugs-fda-cders-new-molecular-entities-and-new-therapeutic-biological-products/new-drug-therapy-approvals-2019. (accessed Jan 18, 2020).
(32) Milik, S. N.; Lasheen, D. S.; Serya, R. A. T.; Abouzid, K. A. M. How to train your inhibitor: design strategies to overcome resistance to epidermal growth factor receptor inhibitors. *Eur. J. Med. Chem.* **2017**, *142*, 131−151.
(33) Cohen, M. H.; Williams, G. A.; Sridhara, R.; Chen, G.; Pazdur, R. FDA drug approval summary: gefitinib (ZD1839) (iressa(R)) tablets. *Oncologista* **2003**, *8*, 303−306.
(34) Cohen, M. H.; Johnson, J. R.; Chen, Y. F.; Sridhara, R.; Pazdur, R. FDA drug approval summary: erlotinib (Tarceva) tablets. *Oncologist* **2005**, *10*, 461−466.
(35) Ryan, Q.; Ibrahim, A.; Cohen, M. H.; Johnson, J.; Ko, C. w.; Sridhara, R.; Justice, R.; Pazdur, R. FDA drug approval summary: lapatinib in combination with capecitabine for previously treated metastatic breast cancer that overexpresses HER-2. *Oncologista* **2008**, *13*, 1114−1119.
(36) Rusnak, D. W.; Affleck, K.; Cockerill, S. G.; Stubberfield, C.; Harris, R.; Page, M.; Smith, K. J.; Guntrip, S. B.; Carter, M. C.; Shaw, R. J.; Jowett, A.; Stables, J.; Topley, P.; Wood, E. R.; Brignola, P. S.; Kadwell, S. H.; Reep, B. R.; Mullin, R. J.; Alligood, K. J.; Keith, B. R.; Crosby, R. M.; Murray, D. M.; Knight, W. B.; Gilmer, T. M.; Lackey, K. The characterization of novel, dual ErbB-2/EGFR, tyrosine kinase inhibitors: Potential therapy for cancer. *Cancer Res.* **2001**, *61*, 7196.
(37) Wood, E. R.; Truesdale, A. T.; McDonald, O. B.; Yuan, D.; Hassell, A.; Dickerson, S. H.; Ellis, B.; Pennisi, C.; Horne, E.; Lackey, K.; Alligood, K. J.; Rusnak, D. W.; Gilmer, T. M.; Shewchuk, L. A unique structure for epidermal growth factor receptor bound to GW572016 (Lapatinib): Relationships among protein conformation, inhibitor off-rate, and receptor activity in tumor cells. *Cancer Res.* **2004**, *64*, 6652−6659.
(38) Roskoski, R. Classification of small molecule protein kinase inhibitors based upon the structures of their drug-enzyme complexes. *Pharmacol. Res.* **2016**, *103*, 26−48.
(39) Sadek, M. M.; Serrya, R. A.; Kafafy, A.-H. N.; Ahmed, M.; Wang, F.; Abouzid, K. A. M. Discovery of new HER2/EGFR dual kinase inhibitors based on the anilinoquinazoline scaffold as potential anti-cancer agents. *J. Enzyme Inhib. Med. Chem.* **2014**, *29*, 215−222.
(40) Trowe, T.; Boukouvala, S.; Calkins, K.; Cutler, R. E.; Fong, R.; Funke, R.; Gendreau, S. B.; Kim, Y. D.; Miller, N.; Woolfrey, J. R.; Vysotskaia, V.; Yang, J. P.; Gerritsen, M. E.; Matthews, D. J.; Lamb, P.; Heuer, T. S. EXEL-7647 inhibits mutant forms of ErbB2 associated with lapatinib resistance and neoplastic transformation. *Clin. Cancer Res.* **2008**, *14*, 2465−2475.
(41) Li, J. Diarrhea With HER2-Targeted Agents in Cancer Patients: A Systematic Review and Meta-Analysis. *J. Clin. Pharmacol.* **2019**, *59*, 935−946.
(42) Lee-Hoeflich, S. T.; Crocker, L.; Yao, E.; Pham, T.; Munroe, X.; Hoeflich, K. P.; Sliwkowski, M. X.; Stern, H. M. A central role for HER3 in HER2-amplified breast cancer: Implications for targeted therapy. *Cancer Res.* **2008**, *68*, 5878−5887.
(43) Jackson-Fisher, A. J.; Bellinger, G.; Shum, E.; Duong, J. K.; Perkins, A. S.; Gassmann, M.; Muller, W.; Kent Lloyd, K. C.; Stern, D. F. Formation of Neu/ErbB2-induced mammary tumors is unaffected by loss of ErbB4. *Oncogene* **2006**, *25*, 5664−5672.
(44) Li, T.; Perez-Soler, R. Skin toxicities associated with epidermal growth factor receptor inhibitors. *Target. Oncol.* **2009**, *4*, 107−119.
(45) Shuch, B.; Bratslavsky, G.; Linehan, W. M.; Srinivasan, R. Sarcomatoid renal cell carcinoma: A comprehensive review of the biology and current treatment strategies. *Oncologist* **2012**, *17*, 46−54.
(46) Milik, S. N.; Abdel-Aziz, A. K.; Lasheen, D. S.; Serya, R. A. T.; Minucci, S.; Abouzid, K. A. M. Surmounting the resistance against EGFR inhibitors through the development of thieno[2,3-d]-pyrimidine-based dual EGFR/HER2 inhibitors. *Eur. J. Med. Chem.* **2018**, *155*, 316−336.
(47) Jani, J. P.; Finn, R. S.; Campbell, M.; Coleman, K. G.; Connell, R. D.; Currier, N.; Emerson, E. O.; Floyd, E.; Harriman, S.; Kath, J. C.; Morris, J.; Moyer, J. D.; Pustilnik, L. R.; Rafidi, K.; Ralston, S.; Rossi, A. M. K.; Steyn, S. J.; Wagner, L.; Winter, S. M.; Bhattacharya, S. K. Discovery and pharmacologic characterization of CP-724,714, a selective ErbB2 tyrosine kinase inhibitor. *Cancer Res.* **2007**, *67*, 9887−9893.
(48) Aertgeerts, K.; Skene, R.; Yano, J.; Sang, B.-C.; Zou, H.; Snell, G.; Jennings, A.; Iwamoto, K.; Habuka, N.; Hirokawa, A.; Ishikawa, T.; Tanaka, T.; Miki, H.; Ohta, Y.; Sogabe, S. Structural analysis of the mechanism of inhibition and allosteric activation of the kinase domain of HER2 protein. *J. Biol. Chem.* **2011**, *286*, 18756−18765.
(49) Verdonk, M. L.; Cole, J. C.; Hartshorn, M. J.; Murray, C. W.; Taylor, R. D. Improved protein-ligand docking using GOLD. *Proteins* **2003**, *52*, 609−623.
(50) Elkamhawy, A.; Farag, A. K.; Viswanath, A. N. I.; Bedair, T. M.; Leem, D. G.; Lee, K.-T.; Pae, A. N.; Roh, E. J. Targeting EGFR/HER2 tyrosine kinases with a new potent series of 6-substituted 4-anilinoquinazoline hybrids: Design, synthesis, kinase assay, cell-based assay, and molecular docking. *Bioorg. Med. Chem. Lett.* **2015**, *25*, 5147−5154.
(51) Ishikawa, T.; Seto, M.; Banno, H.; Kawakita, Y.; Oorui, M.; Taniguchi, T.; Ohta, Y.; Tamura, T.; Nakayama, A.; Miki, H.; Kamiguchi, H.; Tanaka, T.; Habuka, N.; Sogabe, S.; Yano, J.; Aertgeerts, K.; Kamiyama, K. Design and synthesis of novel human epidermal growth factor receptor 2 (HER2)/epidermal growth factor receptor (EGFR) dual inhibitors bearing a pyrrolo[3,2-d]pyrimidine scaffold. *J. Med. Chem.* **2011**, *54*, 8030−8050.
(52) Bellamy, F. D.; Ou, K. Selective reduction of aromatic nitro compounds with stannous chloride in non acidic and non aqueous medium. *Tetrahedron Lett.* **1984**, *25*, 839−842.
(53) Milik, S. N.; Abdel-Aziz, A. K.; Lasheen, D. S.; Serya, R. A. T.; Minucci, S.; Abouzid, K. A. M. Surmounting the resistance against EGFR inhibitors through the development of thieno[2,3-d]-pyrimidine-based dual EGFR/HER2 inhibitors. *Eur. J. Med. Chem.* **2018**, *155*, 316−336.
(54) Porter, H. K. *The Zinin Reduction of Nitroarenes*; John Wiley & Sons, Inc., 2011; Vol. *20*.
(55) Foucourt, A.; Dubouilh-Benard, C.; Chosson, E.; Corbière, C.; Buquet, C.; Iannelli, M.; Leblond, B.; Marsais, F.; Besson, T. Microwave-accelerated Dimroth rearrangement for the synthesis of 4-anilino-6-nitroquinazolines. Application to an efficient synthesis of a microtubule destabilizing agent. *Tetrahedron* **2010**, *66*, 4495−4502.
(56) Von Niementowski, S. Synthesen von chinazolinverbindungen. *J. Prakt. Chem.* **1894**, *51*, 564−572.
(57) Li, R.-D.; Zhang, X.; Li, Q.-Y.; Ge, Z.-M.; Li, R.-T. Novel EGFR inhibitors prepared by combination of dithiocarbamic acid esters and 4-anilinoquinazolines. *Bioorg. Med. Chem. Lett.* **2011**, *21*, 3637−3640.
(58) Forcellini, E.; Boutin, S.; Lefebvre, C.-A.; Shayhidin, E. E.; Boulanger, M.-C.; Rhéaume, G.; Barbeau, X.; Lagüe, P.; Mathieu, P.; Paquin, J.-F. Synthesis and biological evaluation of novel quinazoline-4-piperidinesulfamide derivatives as inhibitors of NPP1. *Eur. J. Med. Chem.* **2018**, *147*, 130−149.
(59) Cai, X.; Zhai, H.-X.; Wang, J.; Forrester, J.; Qu, H.; Yin, L.; Lai, C.-J.; Bao, R.; Qian, C. Discovery of 7-(4-(3-Ethynylphenylamino)-7-

https://dx.doi.org/10.1021/acs.jmedchem.0c01647
J. Med. Chem. XXXX, XXX, XXX−XXX

methoxyquinazolin-6-yloxy)- N -hydroxyheptanamide (CUDC-101) as a Potent Multi-Acting HDAC, EGFR, and HER2 Inhibitor for the Treatment of Cancer. *J. Med. Chem.* **2010**, *53*, 2000−2009.
(60) Hou, X.; Ge, Z.; Wang, T.; Guo, W.; Wu, J.; Cui, J.; Lai, C.; Li, R. Synthesis and Structure-Activity Relationships of A Novel Class of Dithiocarbamic Acid Esters as Anticancer Agent. *Arch. Pharm.* **2011**, *344*, 320.
(61) Ismail, R. S. M.; Abou-Seri, S. M.; Eldehna, W. M.; Ismail, N. S. M.; Elgazwi, S. M.; Ghabbour, H. A.; Ahmed, M. S.; Halaweish, F. T.; Abou El Ella, D. A. Novel series of 6-(2-substitutedacetamido)-4-anilinoquinazolines as EGFR-ERK signal transduction inhibitors in MCF-7 breast cancer cells. *Eur. J. Med. Chem.* **2018**, *155*, 782−796.
(62) Noren, N. K.; Foos, G.; Hauser, C. A.; Pasquale, E. B. The EphB4 receptor suppresses breast cancer cell tumorigenicity through an Abl-Crk pathway. *Nat. Cell Biol.* **2006**, *8*, 815−825.
(63) Gil-Henn, H.; Patsialou, A.; Wang, Y.; Warren, M. S.; Condeelis, J. S.; Koleske, A. J. Arg/Abl2 promotes invasion and attenuates proliferation of breast cancer in vivo. *Oncogene* **2013**, *32*, 2622−2630.
(64) Zhang, S.; Huang, W.-C.; Li, P.; Guo, H.; Poh, S.-B.; Brady, S. W.; Xiong, Y.; Tseng, L.-M.; Li, S.-H.; Ding, Z.; Sahin, A. A.; Esteva, F. J.; Hortobagyi, G. N.; Yu, D. Combating trastuzumab resistance by targeting SRC, a common node downstream of multiple resistance pathways. *Nat. Med.* **2011**, *17*, 461−469.
(65) Golubovskaya, V. Targeting FAK in human cancer: from finding to first clinical trials. *Front. Biosci.* **2014**, *19*, 687−706.
(66) Wang, L.; Ai, M.; Yu, J.; Jin, L.; Wang, C.; Liu, Z.; Shu, X.; Tang, Z.; Liu, K.; Luo, H.; Guan, W.; Sun, X.; Ma, X. Structure-based modification of carbonyl-diphenylpyrimidines (Car-DPPYs) as a novel focal adhesion kinase (FAK) inhibitor against various stubborn cancer cells. *Eur. J. Med. Chem.* **2019**, *172*, 154−162.
(67) Kim, J. W.; Gautam, J.; Kim, J. E.; Kim, J. A.; Kang, K. W. Inhibition of tumor growth and angiogenesis of tamoxifen-resistant breast cancer cells by ruxolitinib, a selective JAK2 inhibitor. *Oncol. Lett.* **2019**, *17*, 3981−3989.
(68) Butti, R.; Das, S.; Gunasekaran, V. P.; Yadav, A. S.; Kumar, D.; Kundu, G. C. Receptor tyrosine kinases (RTKs) in breast cancer: signaling, therapeutic implications and challenges. *Mol. Cancer* **2018**, *17*, 34−51.
(69) Paulsson, J.; Sjöblom, T.; Micke, P.; Pontén, F.; Landberg, G.; Heldin, C.-H.; Bergh, J.; Brennan, D. J.; Jirström, K.; Östman, A. Prognostic significance of stromal platelet-derived growth factor beta-receptor expression in human breast cancer. *Am. J. Pathol.* **2009**, *175*, 334−341.
(70) Carvalho, I.; Milanezi, F.; Martins, A.; Reis, R. M.; Schmitt, F. Overexpression of platelet-derived growth factor receptor alpha in breast cancer is associated with tumour progression. *Breast Cancer Res.* **2005**, *7*, R788−R795.
(71) Bhardwaj, B.; Klassen, J.; Cossette, N.; Sterns, E.; Tuck, A.; Deeley, R.; Sengupta, S.; Elliott, B. Localization of platelet-derived growth factor beta receptor expression in the periepithelial stroma of human breast carcinoma. *Clin. Cancer Res.* **1996**, *2*, 773.
(72) Xu, X.; De Angelis, C.; Burke, K. A.; Nardone, A.; Hu, H.; Qin, L.; Veeraraghavan, J.; Sethunath, V.; Heiser, L. M.; Wang, N.; Ng, C. K. Y.; Chen, E. S.; Renwick, A.; Wang, T.; Nanda, S.; Shea, M.; Mitchell, T.; Rajendran, M.; Waters, I.; Zabransky, D. J.; Scott, K. L.; Gutierrez, C.; Nagi, C.; Geyer, F. C.; Chamness, G. C.; Park, B. H.; Shaw, C. A.; Hilsenbeck, S. G.; Rimawi, M. F.; Gray, J. W.; Weigelt, B.; Reis-Filho, J. S.; Osborne, C. K.; Schiff, R. HER2 reactivation through acquisition of the HER2 L755S mutation as a mechanism of acquired resistance to HER2-targeted therapy in HER2(+) breast cancer. *Clin. Cancer Res.* **2017**, *23*, 5123−5134.
(73) Wen, W.; Chen, W.; Xiao, N.; Bender, R.; Ghazalpour, A.; Tan, Z.; Swensen, J.; Millis, S. Z.; Basu, G.; Gatalica, Z.; Press, M. F. mutations in the kinase domain of the her2/erbb2 gene identified in a wide variety of human cancers. *J. Mol. Diagn.* **2015**, *17*, 487−495.
(74) AACR Project GENIE Consortium. AACR project genie: powering precision medicine through an international consortium. *Cancer Discovery* **2017**, *7*, 818−831.
(75) My Cancer Genome, Genetically Informed Cancer Medicine. https://www.mycancergenome.org/content/alteration/erbb2-l755s/ (accessed Feb 14, 2019).
(76) Zabransky, D. J.; Yankaskas, C. L.; Cochran, R. L.; Wong, H. Y.; Croessmann, S.; Chu, D.; Kavuri, S. M.; Red Brewer, M.; Rosen, D. M.; Dalton, W. B.; Cimino-Mathews, A.; Cravero, K.; Button, B.; Kyker-Snowman, K.; Cidado, J.; Erlanger, B.; Parsons, H. A.; Manto, K. M.; Bose, R.; Lauring, J.; Arteaga, C. L.; Konstantopoulos, K.; Park, B. H. HER2 missense mutations have distinct effects on oncogenic signaling and migration. *Proc. Natl. Acad. Sci. U.S.A.* **2015**, *112*, E6205−E6214.
(77) Bose, R.; Kavuri, S. M.; Searleman, A. C.; Shen, W.; Shen, D.; Koboldt, D. C.; Monsey, J.; Goel, N.; Aronson, A. B.; Li, S.; Ma, C. X.; Ding, L.; Mardis, E. R.; Ellis, M. J. Activating HER2 mutations in HER2 gene amplification negative breast cancer. *Cancer Discovery* **2013**, *3*, 224−237.
(78) Kancha, R. K.; von Bubnoff, N.; Bartosch, N.; Peschel, C.; Engh, R. A.; Duyster, J. Differential sensitivity of ERBB2 kinase domain mutations towards lapatinib. *PLoS One* **2011**, *6*, e26760−e26769.
(79) Trowe, T.; Boukouvala, S.; Calkins, K.; Cutler, R. E., Jr.; Fong, R.; Funke, R.; Gendreau, S. B.; Kim, Y. D.; Miller, N.; Woolfrey, J. R.; Vysotskaia, V.; Yang, J. P.; Gerritsen, M. E.; Matthews, D. J.; Lamb, P.; Heuer, T. S. EXEL-7647 inhibits mutant forms of ErbB2 associated with lapatinib resistance and neoplastic transformation. *Clin. Cancer Res.* **2008**, *14*, 2465−2475.
(80) Dai, X.; Cheng, H.; Bai, Z.; Li, J. Breast cancer cell line classification and its relevance with breast tumor subtyping. *J. Cancer* **2017**, *8*, 3131−3141.
(81) Neve, R. M.; Chin, K.; Fridlyand, J.; Yeh, J.; Baehner, F. L.; Fevr, T.; Clark, L.; Bayani, N.; Coppe, J.-P.; Tong, F.; Speed, T.; Spellman, P. T.; DeVries, S.; Lapuk, A.; Wang, N. J.; Kuo, W.-L.; Stilwell, J. L.; Pinkel, D.; Albertson, D. G.; Waldman, F. M.; McCormick, F.; Dickson, R. B.; Johnson, M. D.; Lippman, M.; Ethier, S.; Gazdar, A.; Gray, J. W. A collection of breast cancer cell lines for the study of functionally distinct cancer subtypes. *Cancer Cell* **2006**, *10*, 515−527.
(82) Lacroix, M.; Leclercq, G. Relevance of breast cancer cell lines as models for breast tumours: an update. *Breast Cancer Res. Treat.* **2004**, *83*, 249−289.
(83) Bacus, S. S.; Kiguchi, K.; Chin, D.; King, C. R.; Huberman, E. Differentiation of cultured human breast cancer cells (AU-565 and MCF-7) associated with loss of cell surface HER-2/neu antigen. *Mol. Carcinog.* **1990**, *3*, 350−362.
(84) Holliday, D. L.; Speirs, V. Choosing the right cell line for breast cancer research. *Breast Cancer Res.* **2011**, *13*, 215.
(85) Riaz, M.; van Jaarsveld, M. T.; Hollestelle, A.; Prager-van der Smissen, W. J.; Heine, A. A.; Boersma, A. W.; Liu, J.; Helmijr, J.; Ozturk, B.; Smid, M.; Wiemer, E. A.; Foekens, J. A.; Martens, J. W. miRNA expression profiling of 51 human breast cancer cell lines reveals subtype and driver mutation-specific miRNAs. *Breast Cancer Res.* **2013**, *15*, R33.
(86) Hollestelle, A.; Nagel, J. H. A.; Smid, M.; Lam, S.; Elstrodt, F.; Wasielewski, M.; Ng, S. S.; French, P. J.; Peeters, J. K.; Rozendaal, M. J.; Riaz, M.; Koopman, D. G.; Ten Hagen, T. L. M.; de Leeuw, B. H. C. G. M.; Zwarthoff, E. C.; Teunisse, A.; van der Spek, P. J.; Klijn, J. G. M.; Dinjens, W. N. M.; Ethier, S. P.; Clevers, H.; Jochemsen, A. G.; den Bakker, M. A.; Foekens, J. A.; Martens, J. W. M.; Schutte, M. Distinct gene mutation profiles among luminal-type and basal-type breast cancer cell lines. *Breast Cancer Res. Treat.* **2010**, *121*, 53−64.
(87) Kao, J.; Salari, K.; Bocanegra, M.; Choi, Y.-L.; Girard, L.; Gandhi, J.; Kwei, K. A.; Hernandez-Boussard, T.; Wang, P.; Gazdar, A. F.; Minna, J. D.; Pollack, J. R. Molecular profiling of breast cancer cell lines defines relevant tumor models and provides a resource for cancer gene discovery. *PLoS One* **2009**, *4*, e6146−e6161.
(88) Anido, J.; Matar, P.; Albanell, J.; Guzmán, M.; Rojo, F.; Arribas, J.; Averbuch, S.; Baselga, J. ZD1839, a specific epidermal growth factor receptor (EGFR) tyrosine kinase inhibitor, induces the formation of inactive EGFR/HER2 and EGFR/HER3 heterodimers

and prevents heregulin signaling in HER2-overexpressing breast cancer cells. *Clin. Cancer Res.* **2003**, *9*, 1274.
(89) Witton, C. J.; Reeves, J. R.; Going, J. J.; Cooke, T. G.; Bartlett, J. M. Expression of the HER1-4 family of receptor tyrosine kinases in breast cancer. *J. Pathol.* **2003**, *200*, 290−297.
(90) Tsutsui, S.; Ohno, S.; Murakami, S.; Hachitanda, Y.; Oda, S. Prognostic value of epidermal growth factor receptor (EGFR) and its relationship to the estrogen receptor status in 1029 patients with breast cancer. *Breast Cancer Res. Treat.* **2002**, *71*, 67−75.
(91) Rakha, E. A.; El-Sayed, M. E.; Green, A. R.; Lee, A. H. S.; Robertson, J. F.; Ellis, I. O. Prognostic markers in triple-negative breast cancer. *Cancer* **2007**, *109*, 25−32.
(92) Lehmann, B. D.; Bauer, J. A.; Chen, X.; Sanders, M. E.; Chakravarthy, A. B.; Shyr, Y.; Pietenpol, J. A. Identification of human triple-negative breast cancer subtypes and preclinical models for selection of targeted therapies. *J. Clin. Invest.* **2011**, *121*, 2750−2767.
(93) Masuda, H.; Zhang, D.; Bartholomeusz, C.; Doihara, H.; Hortobagyi, G. N.; Ueno, N. T. Role of epidermal growth factor receptor in breast cancer. *Breast Cancer Res. Treat.* **2012**, *136*, 331−345.
(94) Chavez, K. J.; Garimella, S. V.; Lipkowitz, S. Triple negative breast cancer cell lines: one tool in the search for better treatment of triple negative breast cancer. *Breast Dis.* **2010**, *32*, 35−48.
(95) Mowafy, S.; Farag, N. A.; Abouzid, K. A. M. Design, synthesis and in vitro anti-proliferative activity of 4,6-quinazolinediamines as potent EGFR-TK inhibitors. *Eur. J. Med. Chem.* **2013**, *61*, 132−145.
(96) Eustace, A. J.; Conlon, N. T.; McDermott, M. S. J.; Browne, B. C.; O'Leary, P.; Holmes, F. A.; Espina, V.; Liotta, L. A.; O'Shaughnessy, J.; Gallagher, C.; O'Driscoll, L.; Rani, S.; Madden, S. F.; O'Brien, N. A.; Ginther, C.; Slamon, D.; Walsh, N.; Gallagher, W. M.; Zagozdzon, R.; Watson, W. R.; O'Donovan, N.; Crown, J. Development of acquired resistance to lapatinib may sensitise HER2-positive breast cancer cells to apoptosis induction by obatoclax and TRAIL. *BMC Cancer* **2018**, *18*, 965.
(97) Tang, L.; Wang, Y.; Strom, A.; Gustafsson, J.-Å.; Guan, X. Lapatinib induces p27(Kip1)-dependent G(1) arrest through both transcriptional and post-translational mechanisms. *Cell Cycle* **2013**, *12*, 2665−2674.
(98) Hanahan, D.; Weinberg, R. A. Hallmarks of cancer: the next generation. *Cell* **2011**, *144*, 646−674.
(99) Shi, Q.; Hao, L.; Pei, J.; Yin, W. Promotion of apoptosis does not necessarily mean inhibition of remodeling. *Hypertension* **2012**, *60*, e3.
(100) Press, M. F.; Lenz, H.-J. EGFR, HER2 and VEGF pathways: validated targets for cancer treatment. *Drugs* **2007**, *67*, 2045−2075.
(101) Ali, H. E. A.; Lung, P.-Y.; Sholl, A. B.; Gad, S. A.; Bustamante, J. J.; Ali, H. I.; Rhim, J. S.; Deep, G.; Zhang, J.; Abd Elmageed, Z. Y. Dysregulated gene expression predicts tumor aggressiveness in African-American prostate cancer patients. *Sci. Rep.* **2018**, *8*, 16335.
(102) Enot, D. P.; Vacchelli, E.; Jacquelot, N.; Zitvogel, L.; Kroemer, G. TumGrowth: An open-access web tool for the statistical analysis of tumor growth curves. *Oncoimmunology* **2018**, *7*, e1462431−e1462433.
(103) Ducray, R.; Ballard, P.; Barlaam, B. C.; Hickinson, M. D.; Kettle, J. G.; Ogilvie, D. J.; Trigwell, C. B. Novel 3-alkoxy-1H-pyrazolo[3,4-d]pyrimidines as EGFR and erbB2 receptor tyrosine kinase inhibitors. *Bioorg. Med. Chem. Lett.* **2008**, *18*, 959−962.
(104) Singla, H.; Munshi, A.; Banipal, R. P. S.; Kumar, V. Recent updates on the therapeutic potential of HER2 tyrosine kinase inhibitors for the treatment of breast cancer. *Curr. Cancer Drug Targets* **2018**, *18*, 306−327.
(105) Mohamed, R.; Storelli, F.; Sidibe, J.; Bararpour, N.; Desmeules, J.; Ausburger, M.; Daali, Y.; Thomas, A. Detection and identification of reactive drug metabolites leading to idiosyncratic toxicity: lapatinib as a case example. *J. Drug Metab. Toxicol.* **2018**, *9*, 1000242.
(106) Li, X.; Yang, C.; Wan, H.; Zhang, G.; Feng, J.; Zhang, L.; Chen, X.; Zhong, D.; Lou, L.; Tao, W.; Zhang, L. Discovery and development of pyrotinib: A novel irreversible EGFR/HER2 dual tyrosine kinase inhibitor with favorable safety profiles for the treatment of breast cancer. *Eur. J. Pharm. Sci.* **2017**, *110*, 51−61.
(107) Wang, R.; Lu, Y.; Wang, S. Comparative evaluation of 11 scoring functions for molecular docking. *J. Med. Chem.* **2003**, *46*, 2287−2303.
(108) Milik, S. N.; Abdel-Aziz, A. K.; Lasheen, D. S.; Serya, R. A. T.; Minucci, S.; Abouzid, K. A. M. Surmounting the resistance against EGFR inhibitors through the development of thieno[2,3-d]-pyrimidine-based dual EGFR/HER2 inhibitors. *Eur. J. Med. Chem.* **2018**, *155*, 316−336.
(109) Smaill, J. B.; Gonzales, A. J.; Spicer, J. A.; Lee, H.; Reed, J. E.; Sexton, K.; Althaus, I. W.; Zhu, T.; Black, S. L.; Blaser, A.; Denny, W. A.; Ellis, P. A.; Fakhoury, S.; Harvey, P. J.; Hook, K.; McCarthy, F. O. J.; Palmer, B. D.; Rivault, F.; Schlosser, K.; Ellis, T.; Thompson, A. M.; Trachet, E.; Winters, R. T.; Tecle, H.; Bridges, A. Tyrosine kinase inhibitors. 20. optimization of substituted quinazoline and pyrido[3,4-d]pyrimidine derivatives as orally active, irreversible inhibitors of the epidermal growth factor receptor family. *J. Med. Chem.* **2016**, *59*, 8103−8124.
(110) Elkamhawy, A.; Farag, A. K.; Viswanath, A. N. I.; Bedair, T. M.; Leem, D. G.; Lee, K.-T.; Pae, A. N.; Roh, E. J. Targeting EGFR/HER2 tyrosine kinases with a new potent series of 6-substituted 4-anilinoquinazoline hybrids: Design, synthesis, kinase assay, cell-based assay, and molecular docking. *Bioorg. Med. Chem. Lett.* **2015**, *25*, 5147−5154.
(111) Ishikawa, T.; Seto, M.; Banno, H.; Kawakita, Y.; Oorui, M.; Taniguchi, T.; Ohta, Y.; Tamura, T.; Nakayama, A.; Miki, H.; Kamiguchi, H.; Tanaka, T.; Habuka, N.; Sogabe, S.; Yano, J.; Aertgeerts, K.; Kamiyama, K. Design and synthesis of novel human epidermal growth factor receptor 2 (HER2)/epidermal growth factor receptor (EGFR) dual inhibitors bearing a pyrrolo[3,2-d]pyrimidine scaffold. *J. Med. Chem.* **2011**, *54*, 8030−8050.
(112) Xu, Y.-Y.; Li, S.-N.; Yu, G.-J.; Hu, Q.-H.; Li, H.-Q. Discovery of novel 4-anilinoquinazoline derivatives as potent inhibitors of epidermal growth factor receptor with antitumor activity. *Bioorg. Med. Chem.* **2013**, *21*, 6084−6091.
(113) Lin, S.; Li, Y.; Zheng, Y.; Luo, L.; Sun, Q.; Ge, Z.; Cheng, T.; Li, R. Design, synthesis and biological evaluation of quinazoline-phosphoramidate mustard conjugates as anticancer drugs. *Eur. J. Med. Chem.* **2017**, *127*, 442−458.
(114) Hamed, M. M.; Abou El Ella, D. A.; Keeton, A. B.; Piazza, G. A.; Abadi, A. H.; Hartmann, R. W.; Engel, M. 6-Aryl and heterocycle quinazoline derivatives as potent EGFR inhibitors with improved activity toward gefitinib-sensitive and -resistant tumor cell lines. *ChemMedChem* **2013**, *8*, 1495−1504.
(115) Forcellini, E.; Boutin, S.; Lefebvre, C.-A.; Shayhidin, E. E.; Boulanger, M.-C.; Rhéaume, G.; Barbeau, X.; Lagüe, P.; Mathieu, P.; Paquin, J.-F. Synthesis and biological evaluation of novel quinazoline-4-piperidinesulfamide derivatives as inhibitors of NPP1. *Eur. J. Med. Chem.* **2018**, *147*, 130−149.
(116) National Cancer Institute, DCTD Division of Cancer Treatment & Diagnosis. Discovery & Development Services. NCI-60 Human Cancer Cell Line Screen NCI-60 Screening Methodology. https://dtp.cancer.gov/discovery_development/nci-60/ (accessed Dec 22, 2019).
(117) Darzynkiewicz, Z.; Bruno, S.; Del Bino, G.; Gorczyca, W.; Hotz, M. A.; Lassota, P.; Traganos, F. Features of apoptotic cells measured by flow cytometry. *Cytometry* **1992**, *13*, 795−808.
(118) Akl, M. R.; Ayoub, N. M.; Mohyeldin, M. M.; Busnena, B. A.; Foudah, A. I.; Liu, Y.-Y.; Sayed, K. A. E. Olive phenolics as c-Met inhibitors: (-)-Oleocanthal attenuates cell proliferation, invasiveness, and tumor growth in breast cancer models. *PLoS One* **2014**, *9*, e97622.
(119) Annexin V-FITC Apoptosis Staining/Detection Kit (ab14085).
(120) Abd Elmageed, Z. Y.; Moore, R. F.; Tsumagari, K.; Lee, M. M.; Sholl, A. B.; Friedlander, P.; Al-Qurayshi, Z.; Hassan, M.; Wang, A. R.; Boulares, H. A.; Kandil, E. Prognostic role of BRAF(V600E)

https://dx.doi.org/10.1021/acs.jmedchem.0c01647
J. Med. Chem. XXXX, XXX, XXX−XXX

cellular localization in melanoma. *J. Am. Coll. Surg.* **2018**, *226*, 526−537.

https://dx.doi.org/10.1021/acs.jmedchem.0c01647
J. Med. Chem. XXXX, XXX, XXX−XXX